

University of Alberta

Metabolic Modulation in Heart Disease

by

Vaninder Kaur Sidhu

A thesis submitted to the Faculty of Graduate Studies and Research
in partial fulfillment of the requirements for the degree of

Master of Science

Pharmacology

©Vaninder Kaur Sidhu

Spring 2013
Edmonton, Alberta

Permission is hereby granted to the University of Alberta Libraries to reproduce single copies of this thesis and to lend or sell such copies for private, scholarly or scientific research purposes only. Where the thesis is converted to, or otherwise made available in digital form, the University of Alberta will advise potential users of the thesis of these terms.

The author reserves all other publication and other rights in association with the copyright in the thesis and, except as herein before provided, neither the thesis nor any substantial portion thereof may be printed or otherwise reproduced in any material form whatsoever without the author's prior written permission.

Dedication

This thesis is dedicated to my grandparents, Jagjit and Pritam, my parents, Inderjit and Iqbal, and my brother, Robbie.

Abstract

Ischemic heart disease and pulmonary arterial hypertension are often accompanied by a drastic change in myocardial energy metabolism that favors fatty acid oxidation and glycolysis, respectively, over glucose oxidation. This form of energy production is both inefficient and detrimental to the myocardium. However, both the glucose and fatty acid oxidative pathways can be targeted to improve cardiac function. Specifically, decreasing fatty acid oxidation and/or increasing glucose metabolism can improve cardiac efficiency in these disease states. This thesis examines the metabolic changes in pulmonary hypertension and demonstrates the therapeutic advantages of metabolic modulation with dichloroacetate through restoring oxidative metabolism. We also investigate the effect of altered fatty acid metabolism on cardiac recovery following an ischemic episode using the acetyl CoA carboxylase-2 knockout mouse. Increased rates of fatty acid oxidation impair cardiac efficiency, but following ischemia these hearts sustain little injury owing to an adaptation in the 5'-AMPK-ACC-malonyl CoA pathway.

Acknowledgements

I would first like to thank my supervisor, Dr. Gary Lopaschuk, for the opportunity to pursue graduate studies in his laboratory and allowing me to complete my M.Sc. while in pharmacy. Dr. Lopaschuk's support, understanding and mentorship were instrumental in bringing me this far along my graduate studies.

I am also thankful to the Department of Pharmacology for accommodating my school schedule.

I would also like to thank my committee members, Dr. Jason Dyck and Dr. Richard Lehner, for their constructive criticism and feedback throughout my graduate studies.

A special thanks to Cory Wagg, Jagdip Jaswal, John Ussher, Wendy Keung, Victoria Lam, Daniel Moroz, Natasha Fillmore, Donna Beker, and Ken Strynadka for their expertise and help during my studies. I would especially like to thank the lab and my summer student, Julia Tan, for their help during the last stage of my experiments.

Finally, I would like to thank my grandparents, parents and brother for their continuous love and support throughout my schooling. I am grateful to have a strong support system that encouraged me to complete my M.Sc. after entering pharmacy.

Table of Contents

CHAPTER 1: Introduction	1
Energy Metabolism in the Heart	2
Myocardial Fatty Acid Metabolism	3
-Fatty acid uptake into the cardiac myocyte	3
-The carnitine shuttle	5
-Fatty acid β -oxidation	6
-Regulation of fatty acid metabolism	7
Myocardial Glucose Metabolism	9
-Glucose uptake into the cardiac myocyte	9
-Glycolysis	9
-Glucose oxidation	10
-Regulation of glucose metabolism	10
The Randle Cycle	10
Energy Metabolism in the Diseased Heart	11
-Ischemic heart disease	11
-Pulmonary arterial hypertension	13

Metabolic Approach to Heart Disease	16
-Pharmacological targets in cardiac energy metabolism	17
-Metabolic modulation of pyruvate dehydrogenase kinase	23
-Metabolic modulation of acetyl CoA carboxylase	25
Hypothesis and Aims	28
-General Hypothesis	28
-Specific Hypotheses/Aims	29
CHAPTER 2: Materials and Methods	31
Introduction	32
Materials	33
Methods	35
-Fawn Hooded rat	35
-Acetyl CoA carboxylase 2 knockout mouse	35
-Ultrasound echocardiography	36
-Isolated working rat heart	37
-Isolated working mouse heart	38

-Measurement of mechanical function in isolated working hearts	38
-Measurement of Glycolysis, Glucose, Lactose, Palmitate Oxidation	39
-Calculation of proton production	40
-Calculation of total TCA acetyl CoA and ATP production	40
-Calculation of cardiac work, power, efficiency	41
-Acetyl CoA carboxylase activity assay	42
-Measurement of short chain CoA esters	42
-Measurement of triacylglycerol	43
-Immunoblot analysis	43
-Statistical analysis	45

CHAPTER 3: Acute Inhibition of Pyruvate Dehydrogenase 46

Kinase Improves the Cardiac Metabolic Profile in the Fawn

Hooded Rodent Model of Pulmonary Hypertension and Right

Ventricular Hypertrophy

Abstract 47

Introduction 49

Materials and Methods 51

Results 53

Discussion 77

CHAPTER 4: Absence of Acetyl Coenzyme A Carboxylase 2 80

in Mice Lowers Cardiac Efficiency During Aerobic Perfusion,

but Does Not Cause Ischemic Injury due to a Compensatory

Increase in Malonyl CoA

Abstract 81

Introduction 83

Materials and Methods 87

Results	89
Discussion	122
CHAPTER 5: Discussion and Conclusions	129
Final Conclusions	130
Future Directions	131
CHAPTER 6: References	133

List of Tables **Page Number**

Table 3-1: Ex vivo cardiac function in aerobically perfused SD and FH hearts in presence of vehicle or 1mM DCA. 66

Table 4-1: Ex vivo cardiac function in WT and ACC2 KO hearts during aerobic and post-ischemic phase of isolated working heart perfusions. 113

List of Figures	Page Number
Figure 1-1: Summary of myocardial energy metabolism and therapeutic targets.	27
Figure 3-1: FH rats manifest PAH, RVH and cardiac dysfunction.	57
Figure 3-2: Glucose oxidation is restored, while glycolysis decreases and proton production is normalized in FH hearts following acute DCA treatment.	60
Figure 3-3: Acute DCA treatment decreases fatty acid oxidation in FH hearts.	62
Figure 3-4: Acute DCA treatment increases total ATP and TCA acetyl CoA production in FH hearts with PAH and RVH.	64
Figure 3-5: Cardiac work in SD and FH hearts over 40 min of perfusion with vehicle or 1mM DCA.	68
Figure 3-6: PDK4 protein expression in RV of SD and FH hearts.	70
Figure 3-7: PDH β and PDK4 mRNA levels in RV of FH and SD hearts.	72
Figure 3-8: Chronic DCA treatment reverses PAH in FH hearts and improves cardiac output.	74
Figure 3-9: Chronic DCA treatment increases PDH activity, while decreasing PDK4 expression in FH hearts.	76

List of Figures	Page Number
Figure 4-1: Southern and Western blot analysis of ACC in WT and ACC2 KO tissue.	94
Figure 4-2: Glucose and palmitate oxidation in isolated working ACC2 KO and WT hearts aerobically perfused with or without insulin.	97
Figure 4-3: Cardiac work and efficiency in ACC2 KO and WT hearts during aerobic perfusion with or without insulin.	99
Figure 4-4: Short chain CoA analysis of aerobically perfused ACC2 KO and WT heart tissue.	101
Figure 4-5: Cardiac energy metabolism in ACC2 KO and WT isolated working hearts during aerobic and reperfusion periods.	103
Figure 4-6: ATP and TCA acetyl CoA production in isolated working ACC2 KO and WT hearts during aerobic and reperfusion periods.	107
Figure 4-7: Ex vivo function in isolated working KO and WT hearts during aerobic perfusion and following ischemia-reperfusion.	110
Figure 4-8: ACC activity, short chain CoA and triacylglycerol levels in cardiac tissue of ACC2 KO and WT mice following ischemia/reperfusion.	115
Figure 4-9: P-AMPK protein expression in ACC2 KO and WT cardiac tissue.	117

Figure 4-10: P-PDH protein expression in ACC2 KO and WT 119

cardiac tissue.

Figure 4-11: MCD protein expression in ACC2 KO and WT 121

cardiac tissue.

List of Abbreviations

-/-	knock out/deficient
+/-	heterozygous
+/+	wild type
3-KAT	3-keto acyl CoA thiolase
ACC	acetyl CoA carboxylase
ADP	adenosine diphosphate
AMI	acute myocardial infarction
AMP	adenosine monophosphate
AMPK	5'-AMP activated protein kinase
AMPKK	AMPK kinase
ANOVA	analysis of variance
ATP	adenosine triphosphate
AU	arbitrary units
BSA	bovine serum albumin
Ca ²⁺	calcium ion
CACT	carnitine acylcarnitine translocase
CAT	carnitine acetyltransferase
CO ₂	carbon dioxide
CO	cardiac output
CoA	coenzyme A
CPT	carnitine palmitoyl transferase
CTR	control
CVD	cardiovascular disease
<i>db/db</i>	leptin receptor deficient
DCA	dichloroacetate
DIO	diet-induced obesity
DNA	deoxyribonucleic acid
DTT	dithiothreitol
EDTA	ethylenediaminetetraacetic acid
EGTA	ethylene glycol tetraacetic acid
ETC	electron transport chain
FABP	fatty acid binding protein
FACS	fatty acyl CoA synthetase
FAD/FADH ₂	flavin adenine dinucleotide
FAO	fatty acid oxidation
FAS	fatty acid synthase
FAT/CD36	fatty acid translocase
FATP	fatty acid transport protein
FDG	2-fluoro-2-deoxy-D-glucose
FFA	free fatty acid
FHR	Fawn Hooded rat
FOXO-1	forkhead transcription factor
GLUT	glucose transporter
H ⁺	proton

HbA1c	glycosylated hemoglobin
HIF	hypoxia-inducible factor
HPLC	high performance liquid chromatography
hr	hour(s)
HR	heart rate
IC ₅₀	inhibitory concentration
IHD	ischemic heart disease
I/R	ischemia reperfusion
kDa	kilo Daltons
KO	knock out
K _v	voltage-gated potassium channel
LDH	lactate dehydrogenase
LV	left ventricle/left ventricular
MEDICA16	β, β, β', β'-tetramethylhexadecanoic acid
MCAD	medium-chain acyl CoA dehydrogenase
MCD	malonyl CoA decarboxylase
min	minute(s)
mRNA	messenger ribonucleic acid
NAD ⁺ /NADH	nicotinamide adenine dinucleotide
NCX	sodium-calcium exchanger
NHE	sodium-hydrogen exchanger
<i>ob/ob</i>	leptin deficient
Pa	Pascal
PA	pulmonary artery
PAAT	pulmonary artery acceleration time
PAB	pulmonary artery banding
PAH	pulmonary arterial hypertension
PaO ₂	partial pressure of oxygen
PASMC	pulmonary artery smooth muscle cells
PCR	polymerase chain reaction
PDH	pyruvate dehydrogenase
PDHK	pyruvate dehydrogenase kinase
PDK	pyruvate dehydrogenase kinase
PFK	phosphofructokinase
PPAR	peroxisome proliferator activated receptor
RNA	ribonucleic acid
ROS	reactive oxygen species
rpm	revolutions per minute
RT-PCR	real-time PCR
RV	right ventricle/right ventricular
RVF	right ventricular failure
RVH	right ventricular hypertrophy
S	septum
SD	Sprague Dawley
SOD	superoxide dismutase
SDS	sodium dodecylsulfate

SDS-PAGE	SDS polyacrylamide gel electrophoresis
sec	second(s)
SEM	standard error of mean
TAG	triacylglycerol
TCA	tricarboxylic acid
TOFA	5-(tetradecyloxy)-2-furan-carboxylic acid
U	unit
UPLC	Ultra performance liquid chromatography
VO ₂	oxygen consumption
v/v	volume/volume
wt	weight
WT	wild type
w/v	weight/volume

CHAPTER 1.

Introduction

CHAPTER 1

Introduction

Cardiovascular disease (CVD) is a broad term that describes a host of conditions affecting the heart and the vasculature such as coronary artery disease, peripheral arterial disease, cerebrovascular disease, and congenital heart disease (1). According to the World Health Organization, CVD is the leading cause of death globally and is estimated to claim the lives of 25 million people worldwide annually by 2030 (2). Since it is no longer exclusive to developed countries, CVD presents a global challenge. As concerns mount over the burden that CVD will have on the healthcare system, there is a pressing need for novel therapeutic strategies to effectively manage this pandemic. One emerging approach to treating CVD is to optimize energy metabolism in the heart. Conventional therapies for CVD mainly focus on the coronary circulation often with the aim of improving oxygen supply (i.e. coronary blood flow), or by decreasing oxygen demand of the heart (3). Optimizing cardiac metabolism could involve improving energy supply to the heart, or improving energetics in the myocardium to increase cardiac efficiency and improve cardiac outcomes.

Energy Metabolism in the Heart

The heart is a metabolically-demanding organ requiring rapid turnover of adenosine triphosphate (ATP) to maintain proper contractile and cellular function. In a normal healthy and aerobic heart, the majority (>90%) of this ATP is generated from mitochondrial oxidative phosphorylation, with the remainder

(~10%) derived from glycolysis (4). The main substrates for oxidation include carbohydrates such as glucose and lactate, as well as the fatty acids (mainly palmitate and oleate). However, fatty acids, particularly long-chain, are preferred due to their high ATP yield (5). In fact, fatty acid oxidation accounts for 60-90% of the total myocardial aerobic ATP and is therefore the major source of fuel for the heart (6).

Normal myocardial energy metabolism ensures optimal cardiac function and efficiency; therefore, any disturbance to the metabolic pathway can adversely affect the heart and contribute to cardiac pathologies such as ischemic heart disease and pulmonary arterial hypertension.

Myocardial Fatty Acid Metabolism

Fatty acid uptake into the cardiac myocyte

Fatty acids are delivered to the heart as either free fatty acids bound to albumin or are released from circulating triacylglycerol (TAG) contained in lipoproteins by virtue of lipoprotein lipase (7). Fatty acids can subsequently enter the cardiac myocyte either by passive diffusion or by protein carriers including fatty acid translocase (FAT)/CD36 (responsible for majority of fatty acid import into the cardiac cell) and fatty acid transport protein (FATP) (7). Under normal physiological conditions, the free fatty acid concentration in the plasma ranges from 0.2 to 0.6 mM, but can dramatically increase during times of myocardial distress, or in obese and diabetic individuals (8). In order for fatty acids to be

oxidized, they must first be transported into the mitochondrial matrix from the cytosol of the cardiac myocyte. Short and medium-chain fatty acids, such as propionic and caproic acid respectively, can easily cross the mitochondrial membranes by passive diffusion. Long-chain fatty acids (palmitate, oleate), however, require a specific transport mechanism: the carnitine-dependent system (9).

The carnitine-dependent transport system consists of three enzymes: carnitine palmitoyltransferase 1 (CPT1), carnitine acylcarnitine translocase (CACT), and carnitine palmitoyltransferase 2 (CPT2) (Figure 1-1) (10). L-carnitine, often considered a “vitamin” for the heart, is essential for the functioning of all three enzymes (11). It is a simple quaternary ammonium compound stored primarily in cardiac muscle following synthesis in the liver and/or kidneys from lysine and methionine (11). The combined efforts of carnitine and these enzymes allow long-chain fatty acids to be oxidized in the mitochondrial matrix to generate energy.

Before long-chain fatty acids can be transported into the matrix, they must be activated in the cytosol by fatty acyl coenzyme A (CoA) synthetase (FACS) (10,12). This enzyme is a transmembrane protein associated with the outer mitochondrial membrane (12,13). Its active site is exposed to the cytosol and it catalyzes the formation of long-chain fatty acyl CoA esters from CoA and long-chain fatty acids (10). Depending on the energy demand, these fatty acyl esters can either be converted to triacylglycerol, membrane phospholipids, or transported into the mitochondria (10). Under normal physiological conditions,

the majority of these activated fatty acids are shuttled to the mitochondria for oxidation (14). However, the mitochondrial inner membrane is impermeable to these long-chain acyl CoA esters, and in order to access the matrix, the carnitine transport system is required (15). Short and medium chain fatty acids, on the other hand, can easily permeate the mitochondrial membrane without the transport system as they are activated to acyl CoA esters in the matrix (13,15).

The carnitine shuttle

Each enzyme of the carnitine transport system has a distinct location and role in transporting fatty acids into the mitochondria. CPT1 catalyzes the first step in the mitochondrial uptake of long-chain fatty acids. There are a few isoforms of this enzyme produced by different genes: liver-CPT1, muscle-CPT1, and CPT1C (mainly expressed in the brain) (15). The muscle isoform predominates in both cardiac and skeletal muscle (15). The muscle-CPT1 is an 82 kDa integral membrane protein with two transmembrane domains located in the mitochondrial outer membrane (12). The catalytic site of CPT1 is found in the intermembrane space and is responsible for transferring the long-chain fatty acyl group from CoA to L-carnitine, thereby generating free CoA and long-chain fatty acylcarnitine (16).

The next step in fatty acid transport is catalyzed by the second enzyme in the carnitine pathway, CACT. It is an integral inner membrane protein that transports long-chain fatty acylcarnitine across the inner mitochondrial membrane

in a 1:1 exchange for free carnitine (returns to extramitochondrial space for reuse) (10,13,17).

CPT2, the third enzyme in the system, is a 70 kDa peripheral protein anchored to the matrix side of the inner membrane (12). It regenerates the long-chain fatty acyl CoAs from long-chain acyl carnitine. This final enzymatic reaction is carried out in the matrix and completes the transport of long-chain fatty acids to the mitochondria, allowing the fatty acyl CoAs to enter the β -oxidation spiral for metabolism (17).

Fatty acid β -oxidation

Fatty acid β -oxidation converts fatty acyl CoA into acetyl CoA through a chain of reactions involving a series of enzymes: acyl CoA dehydrogenase, enoyl CoA hydratase, L-3-hydroxyacyl CoA dehydrogenase, and 3-ketoacyl CoA thiolase (3-KAT) (8). Each cycle nets one molecule of acetyl CoA, which enters the tricarboxylic acid cycle (TCA) to produce flavin adenine dinucleotide (FADH₂) and nicotinamide adenine dinucleotide (NADH) (8). These intermediates then enter the electron transport chain (ETC) to produce the energy currency ATP.

Regulation of fatty acid metabolism

Overall, the carnitine system plays a critical role in cardiac metabolism by facilitating fatty acid oxidation. Of all the components in the system, CPT1 is by far the most significant. It is a key intracellular regulator of fatty acid oxidation by catalyzing the rate-limiting step in mitochondrial fatty acid uptake and consequently committing fatty acids to oxidation (18,19). However, CPT1 is subject to extensive regulation through several direct and indirect pathways.

Malonyl CoA is a potent endogenous CPT1 inhibitor, which binds allosterically to the cytosolic side of the enzyme, distinct from the fatty acyl CoA binding site (4,6). The muscle-CPT1, in particular, is 30-fold more sensitive to this inhibition compared to the liver isoform (6). As a reversible CPT1 inhibitor, malonyl CoA regulates fatty acid metabolism by suppressing fatty acid uptake into the mitochondria. In the heart, the cytosolic concentration of malonyl CoA is approximately 5 μM , while the IC_{50} of CPT1 inhibition lies between 50 and 100 nM (4). However, the majority of this inhibitor is inaccessible to CPT1 since fatty acid oxidation would be completely inhibited if all of the malonyl CoA were available (4). The mechanism for this inaccessibility/compartimentalization is unknown and studies are currently underway to fully elucidate this phenomenon. Regardless, malonyl CoA has a rapid turnover and relatively short half-life of 1.25 min (15). Its synthesis and degradation is important in determining its levels and consequent rate of fatty acid oxidation.

Malonyl CoA is formed from the carboxylation of acetyl CoA by acetyl CoA carboxylase (ACC) (20). ACC exists in two isoforms in the heart as α (1) and β (2); the alpha isoform is primarily involved in fatty acid biosynthesis, while ACC β /2 is responsible for regulating fatty acid oxidation by synthesizing malonyl CoA (16). ACC β /2 is itself regulated by 5'-adenosine monophosphate-activated protein kinase (AMPK), a serine-threonine kinase, often dubbed as “fuel-sensing kinase” which phosphorylates ACC on the serine 221 residue, rendering it inactive (21). Furthermore, malonyl CoA is degraded to acetyl CoA and carbon dioxide by malonyl CoA decarboxylase (MCD), an enzyme found in mitochondria, peroxisomes, and cytosol (4,6). MCD directly regulates the levels of malonyl CoA, and therefore indirectly regulates CPT1 activity and fatty acid oxidation. When MCD is elevated, malonyl CoA levels decrease thereby increasing fatty acid oxidation, whereas the opposite phenomenon occurs when ACC activity is increased. Apart from regulating fatty acid oxidation at the molecular level, new insights have shown that regulation at the gene level is also possible.

Control of fatty acid oxidation at the transcriptional level is carried out by peroxisome proliferator-activated receptor alpha (PPAR α), a ligand-activated transcription factor part of the nuclear receptor superfamily (22). It binds to PPAR response elements in target genes as a heterodimer along with the retinoid X receptor. PPAR α , which is activated by long-chain fatty acids, regulates the expression of certain proteins involved in fatty acid uptake and oxidation such as CD36, FACS, CPT1, and medium-chain acyl CoA dehydrogenase (MCAD) (22).

Studies have found that PPAR α deficient mice have low levels of MCD, but high levels of malonyl CoA, suggesting that PPAR α plays a role in facilitating fatty acid oxidation (23).

Myocardial Glucose Metabolism

Glucose uptake into the cardiac myocyte

Glucose is taken up into the cardiac myocyte via action of glucose (GLUT) transporters, specifically subtypes 1 and 4. GLUT1 is constitutively active, whereas GLUT4 is translocated to the cell membrane in response to insulin or increased work/demand (8).

Glycolysis

Upon entering the cytosol, glucose is phosphorylated by hexokinase into glucose-6-phosphate and is subsequently converted into two pyruvate molecules in a process known as glycolysis (24). In anaerobic conditions, non-oxidative disposal of glycolytically derived pyruvate results in lactate and protons. Under normal physiological conditions, the heart is able to convert lactate into pyruvate by lactate dehydrogenase; however, in times of oxidative stress lactate and protons accumulate, compromising cardiac efficiency and function (see *Ischemic heart disease*) (24).

Glucose oxidation

Under normal aerobic conditions, pyruvate is shuttled into the mitochondria, where it is converted into acetyl CoA by pyruvate dehydrogenase (PDH), the rate-limiting enzyme of glucose oxidation (24). This acetyl CoA then enters the TCA cycle to eventually produce ATP via the ETC, as described previously.

Regulation of glucose metabolism

Pyruvate dehydrogenase (PDH), the rate-limiting enzyme of glucose oxidation, is regulated by pyruvate dehydrogenase kinase (PDHK/PDK). There are four isoforms of PDHK with the PDHK4 isoform predominately expressed in heart and skeletal muscle (25). Acetyl CoA and NADH can feedback to inhibit PDH by activating PDHK, which phosphorylates and inhibits PDH, thereby halting glucose oxidation (25). PDHK will become important when looking at certain disease states such as pulmonary arterial hypertension (discussed later).

The Randle Cycle

Sir Philip Randle was first to describe a reciprocal relationship between fatty acid and glucose metabolism known as the “glucose-fatty acid cycle” in 1963. The cycle has been shown to operate in the heart where the ratio of acetyl CoA/CoA and NADH/NAD increases through fatty acid oxidation resulting in

PDH (and therefore glucose oxidation) being inhibited via PDHK activation (26). Ultimately, the heart is able suppress glucose oxidation in response to elevated rates of fatty acid oxidation. However, this can inadvertently compromise cardiac function, especially in ischemic heart disease.

Energy Metabolism in the Diseased Heart

Ischemic heart disease

Ischemic heart disease is the most common form of CVD and is often the underlying cause of angina, acute myocardial infarction, and heart failure (4). Ischemia is characterized by a reduced coronary blood flow (as a result of stenosis) that is unable to adequately meet the oxygen demands of the heart (27). During ischemia, the rate of glycolysis increases in order to generate ATP anaerobically and compensate for the reduced oxidative ATP production (4). This increase in glycolysis persists into reperfusion. Oxidative phosphorylation is not completely halted during ischemia; in fact, fatty acid oxidation dominates as the source of any remaining oxidative phosphorylation and accounts for more than 90% of the energy production in the reperfused heart (6). This increase in fatty acid oxidation is partly due to the rapid activation of AMPK during periods of stress, combined with an increase in levels of fatty acids during ischemia and reperfusion (8). As mentioned earlier, AMPK inactivates ACC and decreases cytosolic malonyl CoA levels. MCD activity, however, is unchanged during ischemia/reperfusion and thus continues to degrade malonyl CoA so the levels are

even further reduced (4). During ischemia and reperfusion, the heart is also exposed to high levels of fatty acids. This is due to the release of catecholamines that stimulate the release of fatty acids from adipose tissue (lipolysis) (3). In the presence of low malonyl CoA levels combined with the high level of fatty acids, CPT1 activity increases as well as fatty acid oxidation. This is undesirable at a time of oxygen shortage since fatty acids require approximately 10% more oxygen than carbohydrates to produce equal amounts of ATP (4). Furthermore, fatty acid oxidation inhibits glucose oxidation (via Randle Cycle), thereby uncoupling glucose oxidation from glycolysis. The uncoupling eventually leads to a proton overload and intracellular acidosis due to the hydrolysis of glycolytically derived ATP (28). The build-up of protons in the myocyte activates the sodium-hydrogen exchanger (NHE), which will then attempt to extrude excess protons in exchange for sodium (29). As sodium levels rise in the cardiac myocyte, the sodium-calcium exchanger (NCX) reverses in attempt to expel excess sodium in exchange for calcium (29). Thus, as the heart expends energy to maintain ion homeostasis rather than to maintain proper contractile function, cardiac efficiency (i.e. cardiac work/oxygen consumed) dwindles, and the risk for ischemic injury increases as calcium and sodium ions accumulate. Even once coronary flow is restored, cardiac work recovers to a lesser extent than oxygen consumption (30). Myocardial ischemia is a prime example of how alterations in metabolism can compromise heart function.

Pulmonary arterial hypertension

Pulmonary arterial hypertension (PAH) is a lethal disease characterized by a progressive increase in pulmonary arterial (PA) pressure. This elevation in PA pressure is caused by either excessive proliferation and impaired apoptosis of pulmonary artery smooth muscle cells (PASMC), endothelial dysfunction, inflammation, and/or vasoconstriction (31). PAH typically affects individuals between 30 and 50 years with mortality approximately 50% at five years (32). PAH can occur idiopathically, but commonly occurs secondary to connective tissue disease, pulmonary embolism, emphysema, congenital heart disease, or left-sided heart failure (32). Ultimately, the increased afterload on the right ventricle leads to compensatory right ventricle hypertrophy (RVH), which is further complicated by ischemia and contractile dysfunction. Gomez *et al.*, studied patients with PAH and found that the degree of dysfunction in the RV strongly correlates with the degree of ischemia (33). The etiology of this ischemia is still being investigated, however it has been postulated to be the result of either reduced coronary perfusion pressure or loss of small blood vessels (34). Eventually, the right ventricle becomes decompensated and leads to right ventricular failure, which is the major cause of mortality in PAH patients (34).

Aside from the physiological changes in the vasculature, recent studies have implicated a metabolic switch in the pathophysiology of PAH. Specifically, there is a tendency towards increased glycolysis and decreased glucose oxidation (35), characteristic of the Warburg effect (35). The Warburg effect was first used in 1956 by Otto Warburg to describe metabolism in cancerous cells, which

exhibited elevated rates of glycolysis and lactate fermentation compared to normal cells (36). Similarly, the right ventricle reverts to this fetal metabolic profile in the setting of PAH and PAH patients undergoing positron emission tomography scans have exhibited increased 2-fluoro-2-deoxy-D-glucose (FDG) uptake in the right ventricle (37). At the molecular level, these metabolic changes have been associated with abnormal mitochondrial function resulting in the activation of hypoxia-inducible factor-1 α (HIF-1 α), a transcription factor that regulates the transcription of glycolytic genes (i.e. hexokinase, lactate dehydrogenase kinase and GLUT1) and an increase in expression of PDHK, a potent inhibitor of glucose oxidation (31,32).

Numerous groups have studied pulmonary hypertension using different models of the disease ranging from monocrotaline, pulmonary artery banding (PAB), or a specific genetic model of PAH, the Fawn Hooded rat (FHR). Monocrotaline, a pyrrolizidine alkaloid, has been extensively used in animal models to induce PAH. A single subcutaneous injection (60 mg/kg) of the compound is capable of damaging the pulmonary vasculature and producing PAH and RVH in Sprague Dawley (SD) rats after one month (31). In a study by Piao *et al.*, monocrotaline-induced PAH was associated with increased thickness of the right ventricular free wall and reduced RV systolic function. Furthermore, metabolic data demonstrated higher glycolytic rates in the right ventricle as well as higher FDG uptake and lower oxygen consumption. These metabolic changes were accompanied by increased expression of GLUT1 in the cytosol and plasma membrane as well as increased phosphorylation of PDH (31). In the PAB model,

RVH is produced secondary to an elevation in pulmonary artery pressure. This occurs in the absence of any vascular changes, but like monocrotaline is associated with a glycolytic shift, reduction in cardiac output and increase in GLUT1 (31).

The FHR is a strain that spontaneously develops PAH due to abnormalities in chromosome 1. The autosomal recessive disease in this animal model is characterized by high endothelin levels, increased serotonin-induced vasoconstriction, a platelet storage pool disorder, and abnormal PASMC vasoconstriction (38-40). By 40 weeks of age these rats develop PAH, progressing to RVH despite normal systemic blood pressure and partial pressure of oxygen (PaO_2) (41). These changes are a consequence of mitochondrial dysfunction in the PASMC where oxidative function is compromised. The PASMC in the FHR exhibit decreased expression/activity of mitochondrial components superoxide dismutase-2 (SOD-2) and ETC complex I (32). This abnormality has also been documented in pulmonary arteries isolated from PAH patients. SOD-2 is an intramitochondrial antioxidant enzyme that is responsible for converting reactive oxygen species (ROS), superoxide, into hydrogen peroxide. Under normal respiratory conditions, ROS are routinely scavenged by mitochondrial SOD-2; however, in PAH this cycle is disrupted leading to adverse downstream effects. Typically, the product of this reaction, hydrogen peroxide, regulates the activity of redox-sensitive transcription factors HIF-1 α and expression of potassium (Kv) channels. However, in PAH, due to a mitochondrial defect a low ROS or “hypoxia-like” environment is created which triggers the activation of HIF-1 α .

and downregulation of Kv channels (32). The downregulation of Kv channels results in depolarized membrane potential and ultimately activates L-type calcium channels, leading to increased calcium influx and vasoconstriction of the PA (32). On the other hand, the activation of HIF-1 α shifts the heart away from energy rich oxidative metabolism to glycolysis through activation of glycolytic genes and inhibition of glucose oxidation via PDHK (32).

Pulmonary hypertension patients exhibit poor cardiac function as a result of RVH and the heart's increased reliance on glycolytic metabolism. Subcellular changes result in inhibition of glucose oxidation and acceleration of glycolysis. This combination is not only detrimental to the heart but also compromises its efficiency and is associated with impairment of RV function. In the normal heart, as glucose is imported to the cardiac myocyte it is converted into pyruvate, which is shuttled into the mitochondria to PDH for glucose oxidation. However, in PAH patients the uncoupling of glucose oxidation from glycolysis results in pyruvate build-up in the cytosol and its conversion to lactate. This results in a net of two ATP molecules/glucose rather than the complete 36 or 38 from glucose oxidation (8). As described above, this uncoupling eventually leads to a proton overload and cation overload that in combination with the low ATP yield plummets cardiac efficiency.

Metabolic Approach to Heart Disease

Recently, a number of studies have suggested that a novel approach to treating CVD is by means of metabolic modulation, whereby optimizing

energetics in the myocardium can improve cardiac efficiency of the heart muscle (i.e. increase the contractile work achieved per molecule of oxygen consumed). To restore cardiac efficiency, current therapeutic strategies have focused on inhibiting fatty acid oxidation and/or stimulating glucose oxidation. This emerging approach holds the promise of providing added benefit when used alongside existing therapies.

Pharmacological targets in cardiac energy metabolism

There are several pharmacological targets in the cardiac metabolic pathway that have been studied as a potential site for optimizing energy metabolism; such as CPT1, MCD, 3-KAT, AMPK, and PPAR α .

A direct approach to the modulation of fatty acid metabolism is to regulate the import of fatty acids into the mitochondria. CPT1 catalyzes the rate-limiting step in the mitochondrial uptake of long-chain fatty acids (4). This enzyme has become the target of several pharmacological agents known as CPT1 inhibitors, including etomoxir, oxfenicine, and perhexiline (42,43). All three decrease CPT1 activity and thus limit fatty acid oxidation while favoring glucose oxidation (via the Randle Cycle) (42). In animal studies, etomoxir has demonstrated favorable outcomes. Lopaschuk *et al.* (44) showed that etomoxir improved glucose oxidation and cardiac function while protecting the heart from injury after ischemia-reperfusion (I/R). In a separate study, etomoxir was found to reduce myocardial oxygen consumption while sustaining contractile function in ischemic

rat hearts (43,45). Although studies using etomoxir in animals are extensive, epidemiological studies have been limited to a few clinical trials. In one open-label and uncontrolled study, etomoxir was found to improve left ventricular ejection fraction, cardiac output at peak exercise, and clinical status in patients with New York Heart Association Class II–III heart failure (43,46), but the Etomoxir for the Recovery of Glucose Oxidation (ERGO) study was terminated prematurely because of toxicities resulting from irreversible effects on fatty acid oxidation (47). Although etomoxir has been investigated as a treatment for heart failure, its antianginal properties remain to be evaluated. In contrast, perhexiline was introduced in the 1970s as an antianginal agent effective in improving anginal symptoms and increasing exercise tolerance (48). Furthermore, the findings of recent studies have supported its suitability for the treatment of angina pectoris and heart failure, in addition to short-term therapy for ischemia (43). A randomized control trial consisting of 56 patients with heart failure receiving 8 weeks of treatment led to the conclusion that perhexiline was associated with an improved left ventricular ejection fraction and peak oxygen uptake ($VO_2\text{max}$) (49). Although perhexiline may have clinical benefit, its use in treating CVD is limited.

Another approach to inhibiting CPT1 and decreasing mitochondrial fatty acid uptake is via inhibition of MCD. MCD is responsible for degrading malonyl CoA, a potent endogenous reversible inhibitor of CPT1 (4). Several experimental studies have found that pharmacological MCD inhibitors increase malonyl CoA concentrations in the heart, thereby indirectly inhibiting CPT1 and decreasing

fatty acid oxidation (50,51). Stanley *et al.* (52) reported that inhibition of MCD by CBM-301940 was associated with a four-fold increase in malonyl CoA concentration, an 87% decrease in the rate of fatty acid oxidation, and a 50% decrease in lactate production. In a study by Dyck *et al.*, (50) MCD knockout mice demonstrated a lower rate of fatty acid oxidation, greater glucose oxidation, and overall improved cardiac function during and after ischemia. These findings suggest that the inhibition of MCD may be a feasible approach to optimizing energy metabolism and may have potential in the treatment of heart disease. However, clinical studies using this approach have yet to be performed.

Direct inhibition of fatty acid oxidation can be achieved by targeting enzymes in the β -oxidative pathway, particularly long-chain 3-KAT. Trimetazidine is a 3-KAT inhibitor that reduces fatty acid oxidation while promoting glucose oxidation via the Randle Cycle (53). The Trimetazidine in Angina Combination Therapy (TACT) study showed that trimetazidine, in conjunction with long-acting nitrates or β -blockers, improved exercise test duration and anginal symptoms (54). Recently, the Cochrane Collaboration conducted a review of randomized studies comparing trimetazidine with placebo or other antianginal drugs in adults with stable angina (55). This meta-analysis led to the conclusion that trimetazidine is effective in the treatment of stable angina when compared with placebo, alone or combined with conventional antianginal agents, and that trimetazidine may result in fewer failures to continue treatment as a result of adverse events. Furthermore, in the Second Trimetazidine in Poland (TRIMPOL II) study, trimetazidine improved workload, time to 1 mm ST-

segment depression, and anginal symptoms in patients already receiving metoprolol, and was beneficial even after percutaneous coronary intervention (56). A number of studies have shown that trimetazidine can also improve the symptoms of heart failure (57). Currently, trimetazidine is the most common metabolic agent prescribed worldwide to treat CVD, and is available in Europe and more than 80 countries worldwide (58). Ranolazine is an antianginal agent recently approved in the United States for treating chronic stable angina (42). It is structurally similar to trimetazidine and, although substantially less potent than trimetazidine, at clinically relevant concentrations ranolazine partially inhibits fatty acid oxidation while stimulating glucose oxidation under normoxic and ischemic conditions (59). Although the mechanism of action remains under investigation, the therapeutic effect of ranolazine on metabolism may be mediated via inhibition of 3-KAT (43). However, the findings of recent studies suggest that its cardioprotective effects may also be attributable to inhibition of the late sodium current, thereby preventing the sodium-dependent calcium overload that is characteristic of ischemic injury (60). Support for a metabolic mechanism of action comes from a recent study in which it was shown that ranolazine significantly improved glycosylated hemoglobin A (HbA1c) concentrations and recurrent ischemia in patients with diabetes mellitus, and reduced the incidence of increased HbA1c in those without evidence of previous hyperglycemia (61). The anti-ischemic effects of ranolazine have been established in numerous experimental studies (62-64). In an animal model of heart failure, for example, ranolazine increased both ejection fraction and mechanical function without

increasing oxygen consumption (63). In clinical settings, ranolazine has demonstrated favorable cardiac outcomes in patients with angina. The Monotherapy Assessment of Ranolazine in Stable Angina (MARISA) study revealed a significant increase in exercise duration and time to 1 mm ST-segment depression with ranolazine (65). The Efficacy of Ranolazine in Chronic Angina (ERICA) trial also found that, compared with placebo, ranolazine significantly reduced the frequency of angina episodes and consumption of glyceryl trinitrate in patients already receiving the maximum recommended dose of amlodipine (66). In the Metabolic Efficiency with Ranolazine for Less Ischemia in Non-ST-Segment Elevation Acute Coronary Syndromes (MERLIN-TIMI) trial, ranolazine was effective in reducing recurrent ischemic episodes and angina, but not acute myocardial infarction and death in patients with ischemic heart disease (67). Ranolazine is an effective antianginal agent, yet it remains to be clarified whether its cardioprotective effects against ischemia are mediated by metabolic or electrophysiological changes, or both.

AMPK is another pharmacological target for metabolic modulation. By inhibiting AMPK, ACC will no longer be inactivated and can continue to produce malonyl CoA to inhibit CPT1. However, a study using a mouse model with a dominant negative AMPK mutation found that the reperfused hearts had poor recovery following low-flow ischemia (68). There was reduced recovery of left ventricular contractile function and increased levels of intracellular enzymes such as creatine kinase and lactate dehydrogenase, markers of myocardial membrane damage and necrosis (68). Yet, in the reperfused AMPK-deficient hearts, fatty

acid oxidation was lower and glucose oxidation was higher compared to wild type reperfused hearts (68). Although these findings suggest that AMPK is important in regulating metabolism, it also has a cardioprotective role in preventing necrosis and myocardial injury (68). Currently, AMPK has a controversial role in heart and further studies are needed before a therapy can be implemented.

At the transcriptional level, PPAR α indirectly regulates fatty acid oxidation. A study by Yue *et al.* found ischemia/reperfusion downregulated PPAR α expression and its regulated genes such as CPT1 and MCAD (22). As a result, there was an increase in glucose oxidation from 12% in control to 42% in ischemic/reperfused hearts and a reduction in fatty acid oxidation from 88% to 58%. After administering the PPAR α agonist GW7647 to these same hearts, glucose oxidation decreased to 20%, while fatty acid oxidation increased to 79% (22). Furthermore, studies using a PPAR α agonist have been associated with poor post-ischemic recovery and efficiency. The downregulation of PPAR α , during ischemia, likely serves a cardioprotective role by switching to a more efficient fuel source. However, the same study also found that activation of PPAR by GW7647 is associated with decreased release of pro-inflammatory cytokines and a reduction in neutrophil accumulation, which is responsible for reperfusion injury. PPAR activation and inhibition both have beneficial effects on the heart, but more study is needed to delineate its role in metabolic modulation.

The fundamental concept behind each therapeutic strategy is to regulate myocardial energy metabolism. All the approaches discussed above ultimately

target the cardiac metabolic pathway to improve the energetics and function of the heart.

This thesis will focus on the metabolic modulation of two key enzymes in the glucose and fatty acid oxidative pathways, PDHK and ACC.

Metabolic modulation of pyruvate dehydrogenase kinase (PDHK)

As previously described, PAH studies have reported an increase in PDHK expression and subsequent decrease in glucose oxidation. Therefore, this shift in energy metabolism can be offset through metabolic modulation. Glucose oxidation can be directly stimulated with the PDHK inhibitor dichloroacetate (DCA) (69). DCA is a readily available compound, which garnered international attention following the discovery of its anti-cancer properties. Currently, DCA is used to treat metabolic disorders such as lactic acidosis and more recently it has been studied in PAH. Numerous *in vitro* and *in vivo* studies have documented that activation of PDH with DCA increases glucose oxidation, shifting the energy metabolism to an efficient fuel source. Furthermore, DCA improves coupling between glycolysis and glucose oxidation, minimizing intracellular acidosis and contractile dysfunction (25,69).

DCA has been reported to restore mitochondrial function and metabolism in PAH studies. In the FH rat chronic oral treatment was able to reverse PASMC proliferation, inactivate HIF-1 α , and upregulate Kv channel expression. In monocrotaline-induced PAH, chronic DCA treatment with 0.75 g/L (dose

commonly used in human metabolic disorders) reversed RVH and PASMC remodeling (31). In both human and FHR PASMC, DCA treatment resulted in the inhibition of HIF-1 α , and increased both SOD-2 activity and Kv1.5 expression (32). In PAB-RVH, DCA improved cardiac output, but this effect was only 1/3 of that observed in the monocrotaline model (31). The larger effect of DCA in this latter model suggests DCA has beneficial effects on both the pulmonary vasculature and the hypertrophied RV.

Shortly after oral administration in humans, DCA is quickly and extensively absorbed with peak plasma concentrations being achieved in 15 to 30 minutes (70). Furthermore, animal studies have demonstrated that PDH complex activity is significantly stimulated within 15 to 30 minutes of oral, subcutaneous or intravenous dosing (70). Dichloroacetate is minimally bound to plasma proteins and equally distributed to liver and muscle tissue. The distribution and plasma clearance of DCA varies according to species, age and repeated administration. For example, in SD rats following a single, oral dose of 50 mg/kg the plasma half-life of DCA was 0.6 hr and with repeated oral administration it increased to 3.0 hr (70). In healthy adult humans, DCA administered intravenously or orally (50 mg/kg) had an average plasma half-life of 2.7 hr (70). Overall, the half-life of DCA in rats and humans ranges from 0.3 to 3.5 hr and is prolonged with repeated administration (71). Dichloroacetate is believed to inhibit its own metabolism through an unknown mechanism, yet DCA levels do not increase proportionally with chronic administration, rather a plateau effect is observed (72).

Metabolic modulation of acetyl CoA carboxylase (ACC)

During and following ischemia, the heart's metabolic profile shifts to increased fatty acid oxidation and decreased glucose oxidation. This change contributes to contractile dysfunction and reduces cardiac efficiency. Therefore, optimizing cardiac metabolism is a possible treatment for IHD. One strategy is targeting ACC2, an enzyme that regulates fatty acid oxidation. ACC catalyzes the synthesis of malonyl CoA and is therefore a potential drug target in metabolic modulation. Currently, there are no pharmacological activators of ACC; however, there are nonselective ACC inhibitors such as 5-(tetradecyloxy)-2-furan-carboxylic acid (TOFA) and β , β , β' , β' -tetramethylhexadecanoic acid (MEDICA 16) which, once converted to their acyl CoA thioesters, allosterically inhibit ACC (73). In addition, the cyclohexanedione herbicides, alloxodim, clethodim, have demonstrated inhibition of ACC in rat cardiac tissue (74). Although these agents have inhibitory properties, their use in practice is limited due to lack of specificity and limited safety profile, respectively. Instead, an ACC2 knockout (KO) mouse has been developed that demonstrates increased fatty acid oxidation. This metabolic phenotype has been exploited for treating obesity and diabetes, but has not been studied in the heart. Specifically, the impact of ACC2 modulation in IHD, a common manifestation in obese, diabetic patients, will be examined.

Figure 1-1: *Summary of myocardial energy metabolism and therapeutic targets.*

ACC, acetyl CoA carboxylase; MCD, malonyl CoA decarboxylase; FAT/CD36, fatty acid translocase transporter; CPT1/2, carnitine palmitoyltransferase 1/2; PDH, pyruvate dehydrogenase; PDK, pyruvate dehydrogenase kinase; 3-KAT, 3-ketoacyl CoA thiolase.

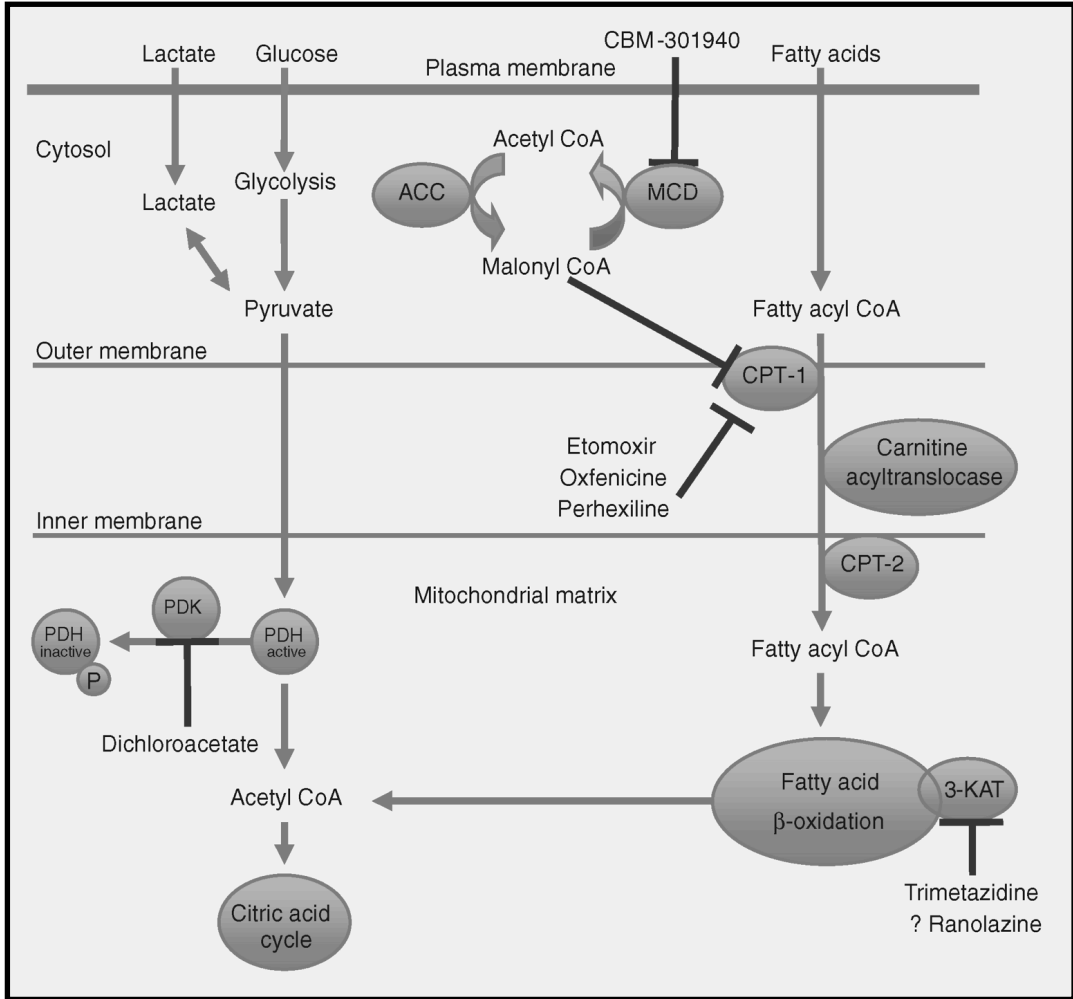


FIGURE 1-1

Hypothesis and Aims

General Hypothesis

The relative contribution of glucose and fatty acid oxidation to myocardial energy production dictates cardiac function and efficiency. Therefore, any disruption to the metabolic homeostasis can adversely affect the heart and contribute to cardiac pathologies. In the ischemic myocardium, fatty acid oxidation dominates as the residual source of oxidative phosphorylation and inhibits glucose oxidation. Whereas in PAH, the heart reverts to a glycolytic phenotype where glucose oxidation is uncoupled from glycolysis.

The premise for a metabolic intervention in PAH is to switch the energy substrate preference to glucose oxidation. By increasing glucose oxidation, the ischemic heart will produce less lactate and protons, thereby increasing cardiac efficiency. The energetics of the heart can be altered to favor this shift by the direct stimulation of glucose oxidation. One emerging therapy involves metabolic modulation to offset the changes seen in PAH in the FH rat by inhibiting PDHK. This enzyme is responsible for phosphorylating and inactivating the rate-limiting enzyme of glucose oxidation, PDH. A well-established and widely available PDHK inhibitor is DCA. DCA will increase mitochondrial oxidative phosphorylation, thereby improving the coupling of glucose oxidation to glycolysis, which may translate into improved cardiac function in PAH.

The goal of metabolic intervention in IHD is to decrease fatty acid oxidation and increase glucose oxidation (secondarily). In the ACC2 KO mouse

low levels of malonyl CoA translate into high rates of fatty acid oxidation. This metabolic phenotype is likely detrimental to cardiac function and efficiency in IHD. Increased fatty acid oxidation will inhibit glucose oxidation, eventually leading to accumulation of lactate and protons. Therefore, this “proof of principle” study will examine some of the cautions to metabolic modulation in the diseased heart.

Specific Hypothesis

The specific hypotheses of this thesis are located in the individual chapters for each study.

Specific Aim 1

To determine whether stimulating glucose oxidation with DCA can improve glucose oxidation-glycolysis coupling, and cardiac function in the FH rat. In this study, we will investigate the metabolic changes associated with RVH by using the FH rat model of spontaneous PAH. We will also assess the effects of the PDK inhibitor DCA, which stimulates glucose oxidation. We hypothesize that DCA restores glucose oxidation in RVH and may therefore improve cardiac function in PAH.

Specific Aim 2

To determine whether high rates of fatty acid oxidation impair recovery (cardiac function and efficiency) of the ACC2 KO heart following I/R. The ACC2 knockout mouse model, which is deficient in malonyl CoA, will be used to assess the effects of increased fatty acid oxidation on post-ischemic recovery of cardiac function.

CHAPTER 2.

Materials and Methods

CHAPTER 2

Materials and Methods

Introduction

The primary aim of this thesis is to examine cardiac metabolism and function in two different animal models, the Fawn Hooded rat (FHR) and the acetyl CoA carboxylase 2 knockout (ACC2 KO) mouse. Much of the methodology in this thesis involves measuring flux through cardiac metabolic pathways as well as cardiac function. *In vivo* function is also assessed by echocardiography. Furthermore, various *in vitro* protocols such as Western blotting, enzyme activity assays, TAG assay, and HPLC will be used to examine the expression of molecular components, measure ACC activity, assess lipid profile and CoA ester levels, respectively.

Materials

Radioisotopes [U-¹⁴C]glucose and D-[5-³H]glucose were obtained from Amersham Canada Ltd. (Oakville, Ontario); [9,10-³H]palmitic acid and [1-¹⁴C]palmitic acid were obtained from NEN Research Products (Boston, Massachusetts); L-[¹⁴C(U)]lactic acid was purchased from Perkin Elmer (Waltham, Massachusetts). Insulin (Novolin™ ge Toronto) was obtained via University of Alberta Hospital stores from Novo Nordisk (Mississauga, Ontario). Bovine serum albumin (BSA fraction V, fatty acid free) was obtained from Equitech-Bio Inc. (Kerrville, Texas). Ecolite™ Aqueous Counting Scintillation fluid was obtained from MP Biomedicals (Solon, Ohio). Hyamine hydroxide (1M in methanol solution) was obtained from NEN Research Products (Boston, Massachusetts). Dichloroacetate was purchased from Sigma-Aldrich (St. Louis, Missouri). Free fatty acid and triacylglycerol assay kits were obtained from Wako Pure Chemicals Industries Ltd. (Osaka, Japan). For HPLC analysis of short-chain CoA esters, an Ascentis Express C18, 2.7 µm particle size, 10 cm x 2.1 mm column was obtained from Supelco/Sigma-Aldrich (St. Louis, Missouri). ECL Supelcosil™ Western Blotting detection reagents were obtained from GE Healthcare (Piscataway, New Jersey) and Western Lighting® Chemiluminescence Reagent Plus was obtained from Perkin Elmer Life and Analytical Sciences (Woodbridge, Ontario). Trans-Blot® Transfer Medium (pure nitrocellulose) was obtained from BioRad (Richmond, California). FUJI Medical X-ray films were obtained from Mandel Scientific (Guelph, Ontario). Monoclonal and polyclonal primary and secondary antibodies were obtained from Jackson ImmunoResearch

Laboratories (West Grove, Pennsylvania), EMD Millipore (Billerica, Massachusetts), Cell Signaling Technology (Danvers, Massachusetts), Santa Cruz Biotechnology (Santa Cruz, California), Calbiochem (San Diego, California), Abgent (San Diego, California) or Abcam (Cambridge, Massachusetts). All other chemicals were purchased from Sigma-Aldrich (St. Louis, Missouri).

Methods

The University of Alberta adheres to the principles for biomedical research involving animals developed by the Council for International Organization of Medical Sciences and complies with the Canadian Council on Animal Care Guidelines. All animal protocols were approved by the University of Alberta Health Sciences Animal Welfare Committee.

Fawn Hooded Rat

Fawn Hooded rats, the genetic strain of PAH, were purchased from Charles River Laboratories International Inc. (Wilmington, Massachusetts). For the controls, age-matched Sprague Dawley rats were also obtained from Charles River Canada.

ACC2 Knockout Mouse

This mouse strain was generated by Dr. David Olson at Beth Israel Deaconess Medical Center Division of Endocrinology and Metabolism in Boston, Massachusetts, as previously described (75).

Genotyping was conducted using tail DNA with Dneasy Blood and Tissue Kit from Qiagen. Polymerase chain reaction was performed using PCR kit from TaKaRa and primers from IDT Technologies, as previously described (75). Southern blotting was conducted to confirm the genotype. The ACC2 KO band is represented at 425bp and WT band at 350bp. The genotyping strategy was based on primers flanking the 5'-lox P site and a reverse primer distal to the 3'-lox P site:

5'-forward primer (P1): TGGTGGCTCCATAATTTGTGGG;

5'-reverse primer (P2): TTCTCTTTGGTGAAGGTCTGGG;

3'-reverse primer (P3): TCTTGGTCTTTGCTCCAAGCAAG.

ACC^{+/-} (heterozygous) littermates were crossed to produce ACC^{-/-} or ACC^{+/+} mice. These mice were backcrossed to a C57BL6/129/FVB WT animal. Homozygous pairs were allowed to propagate to produce ACC2KO and WT littermates.

Ultrasound Echocardiography

In vivo cardiac function (Tei index) and pulmonary artery acceleration time (PAAT) were assessed in isoflurane-anaesthetized rats using a Vevo 770 high-resolution echocardiography imaging system with a 30-MHz transducer (RMV-707B; Visual Sonics, Toronto, Canada) as previously described (76). Rats were anaesthetized with a mixture of 3% isoflurane and 1.5 L/min of oxygen via a hose attached to a nose cone. Anesthetization was maintained at 1-1.5% isoflurane and monitored with heart rate, respiratory rate and body temperature.

Pulmonary artery acceleration time was assessed by pulse Doppler and normalized to heart rate. Tei index was calculated as (isovolumic contraction time + isovolumic relaxation time) / ejection time. Isovolumic contraction time was calculated as the time from aortic valve closure to initiation of the early (E) filling wave (in msec) using pulsed-wave tissue Doppler.

Isolated Working Rat Heart

Rats were anaesthetized with a 60 mg/kg intraperitoneal injection of sodium pentobarbital, after which the heart was excised and placed in ice-cold Krebs Henseleit bicarbonate buffer (118 mM NaCl, 25 mM NaHCO₃, 5.9 mM KCl, 5 mM EDTA pH = 7.4, 1.2 mM MgSO₄•7H₂O, 2.5 mM CaCl₂•2H₂O). Next the aorta was isolated and placed securely over a cannula with a silk suture. The heart was then perfused in Langendorff mode (60 mmHg) with Krebs Henseleit buffer for 10 min while the left atrium was isolated and cannulated. The heart was switched into left working mode by clamping off the Langendorff flow (aortic inflow line) and opening the preload (left atrial inflow) and afterload (aortic outflow) lines (77). In the isolated working heart, oxygenated Krebs Henseleit buffer (37°C; 95% O₂/5% CO₂) was delivered to the left side of the heart via the left atrial cannula. The buffer was then pumped up through the aorta into the compliance chamber to the aortic outflow line and recirculated back into the heart chamber. Preload and afterload pressures were maintained at 11.5 mm Hg and 80 mm Hg, respectively. Perfusion buffer (100 mL) consisted of Krebs-Henseleit solution with 100 μU/mL insulin, 11 mM [5-³H/U-¹⁴C]glucose, 0.8 mM [9,10-³H/1-¹⁴C]palmitic acid pre-bound to 3% fatty acid free bovine serum albumin, as previously described (28,77). Spontaneously beating rat hearts were aerobically perfused for 40 min in the presence of 1 mM DCA or vehicle (Krebs). After the perfusions, hearts were separated into the right ventricle (RV), left ventricle (LV) and septum (S) then flash frozen in liquid nitrogen using Wollenberger clamps and stored at -80°C. Individual structural components were weighed to calculate

the RV/LV+S ratio.

Isolated Working Mouse Heart

Mouse hearts were perfused using the left working heart system as previously described (77,78). To measure oxygen saturation pre and post, an oxygen probe was placed in the preload line as well as the pulmonary arterial cannula, respectively. Preload pressure was set at 11.5 mm Hg and afterload at 50 mm Hg. For the studies in ischemia/reperfusion, perfusion buffer was similar to previously described, with the following exceptions: 5 mM glucose, 1.2 mM palmitate and 1 mM lactate. The perfusion protocol was as follows: 30 min aerobic, 18 min global no-flow ischemia, and 40 min reperfusion. Global no-flow ischemia was induced by clamping the preload and afterload lines. For the aerobic insulin study, the perfusion buffer was similar to the I/R study with the following modification in fatty acid concentration: 0.8 mM palmitate. Hearts were aerobically perfused for 30 min after which 100 μ U/mL insulin was added to the perfusate and then perfused for an additional 30 min. After the perfusions, hearts were immediately frozen in liquid nitrogen using Wollenberger clamps and stored at -80°C.

Measurement of Mechanical Function in Isolated Working Hearts

Cardiac pressures (diastolic, systolic) as well as heart rate were measured using a Harvard Apparatus Gould P21 pressure transducer connected to aortic outflow line. Cardiac output and aortic outflow (mL/min) were measured using

ultrasonic flow probes (Transonic T206) connected to the preload and afterload lines, respectively. Coronary flow was calculated as the difference between cardiac output and aortic outflow (78). Physiographic data was collected on a MP100 system from AcqKnowledge (BIOPAC Systems Inc., USA).

Measurement of Glycolysis, Glucose, Lactose, Palmitate Oxidation

Glucose oxidation, lactate oxidation and glycolysis rates were quantified by perfusing hearts with [U-¹⁴C]glucose, L-[¹⁴C(U)]lactic acid, and D-[5-³H]glucose, respectively. Palmitate oxidation was quantified using [9,10-³H] palmitic acid or [1-¹⁴C]palmitic acid. Oxidative rates were calculated by measuring total myocardial production of ¹⁴CO₂ from buffer samples containing ¹⁴CO₂ dissolved as H¹⁴CO₃⁻ and by trapping ¹⁴CO₂ released from the system in hyamine hydroxide at 10 min intervals of the perfusion period. ¹⁴CO₂ was released from buffer samples by mixing the bicarbonate buffer with 1mL of 9 N H₂SO₄ and trapped in hydroxide hydroxide filter papers placed over 25 mL stoppered test tubes. Scintillation fluid was added to both sets of scintillation vials and then placed in the liquid scintillation counter (Perkin Elmer Liquid Scintillation Analyzer Tri-Carb 2800TR) to quantify ¹⁴C. Total ³H₂O production was measured in 10 min intervals by a vapor transfer method as previously described (28,79). In this protocol 500 mL of distilled water was placed into a 5 mL scintillation vial along with a 1.5 mL capless microcentrifuge tube. A 200 μL sample from the perfusate was added to the microcentrifuge tube and the vial was capped and placed in a 50°C oven for 24 hr and then at 4°C for another 24 hr. Following

refrigeration, the microcentrifuge tube was discarded and the scintillation vial was filled with scintillation fluid and placed in the counter (28,79).

Dry to wet ratios were calculated based on the wet weight of the atria and the dry weight following incubation in a 50°C oven overnight.

Calculation of Proton Production

Relative proton production was calculated based on the rates of glucose oxidation and glycolysis. Non-oxidative disposal of glycolytically derived pyruvate yields lactate and ATP. If the ATP is hydrolyzed, there is a net production of 2 H⁺ per molecule of glucose. However, if glycolysis is coupled to glucose oxidation, there is no net production of protons. Therefore, the difference between the rate of glycolysis and glucose oxidation multiplied by two yields the overall rate of proton production from glucose utilization (80).

Calculation of Total TCA Acetyl CoA and ATP Production

Cardiac acetyl CoA production was calculated from lactate, glucose and palmitate oxidation rates assuming oxidation of 1 mol of glucose yields 2 mol of acetyl CoA, 1 mol of palmitate produces 8 mol of acetyl CoA and 1 mol of lactate yields 1 mol of acetyl CoA (81).

Total ATP production was calculated from each of the metabolic rates for glycolysis, glucose, lactate and palmitate oxidation using the following values based on fractional P/O ratios: 2 mol of ATP per mol of glucose undergoing

glycolysis, 29 mol ATP per mol of glucose oxidized, 14.5 mol of ATP per mol of lactate oxidized, and 104 mol ATP per mol of palmitate oxidized (81).

Calculation of Cardiac Work, Power, Efficiency

Cardiac work was calculated as the product of cardiac output and LV developed pressure (peak systolic pressure – preload pressure): [volume displaced in 1 min (in m^3)] • [pressure (in Pa)]. Cardiac output (mL/min) was expressed in m^3 as $1 \text{ mL} = 1 \cdot 10^{-6} \text{ m}^3$; developed pressure (mm Hg) was expressed in Pa as $1 \text{ mm Hg} = 133.322 \text{ Pa} = 133.322 \text{ kg}/(\text{m} \cdot \text{s}^2)$. The final product was presented in units of Joules/min ($\text{J} = \text{m}^2 \cdot \text{kg}/\text{s}^2$) (82).

Cardiac power was calculated as the product of cardiac output and LV developed pressure (peak systolic pressure – preload pressure): [volume/s (in m^3/s)] • [pressure (in Pa)]. Cardiac output (mL/min) was expressed in terms of m^3/s as $1 \text{ mL} = 1 \cdot 10^{-6} \text{ m}^3$ and $1 \text{ min} = 60 \text{ s}$; developed pressure (mm Hg) was expressed in Pa as $1 \text{ mm Hg} = 133.322 \text{ Pa} = 133.322 \text{ kg}/(\text{m} \cdot \text{s}^2)$. The final product was presented in SI units of Watts ($\text{W} = \text{m}^2 \cdot \text{kg}/\text{s}^3$) (82).

Cardiac efficiency was calculated as cardiac work per μmol of oxygen consumed per min per gram dry weight. Percent oxygen consumption was measured using a 16-730 Flow-thru O_2 Microelectrode (Microelectrodes, Inc.) placed in the pulmonary arterial cannula. Cardiac work was calculated in joules/min as described above and oxygen consumption was calculated in $\mu\text{mol}/\text{min}$ using $(a/22.414) \times (760-P)/760 \times (r\%/100) \times \text{CF}$ where a = absorption

coefficient of gas at temperature, P = vapor pressure of water in mm Hg at temperature, $r\%$ = actual reading in percent oxygen, and CF = coronary flow in mL/min.

Acetyl CoA Carboxylase Activity Assay

ACC activity assay was performed according to the protocol from Olson *et al* (75).

Measurement of Short Chain CoA Esters

For CoA extraction, approximately 20 mg of cardiac tissue was homogenized (Polytron® Homogenizer) on ice for 30 sec with 200 μ L of extraction buffer consisting of 6% perchloric acid. Homogenized samples were placed on ice for 10 min and then centrifuged at 12 000 x g for 5 min at 4°C and the supernatant was removed for analysis.

For short-chain CoA analysis, a Waters Ultra Performance Liquid Chromatography (UPLC) system was employed. Each sample was run at a flow rate of 0.4 mL/min through an Ascentis Express C18 column maintained at a temperature of 40°C. The analyte was detected at an absorbance of 260 nm. The mobile phase consisted of a mixture of buffer A (0.25 M NaH_2PO_4 and water, pH = 2.5; ratio 80/20) and buffer B (0.25 M NaH_2PO_4 and acetonitrile, pH 2.5; ratio 80/20). The gradient elution profile consisted of the following: initial conditions: 2% B; 2-4 min. 25% B; 4-6 min. 40% B; 6-8 min. 100% B; 10-12 min then back

to initial conditions and maintained to 15 min. All gradients were linear. Waters Empower Software was used for data acquisition and integration of peaks (83).

Measurement of Triacylglycerol

To measure TAG content, approximately 20 mg of powdered ventricular tissue was first homogenized in 20-fold volume 2:1 chloroform:methanol mixture for 45 seconds. Next 0.2 volume methanol was added to each sample and vortexed for 30 sec. The samples were centrifuged at 3500 revolutions per minute (rpm) for 10 min and the supernatant was collected and volume recorded. Next 0.2 volume of 0.04% CaCl₂ was added to supernatant to allow the mixture to separate into two phases. The mixture was again centrifuged at 2400 rpm for 20 min after which the upper phase was removed and the interface was rinsed with 150 µL of pure solvent upper phase three times. After removing the last wash, 50 µL of methanol was added to obtain one phase and the samples were dried under nitrogen gas at 60°C. Finally, the samples were redissolved in 50 µL of 3:2 *tert*-butyl alcohol:triton X-100/methyl alcohol (1:1) mixture. The Wako Triglyceride E Kit was used to quantify TAG levels.

Immunoblot Analysis

Approximately 20 mg of frozen powdered cardiac tissue was homogenized in buffer containing 50 mM Tris-HCl (pH 8 at 4°C), 1 mM EDTA, 10% glycerol (w/v), 0.02% Brij-35 (w/v), 1 mM DTT, protease and phosphatase inhibitors (Sigma). Following homogenization for 10 sec, the homogenate was

placed on ice for 10 min and then centrifuged at 10 000 x g for 15 min at 4°C. The supernatant was used for immunoblotting. The protein concentration of the homogenate was determined using the Bradford protein assay kit (Bio-Rad). A BSA standard curve from 0 to 10 µg was prepared on a 96-well plate and homogenates were loaded in triplicates with 200 µL of the BioRad reagent. The plate was read on a spectrophotometer at 595 nm. Sodium dodecyl sulfate polyacrylamide gel electrophoresis (5%, 8% SDS-PAGE) was conducted using 20 µg samples and separated protein was transferred onto a 0.45 µm nitrocellulose membrane. SDS-PAGE gel was stained with 0.05 % (w/v) of Coomassie Brilliant Blue R250 (Sigma), 25% (v/v) 2-propanol, 10% (v/v) acetic acid for 5-10 min and then de-stained with 7.5% (v/v) acetic acid, and 10% (v/v) methanol. Membranes were blocked with 5% fat free skim milk for 1 hr and probed with either anti-phosphoSerine-79 ACC (Millipore, 1/500 dilution), peroxidase-labeled streptavidin (Jackson ImmunoResearch Laboratories, 1/500 dilution), anti-MCD H240 (prepared as previously described (50), 1/500 dilution), anti-phosphoThreonine-172 AMPK (Cell Signaling Technologies, 1/1000 dilution), anti-AMPKalpha (Cell Signaling Technologies, 1/1000 dilution), anti-PDK4 (Abcam, 1/500 dilution), anti-PDH (Cell Signaling Technologies, 1/1000 dilution), anti-phosphoSerine-293 PDH (Calbiochem, 1/1000 dilution), or anti-alpha-tubulin (Cell Signaling, 1/2000) antibodies in 5% fatty acid free BSA or 5% fat free skim milk. Following incubation in primary antibody, membranes were washed with 1x Tris buffered saline and probed with secondary antibody goat anti-rabbit (Santa Cruz Biotechnology, 1/2000 dilution) in 5% fat free milk.

Western blots were visualized using enhanced chemiluminescence Western blot detection kit (Perkin Elmer) and quantified with Image J 1.46q (NIH, USA).

Statistical Analysis

Data are represented as mean \pm SE (n observations). One-way and two-way analyzes of variance (1, 2-way ANOVA) with the Bonferroni *post hoc* test and the unpaired two-tailed Student's *t*-test was used to determine the significance of observed differences. $P < 0.05$ was considered significantly different.

The Bonferroni *post hoc* test was selected as it limits the number of tests that can be conducted in the analysis and thereby reduces the chance of a Type 1 error (false positive). This test can also assess differences among experimental groups and between experimental and control groups (84).

CHAPTER 3.

Acute Inhibition of Pyruvate Dehydrogenase Kinase Improves the Cardiac Metabolic Profile in the Fawn Hooded Rodent Model of Pulmonary Hypertension and Right Ventricular Hypertrophy

Some of the data in this chapter has been published. Piao L, **Sidhu VK**, Fang Y, Ryan JJ, Parikh KS, Hong Z, Toth PT, Morrow E, Kutty S, Lopaschuk GD, Archer SL. FOXO1-mediated upregulation of pyruvate dehydrogenase kinase-4 (PDK4) decreases glucose oxidation and impairs right ventricular function in pulmonary hypertension: Therapeutic benefits of dichloroacetate. *Journal of Molecular Medicine*. 2012 Dec 18. [Epub ahead of print]

In this study my role involved performing the isolated working heart perfusions, biochemical assays (Western blot) as well as writing part of the manuscript. Donna Beker conducted the echocardiography and Lin Piao (Section of Cardiology, Department of Medicine, University of Chicago) measured PDK4 mRNA and protein expression, PDH activity and cardiac function in chronic DCA treatment.

CHAPTER 3

Acute Inhibition of Pyruvate Dehydrogenase Kinase Improves the Cardiac Metabolic Profile in the Fawn Hooded Rodent Model of Pulmonary Hypertension and Right Ventricular Hypertrophy

Abstract

Objective – Right ventricular failure is the major cause of death in patients with pulmonary arterial hypertension (PAH). Currently, there are no therapies to specifically treat right ventricular failure in PAH. We have previously shown that chronic administration of dichloroacetate (DCA), a pyruvate dehydrogenase kinase (PDHK) inhibitor, increases glucose oxidation and improves cardiac output and contractility in monocrotaline-induced PAH and right ventricular hypertrophy (RVH). Here we studied the effects of DCA on glucose and fatty acid oxidation in the Fawn Hooded rat (FHR), a strain that spontaneously develops PAH/RVH.

Methods and Results – Two groups were used: (i) control (age-matched Sprague Dawley (SD) rats); and (ii) FHR. PAH was confirmed by decreased pulmonary artery acceleration time, corrected by heart rate (FHR, 0.08 ± 0.01 ; SD, 0.11 ± 0.00 ms·min·beats⁻¹) and increased RV/LV+septum (FHR, 0.30 ± 0.02 ; SD, 0.22 ± 0.01). The expression of PDH β subunit was reduced 35% in FHR and there was a trend toward increased PDK4 expression in the RV. Cardiac metabolism and the effects of DCA were evaluated in isolated working hearts. Glucose oxidation was decreased in FHR compared with SD [FHR, 432 ± 73 ; SD, 1030 ± 175 nmol·(g·min)⁻¹] and glycolysis was increased [FHR, 6793 ± 665 ; SD, 4987 ± 248

nmol·(g·min)⁻¹]. DCA (1 mM), added to the perfusate, caused a 3.6-fold increase in glucose oxidation and decreased glycolysis in FHR. This was accompanied by a 37% reduction in proton production and a 34% decrease in fatty acid oxidation. Acetyl CoA production and ATP production rates were reduced in FHR compared with SD (P<0.01; P<0.05, respectively). DCA increased both acetyl CoA and ATP production in FHR. The improvement of glucose oxidation in FHR, treated with DCA, was accompanied by an increase in cardiac work towards the end of perfusion.

Conclusions – RVH is associated with reduced PDH and increased PDK expression. DCA improves glucose oxidation and reduces glycolysis and fatty acid oxidation in FHR RVH, suggesting that PDK inhibition may be a promising therapy for RVF.

Introduction

Pulmonary arterial hypertension (PAH) is a lethal disease characterized by a progressive increase in pulmonary arterial pressure. As a consequence of this pressure overload, one of the major causes of mortality in PAH patients is right ventricular failure, which results from decompensated right ventricular hypertrophy (RVH) (31).

Traditionally, PAH is treated by pharmacological or mechanical means that target the vasculature in order to decrease the pulmonary arterial pressure. These therapies primarily focus on reducing symptoms of dyspnea, edema and improving quality of life. These include vasodilators, endothelin receptor antagonists, calcium channel blockers, diuretics, and anticoagulants, as well as more invasive treatments such as atrial septostomy, lung or heart-lung transplants (32). However, the degree of RVH is the main predictor of prognosis in PAH patients and is often overlooked when treating the disease.

Accompanying the RVH is an altered cardiac metabolic profile, where there is increased expression of pyruvate dehydrogenase kinase (PDHK/PDK) as well as a tendency towards increased glycolysis and decreased glucose oxidation, characteristic of the Warburg effect (31,34). This uncoupling of glycolysis from glucose oxidation may be partly responsible for the some of the cardiac morbidities associated with PAH.

Currently, there is no direct treatment for the associated metabolic disturbance in PAH. In order to successfully treat this disease, vascular therapy is

critical, but treating the right ventricular metabolic disturbance is equally important. Archer *et al.* explain that an effective treatment for RVH/RVF may substantially improve prognosis even after vascular treatment. Thus, a metabolic intervention to offset these changes could be beneficial. In this study, we investigated the metabolic changes associated with RVH by using the FH rat model of spontaneous PAH. We also tested the effects of the PDHK inhibitor DCA, which stimulates glucose oxidation. The therapeutic benefits of chronic PDK inhibition were also evaluated in RVH and RV failure. We hypothesize that DCA restores glucose oxidation in RVH and may therefore improve cardiac function in PAH.

Materials and Methods

The FH rat strain spontaneously develops PAH and was used to assess the effect of acute DCA administration on both functional and metabolic parameters in isolated working heart perfusions. *In vivo* echocardiography was first conducted to assess the degree of PAH, RVH, and cardiac dysfunction in female FH rats from 10 to 20 months, which were compared to age-matched SD controls. Hearts were then isolated and aerobically perfused for 40 min in the presence of 11 mM glucose, 0.8 mM palmitate, 100 μ U/mL insulin, 3% bovine serum albumin and either vehicle or 1 mM DCA. Glucose oxidation, glycolysis, and fatty acid oxidation were quantified using radiolabeled substrates and various functional parameters (heart rate, pressure, cardiac output, etc.) were measured during the course of the perfusion. Detailed protocols can be found in **Chapter 2** of this thesis. All animals received care according to the Canadian Council on Animal Care and the University of Alberta Health Sciences Animal Welfare Committee.

In the chronic DCA experiment, three groups of 1-year old rats were used: Brown Norway rats (as CTR), FHR and age-matched FHR with chronic DCA treatment (FHR+DCA). DCA (0.75 g/L) was added into drinking water for six months.

Quantitative RT-PCR was conducted on RV heart tissue to determine mRNA levels of pyruvate dehydrogenase beta (PDH β) and PDK4. Briefly, tissue total RNA was extracted using the Pure Link Micro-to-Midi Total RNA Isolation Kit from Invitrogen (Carlsbad, California). The mRNA levels of PDH- β and

PDK4 were measured using an ABI PRISM 7900HT PCR system (Applied Biosystems, Foster City, CA) and normalized to β 2 microglobulin mRNA expression. Protein levels of PDK4 were also measured in RV, LV homogenates with SDS-PAGE and Western blotting. PDH activity was measured as described previously (35). Briefly, PDH was immunocaptured with anti-PDH antibody immobilized on a dipstick using the manufacturer's instructions (Abcam, Cambridge, Massachusetts). The colored precipitate was quantified using Image J from NIH (Bethesda, Maryland). Echocardiography was used to assess cardiac output *in vivo*. Cardiac output was quantified by measuring maximal diameter of pulmonary artery (PAd) and velocity time integral (VTI_{PA}) of pulsed wave Doppler. Cardiac output was then calculated from the formula Cardiac Output = SV x heart rate, where $SV = 3.14 \times (PAd/2)^2 \times VTI_{PA}$. The University of Chicago Institutional Animal Care and Use Committee approved all protocols. For the perfusion studies conducted at the University of Alberta, the University of Alberta Health Sciences Animal Welfare Committee approved all animal protocols.

Results

Ultrasound echocardiography and the RV/LV+S ratio were used to confirm the presence of PAH and RVH, respectively. By ten months, PAH was well established in the FHRs, as the PAAT (inversely related to PA pressure) was significantly shorter in the FHR compared to SD (Figure 3-1A). Furthermore, there was evidence of significant RVH in the FH hearts as the RV weighed 1.4-fold more than SD after normalizing for LV and septum (Figure 3-1B). The Tei index, a measure of cardiac dysfunction, was elevated indicating the presence of diastolic/systolic dysfunction in the FHR hearts (Figure 3-1C).

In addition to the physiological changes, the FHRs manifested metabolic changes. Aerobic perfusion of the FHR hearts showed a shift away from oxidative metabolism. Glucose oxidation was significantly reduced in the FH hearts compared to SD [FHR, 432 ± 73 ; SD, $1030 \pm 175 \text{ nmol}\cdot(\text{g}\cdot\text{min})^{-1}$] (Figure 3-2A), while glycolysis was markedly increased [FHR, 6793 ± 665 ; SD, $4987 \pm 248 \text{ nmol}\cdot(\text{g}\cdot\text{min})^{-1}$] (Figure 3-2B). This was accompanied by higher proton production in the FHR hearts compared to SD (Figure 3-2C). Furthermore, fatty acid oxidation was depressed in the FH hearts under normal perfusion conditions [161 ± 13 vs. $235 \pm 11 \text{ nmol}\cdot(\text{g}\cdot\text{min})^{-1}$] (Figure 3-3). Following the addition of 1 mM DCA, glucose oxidation was restored to rates comparable to SD hearts [by a 3.6-fold increase to $1552 \pm 141 \text{ nmol}\cdot(\text{g}\cdot\text{min})^{-1}$] (Figure 3-2A). Moreover, glycolytic rates showed a trend towards normalization with DCA to $5692 \pm 450 \text{ nmol}\cdot(\text{g}\cdot\text{min})^{-1}$ (Figure 3-2B). Fatty acid oxidation decreased by 34% and by 37% with DCA in FH and SD hearts, respectively (Figure 3-3). Acute DCA treatment

also normalized the proton production in the FH hearts to levels similar to the control group (Figure 3-2C). In terms of relative ATP production, glycolysis accounted for more than 23% of the ATP production in FH hearts (versus 15% in SD), but with DCA this decreased to 14% (similar to control SD). On the other hand, glucose oxidation accounted for 37% of total ATP (compared to 48% in SD), but with DCA it increased close to two-fold (Figure 3-4A-C).

Although cardiac function was depressed in FH hearts, little improvement was seen with acute DCA treatment (Table 3-1). Cardiac parameters measured during the course of the perfusion (i.e. cardiac output, heart rate, peak systolic pressure) did not significantly change with addition of DCA over the 40 min perfusion (Table 3-1). However, cardiac work slightly improved in FHR hearts towards the end of the perfusion with DCA from 0.32 J/min initially to 0.36 J/min at 40 min compared to 0.27 J/min without DCA (Figure 3-5).

Biochemical analysis of RV and LV tissue did not reveal any substantial changes in PDK4 protein expression between the two groups (Figure 3-6). However, quantitative RT-PCR revealed PDH β mRNA levels were 35% lower in FH hearts (Figure 3-7A), while PDK4 mRNA was slightly increased relative to SD (Figure 3-7B).

Chronically, DCA treatment improved the PAAT/HR ratio compared to treatment-naïve FHRs (Figure 3-8A). The RV/LV+S ratio also slightly decreased (not statistically significant) following chronic DCA treatment in the FHR group (Figure 3-8B), while cardiac output increased in FHR+DCA group (Figure 3-8C).

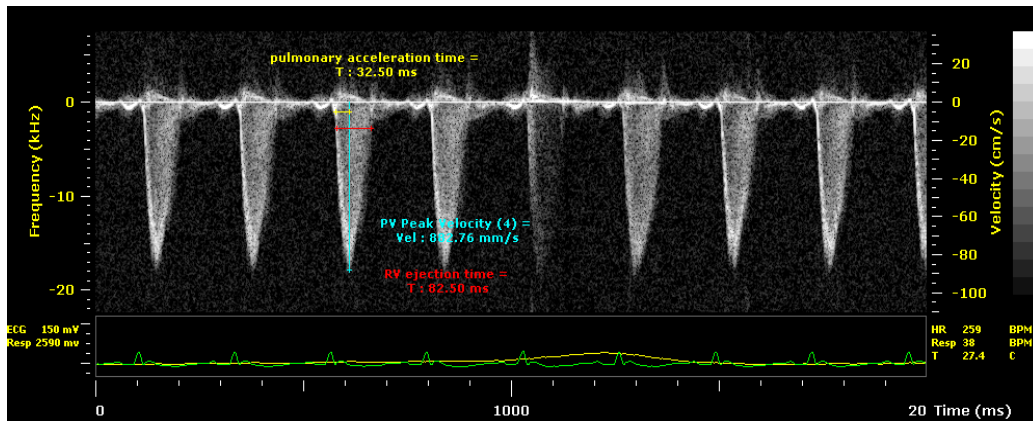
At the molecular level, PDK4 protein expression was elevated in FHR hearts, but regressed with chronic DCA treatment (Figure 3-9A). Furthermore PDH activity was significantly depressed in FHR hearts, but improved to levels comparable to control with six months of DCA treatment (Figure 3-9B).

Figure 3-1: *FH rats manifest PAH, RVH and cardiac dysfunction.*

A: Pulmonary artery acceleration time (PAAT) corrected by heart rate (HR) is reduced in Fawn Hooded rats, thus confirming the presence of PAH in FHR (*P<0.05, n=7-8, two-tailed Student's *t* test). **B:** Assessment of right ventricular hypertrophy (mass of right ventricle/(mass of left ventricle + septum). FHR develop RVH as evidenced by the increased RV/LV+S ratio (*P<0.001, n=15, two-tailed Student's *t* test). **C:** Assessment of cardiac diastolic and systolic dysfunction by *in vivo* echocardiography (*P<0.05, n=8, two-tailed Student's *t* test). Values represent mean \pm SE.

A

SD



FH

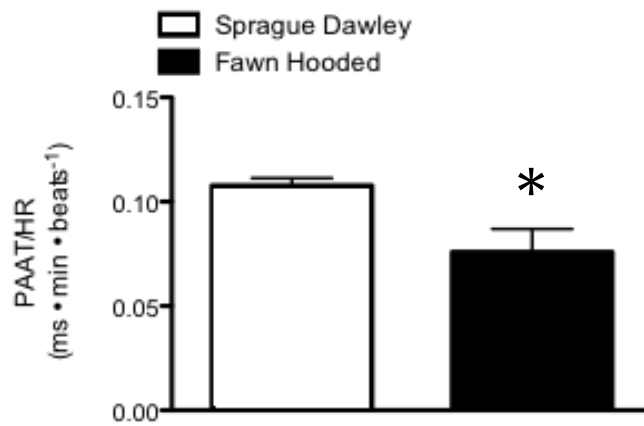
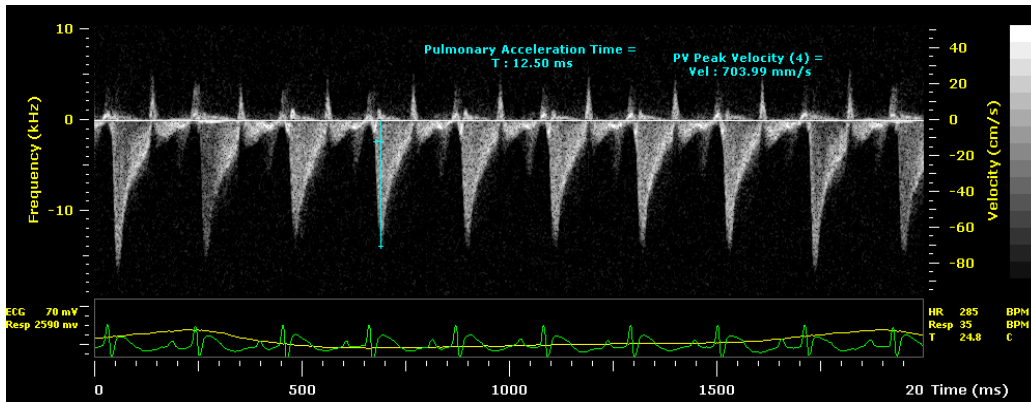
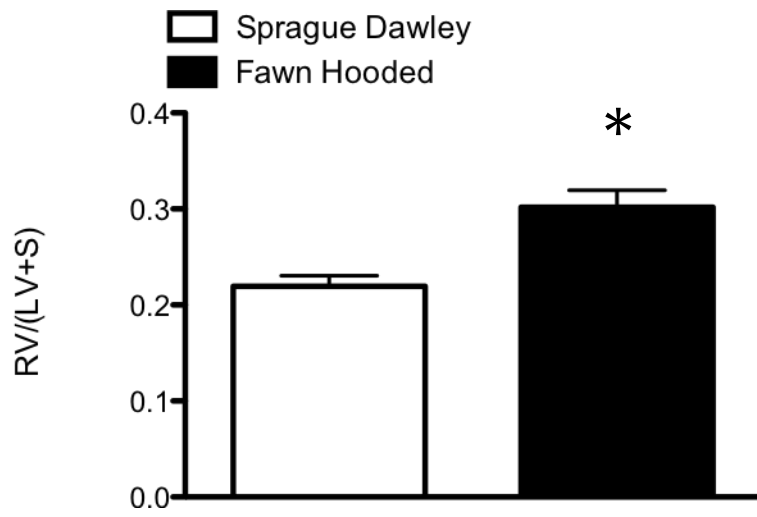


FIGURE 3-1

B



C

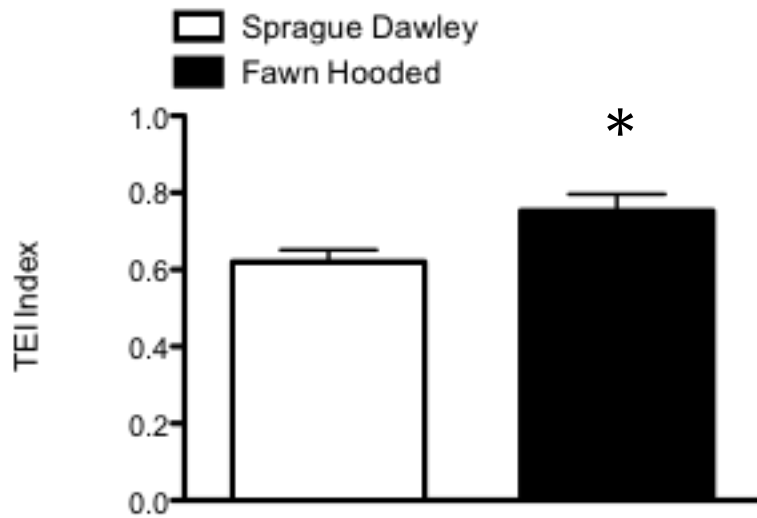


FIGURE 3-1

Figure 3-2: *Glucose oxidation is restored, while glycolysis decreases and proton production is normalized in FH hearts following acute DCA treatment.*

A: Glucose oxidation in aerobically perfused isolated working hearts from SD and FH rats in the presence of vehicle or 1 mM DCA. Glucose oxidation is reduced in FHR hearts and restored by the addition of 1 mM DCA in the perfusate (*P<0.01 vs. SD; **P<0.001 vs. FH baseline; #P<0.01 vs. SD baseline; n=6, 2-way ANOVA). **B:** Glycolysis in aerobically perfused isolated working hearts from SD and FH rats in the presence of vehicle or 1 mM DCA. Glycolysis is increased in FHR hearts and shows a trend towards normalization following the addition of 1 mM DCA in the perfusate (*P<0.05 vs. SD, n=8, 2-way ANOVA). Values represent mean \pm SE. **C:** Proton production in SD and FH hearts in presence of vehicle or 1mM DCA. Proton production is increased in FH rat hearts, but it is significantly reduced by the addition of 1 mM DCA (*P<0.01 vs. SD, n=6; **P<0.01 vs. FH baseline, n=5; 2-way ANOVA).

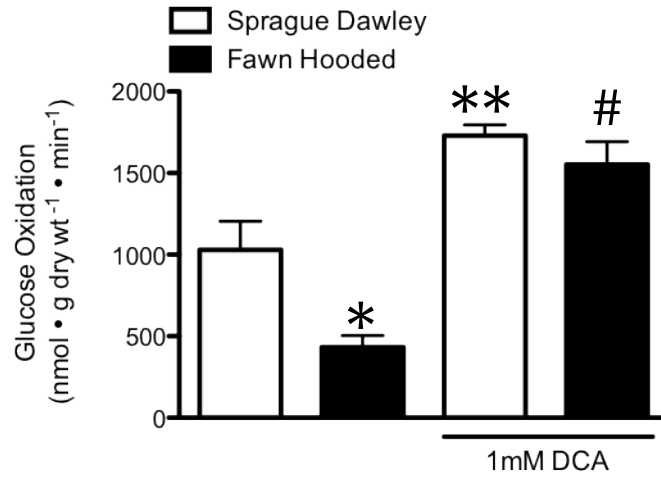
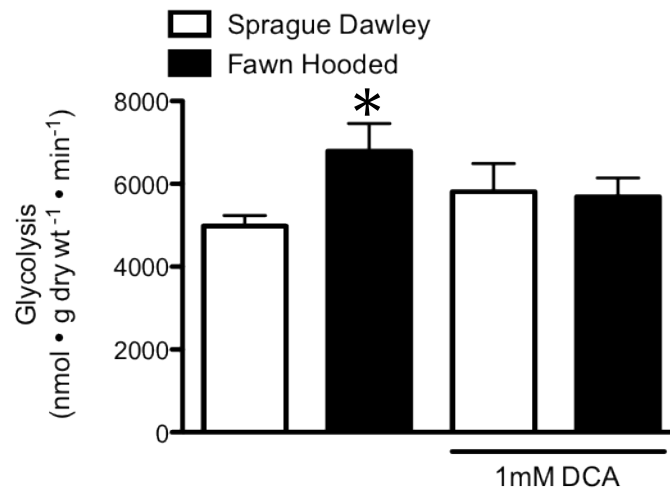
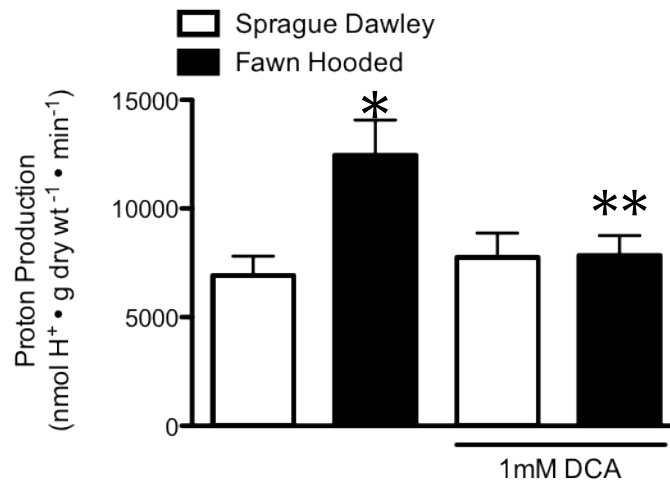
A**B****C****FIGURE 3-2**

Figure 3-3: *Acute DCA treatment decreases fatty acid oxidation in FH hearts.*

Palmitate oxidation in aerobically perfused isolated working hearts in the presence of vehicle or 1 mM DCA. Fatty acid oxidation, as measured by using radiolabeled palmitate, is decreased in FHR hearts and further reduced by the addition of 1 mM DCA (*P<0.05 vs. SD; **P<0.01 vs. SD baseline; #P<0.01 vs. FH baseline; n=4, 2-way ANOVA). Values represent mean \pm SE.

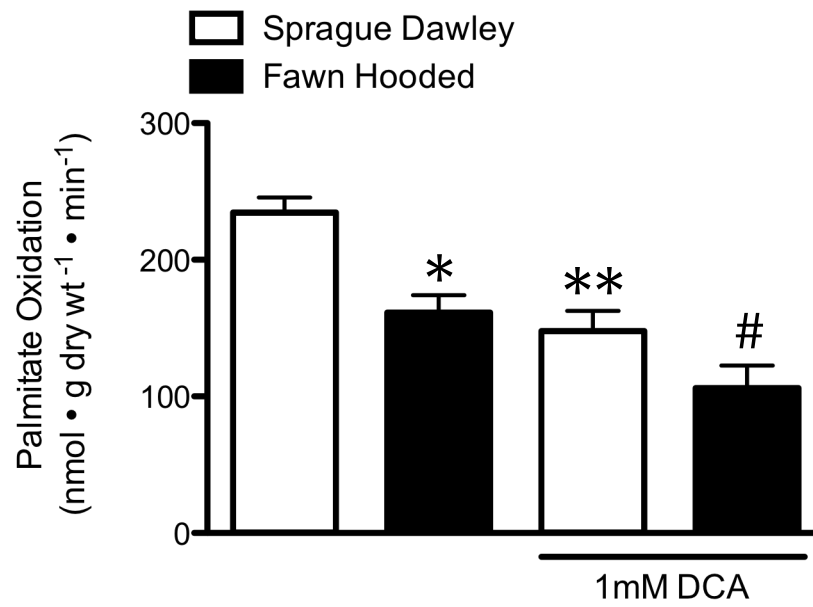


FIGURE 3-3

Figure 3-4: *Acute DCA treatment increases total ATP and TCA acetyl CoA production in FH hearts with PAH and RVH.*

A: Total ATP production was reduced in FH hearts (* $P < 0.05$ vs. SD, $n = 3-4$; 2-way ANOVA), but increased markedly with DCA (** $P < 0.05$ vs. FH baseline, $n = 3-4$; 2-way ANOVA). **B:** In terms of relative ATP production, glycolysis accounted for more than 23% of the ATP production in FH hearts (versus 15% in SD), but with DCA this decreased to 14% (similar to control SD). Glucose oxidation accounted for 37% of total ATP (compared to 48% in SD), but with DCA it increased close to two-fold. **C:** TCA acetyl CoA production was significantly lower in FH hearts (* $P < 0.05$ vs. SD, $n = 3-4$; 2-way ANOVA), but improved with DCA treatment (** $P < 0.05$ vs. FH baseline, $n = 3-4$; 2-way ANOVA). Values represent mean \pm SE.

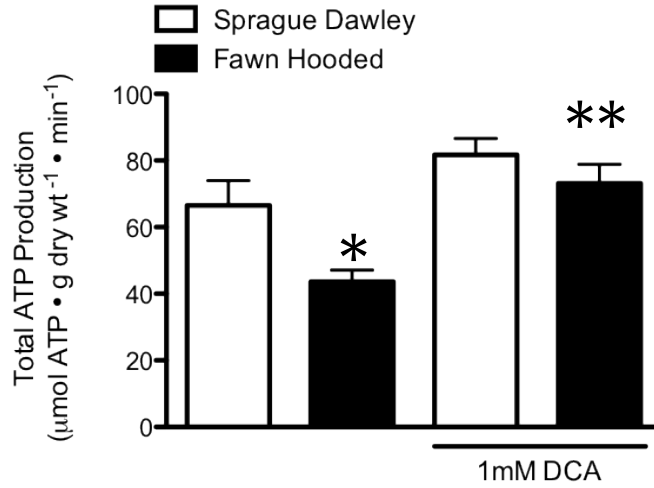
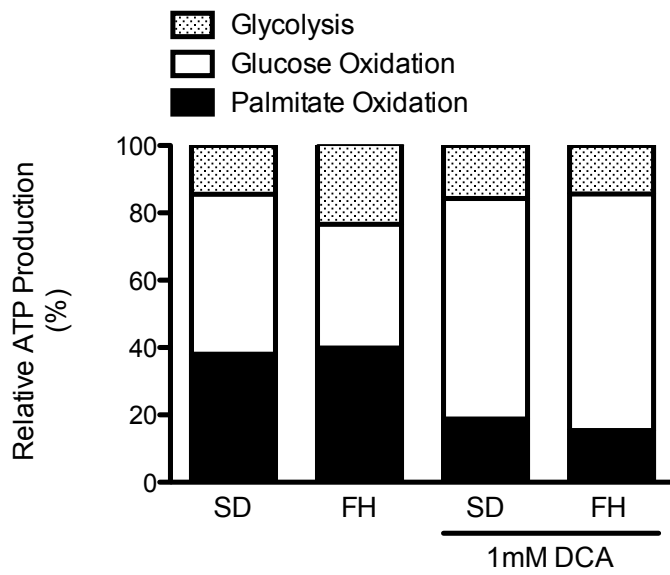
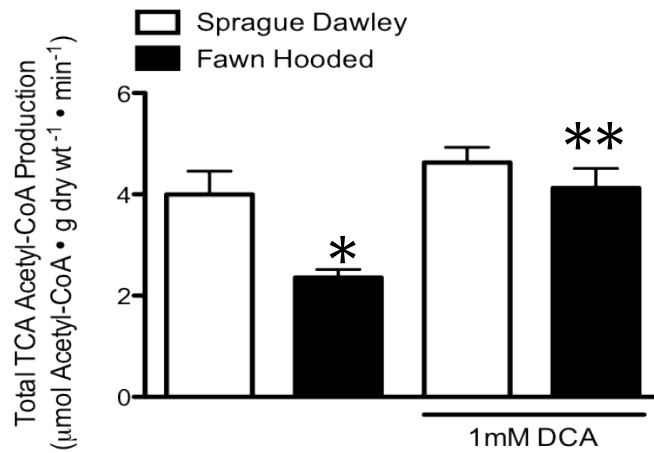
A**B****C****FIGURE 3-4**

Table 3-1: *Ex vivo cardiac function in aerobically perfused SD and FH hearts in presence of vehicle or 1 mM DCA.*

Cardiac function is markedly depressed in FH hearts, but is slightly improved by the addition of 1 mM DCA in the perfusate for 40 min (* $P < 0.05$ vs. SD, $n = 10-11$, two-tailed Student's t test). Values represent mean \pm SE.

	SD (n=11)	SD+DCA (n=10)	FH (n=11)	FH+DCA (n=10)
Heart Rate (beats/min)	227 ± 12	237 ± 11	211 ± 10*	207 ± 11
Peak Systolic Pressure (mm Hg)	140 ± 4	136 ± 5	112 ± 2*	114 ± 3
Developed Pressure (mm Hg)	87 ± 6	81 ± 7	48 ± 3*	50 ± 4
Cardiac Output (ml/min)	54.5 ± 3.9	52.2 ± 2.3	22.7 ± 1.7*	24.1 ± 1.6
Aortic Outflow (ml/min)	34.2 ± 2.9	32.0 ± 1.4	13.1 ± 1.7*	14.4 ± 1.2
Coronary Flow (ml/min)	20.3 ± 1.5	20.2 ± 1.7	12.0 ± 0.6*	9.7 ± 0.8
Cardiac Function (hr x psp x 10⁻³)	31.6 ± 1.5	31.8 ± 1.0	23.4 ± 1.0*	23.5 ± 1.0
Cardiac Power (mW)	17.1 ± 1.4	15.9 ± 1.1	5.6 ± 0.4*	6.1 ± 0.5

Table 3-1

Figure 3-5: *Cardiac work in SD and FH hearts over 40 min of perfusion with vehicle or 1 mM DCA.*

Time-dependent changes in cardiac work over 40 min of aerobic perfusion in SD, FH hearts with or without 1 mM DCA. Although there were no significant changes, cardiac work did slightly increase in FH hearts towards the end of perfusion with DCA. Values represent mean \pm SE (n=10-11).

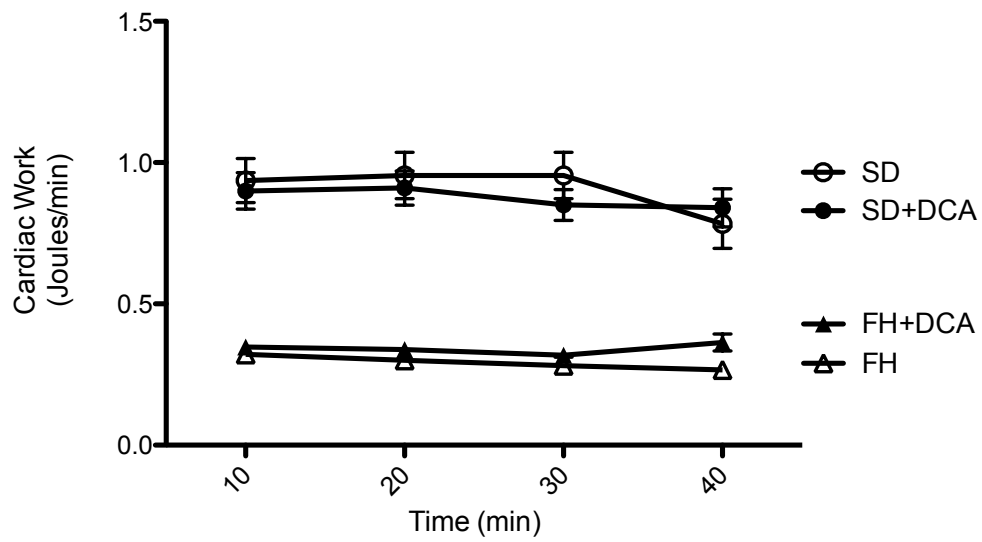


FIGURE 3-5

Figure 3-6: *PDK4* protein expression in RV of SD and FH hearts.

There is no change in expression of PDK4 between the RV of FHR and SD rat hearts. Values represent mean \pm SE.

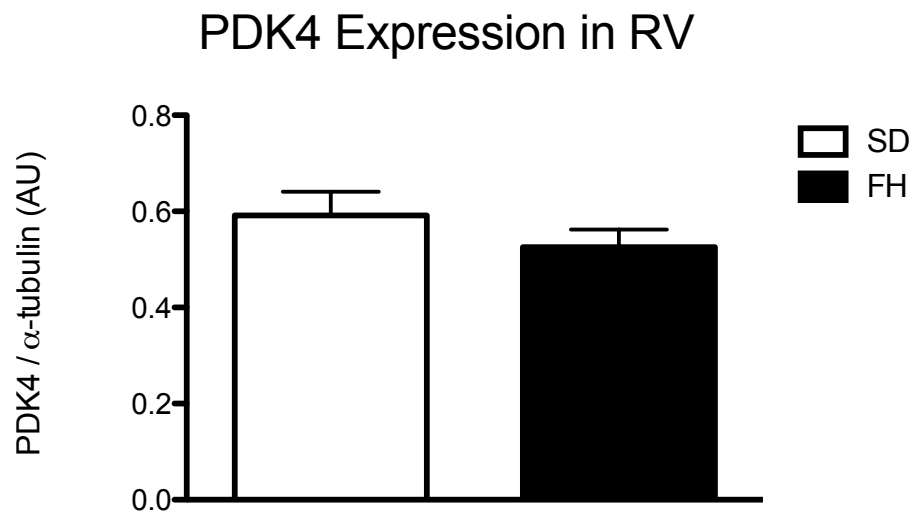
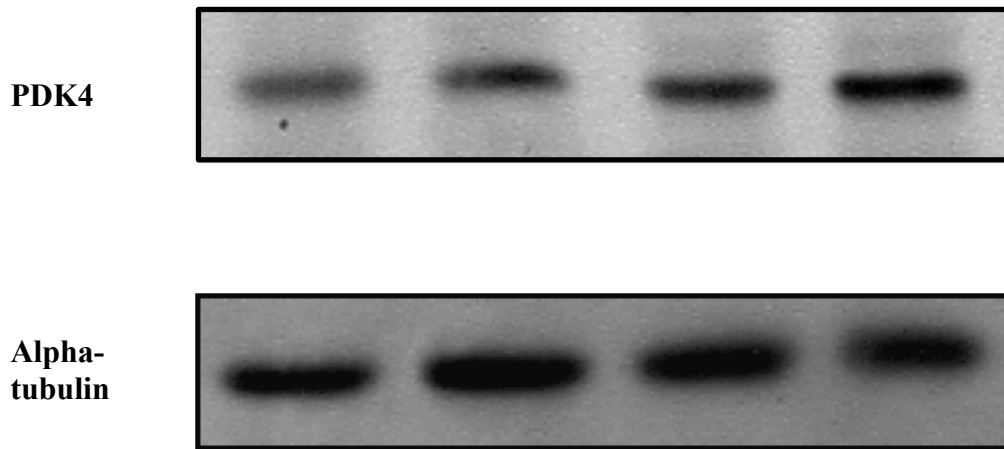
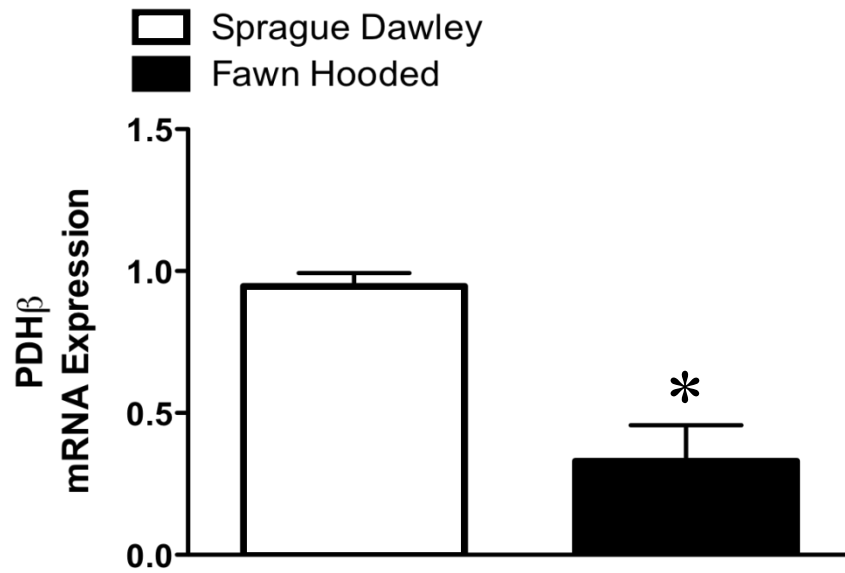


FIGURE 3-6

Figure 3-7: *PDH β and PDK4 mRNA levels in RV of FH and SD hearts.*

A: The mRNA level of PDH β is reduced in the RV of FH rats (*P<0.05 vs. SD, n=3, two-tailed Student's *t* test). **B:** The mRNA level of PDK4 is slightly increased in the RV of FH hearts relative to SD controls. Values represent mean \pm SE. These data were obtained from Lin Piao (University of Chicago).

A



B

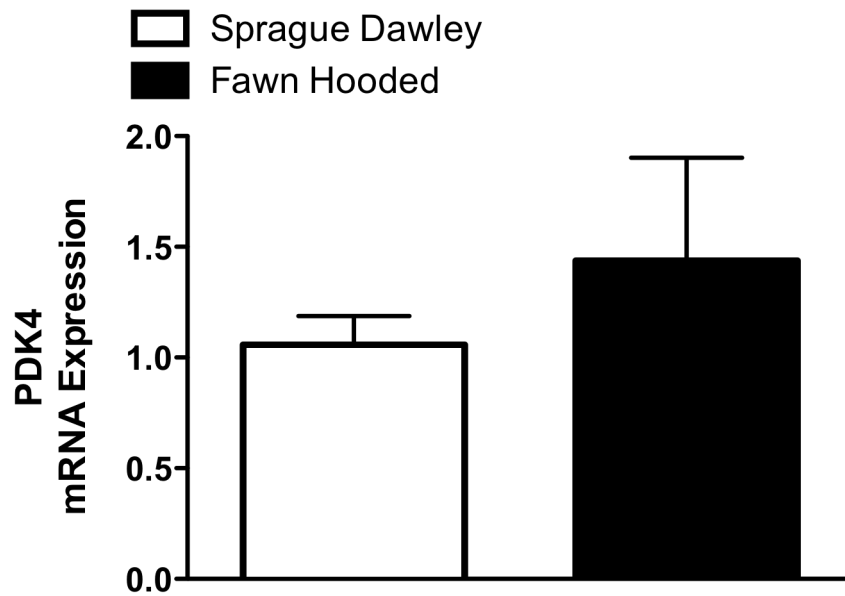
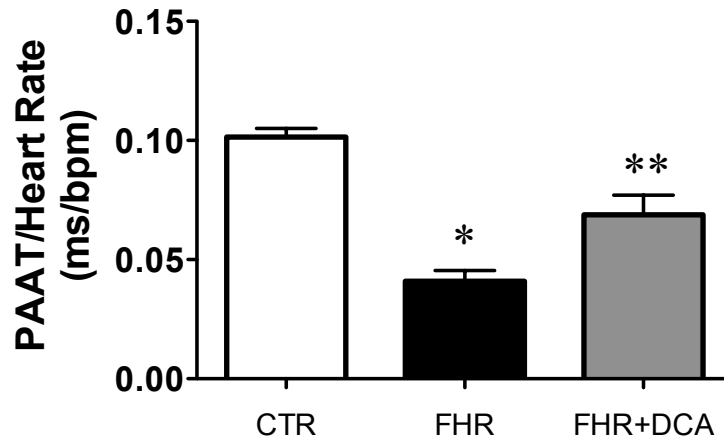


FIGURE 3-7

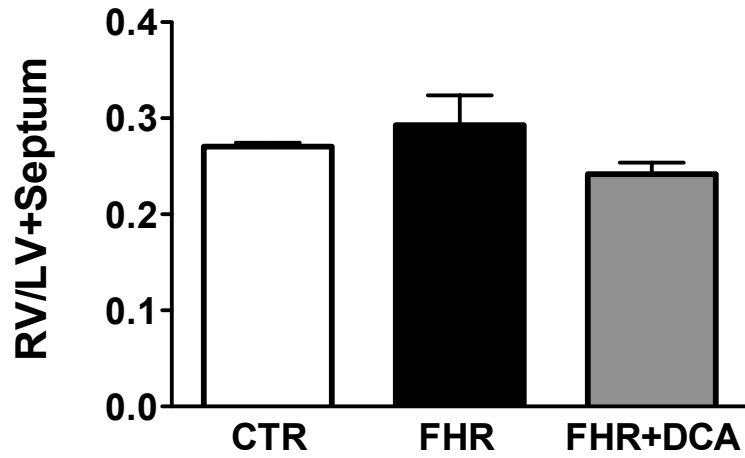
Figure 3-8: *Chronic DCA treatment reverses PAH in FH hearts and improves cardiac output.*

A: PAAT normalized to HR in FHR hearts treated with vehicle or DCA for six months (*P<0.05 vs. CTR; **P<0.05 vs. FHR). **B:** RV to LV+S ratio in CTR, FHR and FHR hearts treated with DCA. **C:** Cardiac output (assessed by echocardiography) comparing CTR, FHR and FHR with chronic DCA treatment (*P<0.05 vs. CTR; **P<0.05 vs. FHR). An unpaired two-tailed *t*-test was used for determining the differences between FHR and FHR with chronic DCA treatment. P<0.05 was considered statistically significant. Values represent mean \pm SE (n=8-10). These figures have been adapted from a previous publication (85).

A



B



C

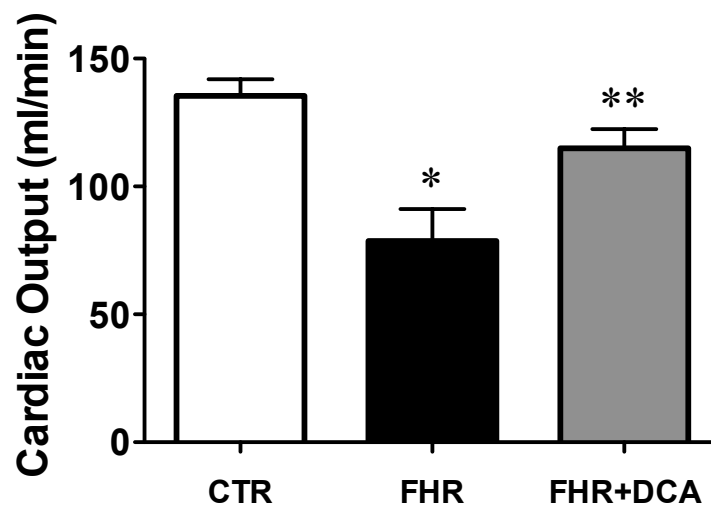
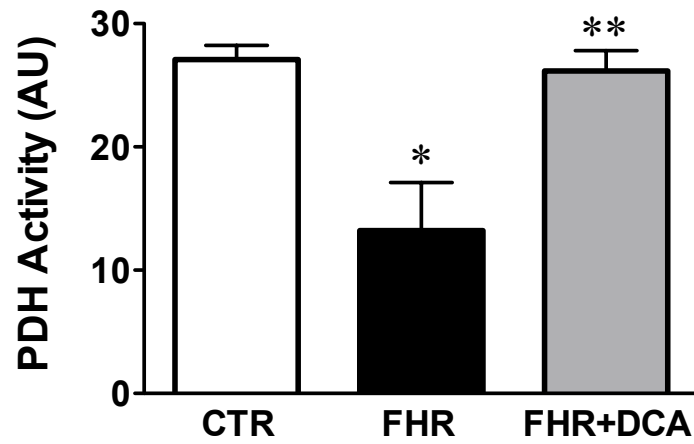


FIGURE 3-8

Figure 3-9: *Chronic DCA treatment increases PDH activity, while decreasing PDK4 expression in FH hearts.*

A: PDH activity is significantly depressed in FHR hearts (* $P < 0.01$ vs. CTR), but following DCA treatment for six months, activity is normalized to that of control hearts (** $P < 0.05$ vs. FHR). **B:** PDK4 protein expression in RV is significantly decreased with chronic DCA treatment to levels comparable to control. An unpaired two-tailed *t*-test was used for determine the differences between FHR and FHR with chronic DCA treatment. $P < 0.05$ was considered statistically significant. Values represent mean \pm SE (n=4-5). These figures have been adapted from a previous publication (85).

A



B

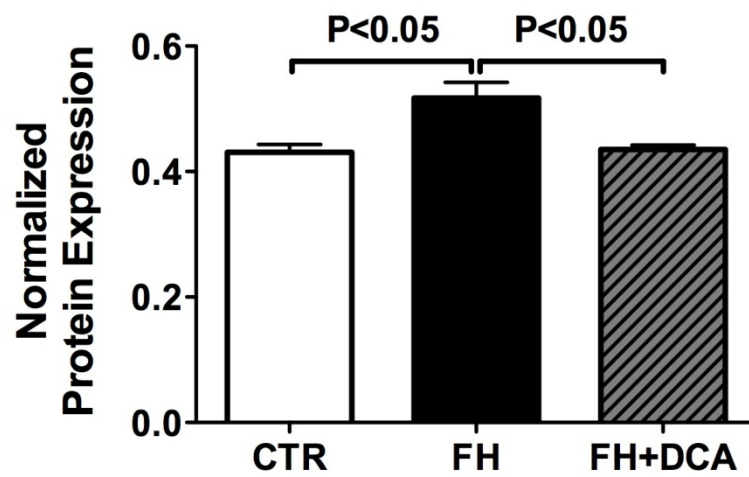
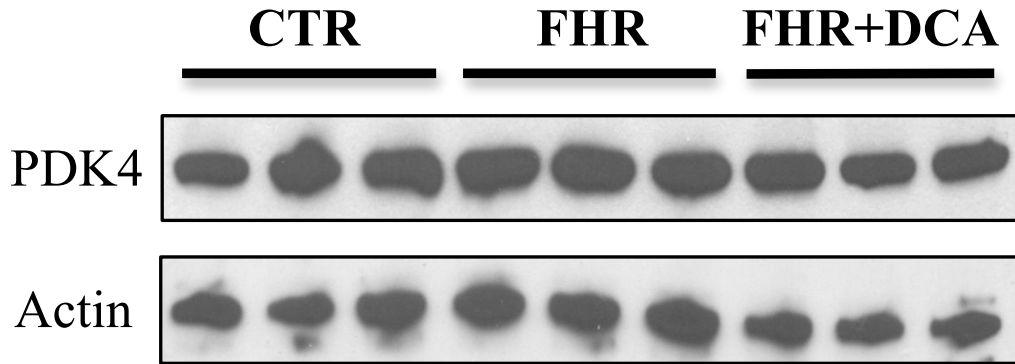


FIGURE 3-9

Discussion

Using a rodent model of spontaneous PAH, we demonstrate that RVH results in a marked elevation of glycolysis and a concomitant suppression of glucose oxidation. This metabolic switch is also accompanied by a reduction of fatty acid oxidation. At the molecular level, the changes in metabolism can be attributed to an increased expression of PDK and decreased expression and activity of PDH in the right ventricle. However, following acute DCA treatment in isolated working hearts, glucose oxidation is restored to rates comparable to that of control hearts, while fatty acid oxidation is significantly reduced. The reduction of fatty acid oxidation is also indicative of the restoration of glucose oxidation, since glucose oxidation and fatty acid oxidation are coupled via the Randle Cycle. Furthermore, proton production in the FH hearts was markedly lowered following DCA treatment, suggesting improved coupling between glycolysis and glucose oxidation. DCA also significantly increased both total ATP production and acetyl CoA production rates in the FH hearts. Specifically, DCA shifted ATP production from glycolysis to glucose oxidation. Although there were no significant changes in function following DCA treatment, there was a trend for cardiac work to increase in a time-dependent manner towards the end of 40 min perfusion with DCA in the FH hearts. Further study using a chronic DCA treatment demonstrated that DCA has the ability improve cardiac function in the setting of RV failure as it improved the RV/LV+S, PAAT/HR and CO. At the molecular level these physiological changes were associated with increased PDH activity and decreased PDK4 expression, suggesting a reversal of the metabolic

changes in PAH by restoring glucose oxidation in FH hearts. Thus, these findings suggest that modulating cardiac energy metabolism via PDK inhibition by DCA holds promise for treating cardiac abnormalities such as RVH and RVF.

While previous studies have demonstrated that directly increasing glucose oxidation improves RV function, recently published work from Fang *et al.* studied the effect of modifying fatty acid oxidation. The authors used the partial fatty acid oxidation inhibitors trimetazidine and ranolazine to indirectly increase glucose oxidation in pulmonary artery banded (PAB) rats. Not only did the inhibitors decrease fatty acid oxidation, but they also restored PDH activity and improved cardiac output. Trimetazidine and ranolazine lowered the RV/LV+S ratios in PAB, indicating a regression of RVH (35). These findings support the notion of optimizing oxidative metabolism to improve cardiac function. While our study demonstrates that stimulating glucose oxidation restores normal cardiac metabolic profile, this recent study corroborates our data showing that increasing glucose oxidation via the Randle Cycle also has therapeutic potential. Sutendra *et al.* extended these findings in their recent study using malonyl CoA decarboxylase (MCD) deficient mice (MCD KO). These mice, which have low rates of fatty acid oxidation, were resistant to development of PAH with chronic normobaric hypoxia. The MCD KO mice did not exhibit the hallmarks of PAH such as reduced mitochondrial ROS, mitochondrial hyperpolarization or inhibition of Kv current in response to acute hypoxia. In addition, the PAAT and RV/LV+S remained unchanged in MCD KO mice compared to wild type. Alternatively, treatment with metabolic modulators trimetazidine and DCA for three weeks was

able to reduce PA pressure and RVH while enhancing functional capacity on the treadmill test. MCD inhibition with CBM-301106 was also able to restore normal mitochondrial function in PASMCs (86).

Although acute DCA treatment did not dramatically improve cardiac function in our studies, the metabolic profile was normalized in the FH hearts. The perfusions were conducted over 40 min and it is likely that extending the perfusion period with DCA would reveal some improvements in functional parameters. Nonetheless, the chronic DCA experiments conducted by Lin Piao demonstrate physiological benefits with DCA, namely regression of RVH, PAH and increase in CO.

While we observed increases in PDK4 protein expression in FH hearts, we also show that PDK4 was also not altered and this may have been due to incorrect dissection and separation of the RV tissue from the LV and septum following perfusion. The upregulation of forkhead transcription factor (FOXO-1), which regulates PDK4 expression by binding to its promoter, has been documented in energy-starved skeletal muscle and diabetic cardiomyopathy (87,88). Preliminary data suggest that FOXO-1 may be responsible for the increased PDK4 expression/activity and subsequent metabolic derangements in PAH. Future studies focusing on FOXO-1 will be instrumental in determining the etiology of the metabolic switch in PAH.

CHAPTER 4.

Absence of Acetyl Coenzyme A Carboxylase 2 in Mice Lowers Cardiac Efficiency During Aerobic Perfusion, but Does Not Cause Ischemic Injury due to a Compensatory Increase in Malonyl CoA

In this study my role involved writing the manuscript and performing all the experiments except for the isolated working heart perfusions, which were done by Cory Wagg, and the short chain CoA HPLC analysis done by Ken Strynadka. Julia Tan and Sownd Sankaralingam assisted with the Western blotting and CoA assay, respectively.

Manuscript Status: This manuscript is currently being prepared to be submitted for publication as an original article.

CHAPTER 4

Absence of Acetyl Coenzyme A Carboxylase 2 in Mice Lowers Cardiac Efficiency During Aerobic Perfusion, but Does Not Cause Ischemic Injury due to a Compensatory Increase in Malonyl CoA

Abstract

Objective – Acetyl coenzyme A carboxylase 2 (ACC2) knockout (KO) mice demonstrate high rates of cardiac fatty acid oxidation. In ischemia/reperfusion (I/R), elevated fatty acid oxidation rates hinder the heart's ability to produce energy efficiently and ultimately lead to ischemic damage. To date, the role of ACC2 in ischemic heart disease has not been characterized.

Methods – The effects of knocking out ACC2 on *ex vivo* cardiac function and energy metabolism were investigated in the context of I/R using isolated working hearts. Twelve-week old male ACC2 KO mice were compared to age-matched wild types (WT). In the I/R study, hearts were isolated and aerobically perfused (30 min) followed by global no-flow ischemia (18 min) and reperfusion (40 min). Oxidative metabolism was quantified with radioisotopes and functional parameters were measured during the perfusions. Hearts were then biochemically analyzed.

Results – During the aerobic perfusion phase of the I/R study, fatty acid oxidation rates were significantly higher in the ACC2 KO, while glucose oxidation rates were depressed compared to WT. Following ischemia fatty acid oxidation

markedly decreased in the KO hearts, while there was little change in glucose oxidation from the aerobic phase. Both WT and KO animals had similar function, but the KOs had higher cardiac work (not statistically significant) and correspondingly higher oxygen consumption during reperfusion. Despite the metabolic changes, ACC2 KO sustained little to no injury following ischemia and maintained cardiac efficiency comparable to WT. Interestingly, at the end of reperfusion malonyl CoA levels in ACC2 KO and WT hearts were similar; however, the acetyl CoA/CoA ratio was significantly elevated in hearts from ACC2 KO mice.

Conclusions – The data suggest ACC isoform, ACC1, may be acutely compensating for the loss of malonyl CoA from ACC2 and thereby responsible for the observed metabolic/functional profile.

Introduction

Ischemic heart disease (IHD) is the most common form of cardiovascular disease and is often the underlying cause of angina, acute myocardial infarction and heart failure (3,15,42). Traditionally, ischemic heart disease has been treated by pharmacological or mechanical means that act primarily to increase oxygen supply to the heart or to decrease oxygen demand of the heart muscle (3). However, these treatments are not always successful and IHD continues to be the leading cause of death in North America, warranting more effective therapies. A number of recent studies of cardiac metabolism have suggested that a novel approach to treating ischemic heart disease is by means of metabolic modulation, whereby optimizing energetics in the myocardium can increase cardiac energy production and/or improve cardiac efficiency of the heart muscle (i.e. increase the contractile work achieved per molecule of oxygen consumed).

In a normal healthy and aerobic heart, fatty acid oxidation (FAO) accounts for 60-90% of total ATP production (8). However, in the ischemic myocardium FAO dominates as the residual source of oxidative phosphorylation as a result of both an increase in fatty acid concentrations in the coronary circulation and subcellular changes that result in dysregulation of FAO (89,90). This increased dependence on fatty acids as a fuel source is both inefficient and undesirable at a time of oxygen shortage. Furthermore, high rates of FAO inhibit glucose oxidation via the Randle Cycle phenomenon (26) and contributes to a proton overload (intracellular acidosis) during reperfusion. This proton overload not only further decreases cardiac efficiency, but also increases the risk for ischemic injury

while compromising cardiac contractility (90). In order to restore cardiac efficiency and function, cardiac energy metabolism can be optimized to decrease FAO and/or stimulate glucose oxidation.

Acetyl CoA carboxylase (ACC), a biotin-containing enzyme, catalyzes the synthesis of malonyl coenzyme A (malonyl CoA) via the carboxylation of acetyl CoA (6,19,91). Malonyl CoA is a reversible inhibitor of carnitine palmitoyltransferase (CPT1), which further regulates fatty acid metabolism by suppressing fatty acid uptake into the mitochondria. In addition, malonyl CoA can serve as a substrate for fatty acid synthase (FAS) (6). Malonyl-CoA is degraded by malonyl CoA decarboxylase (MCD), an enzyme found in mitochondria, peroxisomes, and cytosol (6). MCD directly regulates the levels of malonyl CoA, and therefore indirectly regulates FAO. ACC, on the other hand, is directly regulated by AMPK. AMPK is capable of phosphorylating ACC1, 2 on the serine-79 and 221 sites, respectively, rendering the enzyme inactive. AMPK is activated by either AMP or AMPK kinase (AMPKK), especially during times of metabolic stress.

There are two isoforms of ACC: ACC-1 and 2. ACC1 is typically found in lipogenic tissues such as liver and adipose, whereas ACC2 is mainly found in oxidative tissues such as skeletal muscle and heart (91). As a result, most malonyl CoA produced by ACC1 and ACC2 is used for fatty acid synthesis and regulating fatty acid oxidation, respectively. Therefore, ACC2 can indirectly regulate FAO.

The ACC2 mutant mouse model was first produced by Abu-Elheiga *et al.* and exhibited 10-fold lower levels of malonyl CoA in the heart and elevated rates of FAO and glucose oxidation in adipocytes (92,93). These mice weighed 20% less and accumulated less fat in liver and adipose tissue compared to their wild type counterparts (92). The key finding was that these mice were protected against diet-induced obesity and insulin resistance (94). The ACC2 KO mice had higher energy expenditure with simultaneous increases in whole body fatty acid and glucose oxidation (95), suggesting the absence of any fuel competition. Together, these studies found that stimulating FAO is an effective anti-obesity and anti-diabetic strategy and support the use of an ACC2 inhibitor for treating these diseases. However, a recent publication from Olson *et al.* challenged these findings. This group developed an ACC2 KO mouse that not only weighed similar to controls following high-fat feeding, but also showed no increase in skeletal muscle FAO (75).

The controversy over ACC2 concerns the fate of FAO. Numerous studies, including from our lab, have shown that cardiac fatty acid oxidation is in fact elevated in obesity and insulin resistance (8). Findings from *ob/ob*, *db/db*, and diet-induced obese mice illustrate high circulating fatty acid and triacylglycerol levels; therefore increased uptake and subsequent oxidation in the heart (8). By virtue of the Randle Cycle, there is a parallel decrease in glucose oxidation leading to insulin resistance. Thus, these data contradict previously published studies that support accelerating FAO as a strategy to combat obesity and diabetes.

The effect of knocking out ACC2 on cardiac metabolism has been studied by Essop *et al.* where both glucose and fatty acid oxidation were found to be elevated (relative to control) in the presence of increased glucose uptake and decreased triacylglycerol levels (96). Under aerobic conditions, these KO hearts functioned similar to WT hearts despite a 25% reduction in left ventricle mass (96). However, it remains unknown how ischemia may impact these hearts.

We hypothesize that knocking-out ACC2 leads to a decrease in malonyl CoA, resulting in increased FAO and a secondary decrease in glucose oxidation. This will reduce the functional recovery of hearts subject to ischemia and increase their susceptibility to ischemia/reperfusion injury. To address these issues, an ACC2 knockout model was used to determine whether the absence of ACC2 adversely affects the recovery of hearts following ischemia.

Materials and Methods

All animals received care according to the Canadian Council on Animal Care and the University of Alberta Health Sciences Animal Welfare Committee.

Twelve-week old male ACC2 KO mice were used and compared to age-matched littermate wild types. Animals were fed a standard chow and had access to food and water *ad libitum*. Mice were anesthetized with a 12 mg intraperitoneal injection of sodium pentobarbital USP. For the I/R study hearts were isolated and aerobically perfused for 30 min followed by 18 min of global no-flow ischemia and 40 min of reperfusion in the presence of 5 mM glucose, 1.2 mM palmitate, 1 mM lactate, 100 μ U/mL insulin, 2.5 mM calcium and 3% bovine serum albumin, as previously described (97). An aerobic perfusion study was also conducted to assess cardiac energy metabolism and efficiency in response to insulin. For the aerobic insulin study, the perfusion buffer was similar to the I/R study, however 0.8 mM palmitate was used in place of 1.2 mM palmitate. Hearts were aerobically perfused for 30 min, after which 100 μ U/mL insulin was added to the perfusate and then the hearts were perfused for an additional 30 min. Glycolysis, glucose, lactate and fatty acid oxidation were quantified using radiolabeled substrates and various functional parameters (heart rate, pressure, cardiac output, etc.) were measured during the course of the perfusions, as previously described (97,98).

Following perfusion, hearts were immediately frozen in liquid nitrogen for biochemical analysis. Extraction of CoA esters and assessment of acetyl CoA, malonyl CoA and cardiac triacylglycerol levels in heart tissue was performed as

previously described (51). Total ACC activity was measured from homogenized frozen heart tissue using a radioassay procedure previously described (75). Protein levels of ACC, MCD, PDH and AMPK were measured in whole heart homogenates with SDS-PAGE and Western blotting. Detailed protocols can be found in **Chapter 2** of this thesis.

Results

To date the ACC2 KO mouse model has not been studied in a setting of ischemic heart disease. The purpose of this study was to assess cardiac function and metabolism in these hearts following an ischemic episode. The heterozygous strain was obtained from Dr. David Olson (Division of Endocrinology and Metabolism, Beth Israel Deaconess Medical Center, Boston, Massachusetts) and interbred to produce whole body knockouts of ACC2. Southern blot analysis confirmed the desired genotype (Figure 4-1A) and Western blot analysis with streptavidin demonstrated the absence of ACC2 protein in heart tissue (Figure 4-1B).

Initially, to examine the metabolic plasticity of the ACC2 KO hearts, insulin was added to the perfusate following 30 min of aerobic perfusion. In the absence of insulin, both WT and KO hearts had similar rates of glucose and palmitate oxidation (Figure 4-2A, B, respectively). Furthermore, cardiac work, TCA acetyl CoA and cardiac efficiency were comparable across the two groups (Figure 4-3A-C, respectively). Following the addition of insulin to the perfusate, glucose oxidation sharply increased in the WT and KO hearts while FAO significantly decreased (Figure 4-2A, B, respectively). However, FAO remained considerably higher in the KO hearts compared to WT (848 ± 113 vs. 327 ± 60 nmol per gram dry weight). Cardiac work was not affected with insulin (Figure 4-3A), but TCA acetyl CoA production significantly decreased in the WT hearts while it remained the same in the KO group (Figure 4-3B). As a result, the KO hearts were less efficient than WT in the presence of insulin (0.27 ± 0.02 vs. 0.44

± 0.06) (Figure 4-3C). In addition, malonyl CoA levels were significantly lower in the KO hearts compared to WT (Figure 4-4A), whereas the acetyl CoA to free CoA ratio was significantly elevated in KO hearts following aerobic perfusion (Figure 4-4B).

Next, to assess the impact of knocking out ACC2 on cardiac function and energy metabolism in I/R hearts, isolated working heart perfusions were performed. As anticipated, KO mice had two-fold higher rates of palmitate oxidation than WT and displayed a trend towards decreased glucose oxidation in the aerobic period, indicating the presence of the Randle Cycle (Figure 4-5A, 4-5C, respectively). Following ischemia there was little change in cardiac metabolism between the groups; however, in the KO mice palmitate oxidation was significantly reduced to 605 ± 65 from 1141 ± 110 nmol per gram dry weight (Figure 4-5A) and glucose oxidation slightly decreased (not statistically significant) (Figure 4-5C). Fatty acid oxidation per unit work was elevated during reperfusion in both KO and WT hearts to an equal extent compared to the aerobic values (not statistically significant) (Figure 4-5B). Glucose oxidation, normalized to cardiac work, significantly increased in the WT hearts in reperfusion compared to the aerobic period, and a similar trend was also seen in the KO hearts (Figure 4-5D). Lactate oxidation was 1.7-fold lower in ACC2 KO compared to WT at baseline, yet was similar to WT in reperfusion (Figure 4-5E). The rates of glycolysis were not significantly different between the groups in either the aerobic or reperfusion phases (Figure 4-5F). In terms of energy yield, total ATP and tricarboxylic acid (TCA) cycle acetyl CoA production were higher in aerobic KO

hearts compared to WT, but markedly decreased after ischemia (Figure 4-6B,D, respectively) by 1.7-fold and 2-fold, respectively.

Both the KO and WT animals had similar function during the aerobic period (Table 4-1, Figure 4-7), but following ischemia the KOs tended to have higher, but not statistically significant, cardiac work and significantly higher oxygen consumption relative to WT (Figure 4-7A, 4-7B, respectively). Specifically, cardiac work recovered to 41% of pre-ischemic values in the KO heart compared to only 24% in WT. As a result of the higher cardiac work and oxygen consumption, cardiac efficiency was preserved in the KO mice (Figure 4-7C).

Previously published work from Olson *et al.* using this same mouse model was unable to find any marked changes in metabolism in response to global deletion of ACC2. Specifically, there was little change in body mass, food intake and blood glucose. Even after high-fat feeding these mice had similar body weights as the controls (75). These findings directly challenge data from Wakil *et al.*, which concluded ACC2 KO mice are protected from diet-induced obesity and insulin resistance due to increased energy expenditure, namely increased oxidation of fat. Although our study did not focus on whole-body energy metabolism, cardiac metabolism was affected by systemic deletion of ACC2, where FAO increased and was accompanied by a secondary decrease in glucose oxidation. These results correlate with Olson *et al.*, where metabolic monitoring showed this strain preferentially oxidizes fat with an increase in oxygen consumption. However, where Olson reported 30% lower levels of malonyl CoA

in the KO hearts (75), our results show that malonyl CoA levels were unchanged from WT at 6.3 ± 0.5 nmol per gram dry weight following reperfusion (Figure 4-8A), despite a marked elevation in acetyl CoA to free CoA (Figure 4-8B). Malonyl CoA was however significantly lower in the aerobic KO hearts (Figure 4-4A), even though the absolute values were higher than in I/R hearts. Furthermore, ACC1 expression (both P-ACC1 and T-ACC1) in heart tissue was significantly reduced in the KO strain (Figure 4-1B) even though there was no difference in total ACC enzymatic activity between the two groups (Figure 4-8C). Total cardiac triacylglycerol levels, on the other hand, were significantly lower in tissue of KO mice (18.2 ± 0.9 versus 24.9 ± 2.4 μ mol per gram dry weight in WT), which correlated with the metabolic data (Figure 4-8D). P-AMPK expression normalized to T-AMPK was reduced in the KO hearts. However, analysis of P-AMPK densitometry values, alone, showed no difference between KO and WT hearts, while T-AMPK was significantly decreased in KOs (Figure 4-9A-C). Furthermore, P-PDH/PDH and MCD protein expression following ischemia/reperfusion were unchanged between the two groups of mice (Figure 4-10, 4-11, respectively).

Figure 4-1: *Southern and Western blot analysis of ACC in WT and ACC2 KO tissue.*

A: For genotyping, Southern blot analysis was conducted on tail tissue. The ACC2 KO band is represented at 425bp and WT band at 350bp. The blot depicts (from left to right): a homozygous mouse with the wild type allele, a homozygous mouse with the mutant allele and a heterozygous mouse. **B:** P-ACC1 and T-ACC1 protein expression in ACC2 KO and WT cardiac tissue. Western blot analysis demonstrates the absence of ACC2 (280 kDa) protein expression in KO heart tissue, confirming the desired phenotype. ACC1 (265 kDa) protein expression was significantly reduced in ACC2 KO compared to WT (* $P < 0.05$, $n = 5$; Student's two-tailed t test). Values represent mean \pm SE.

A

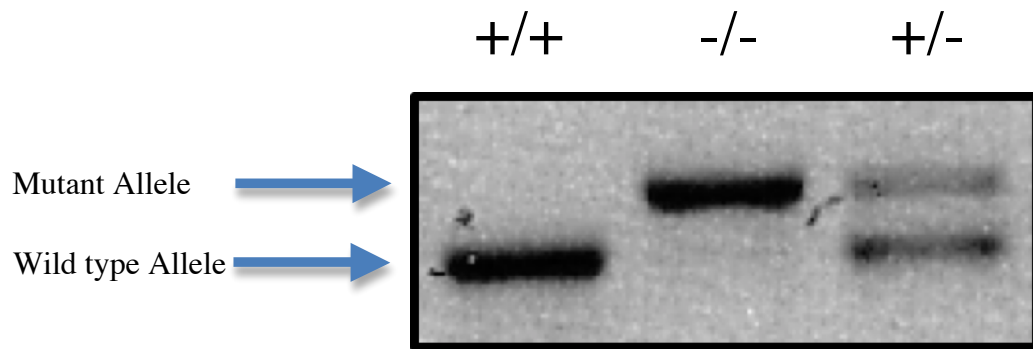


FIGURE 4-1

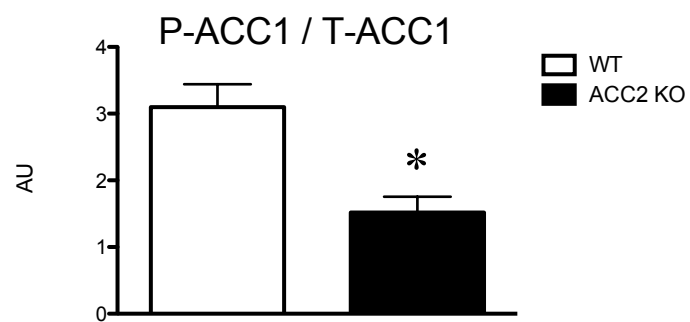
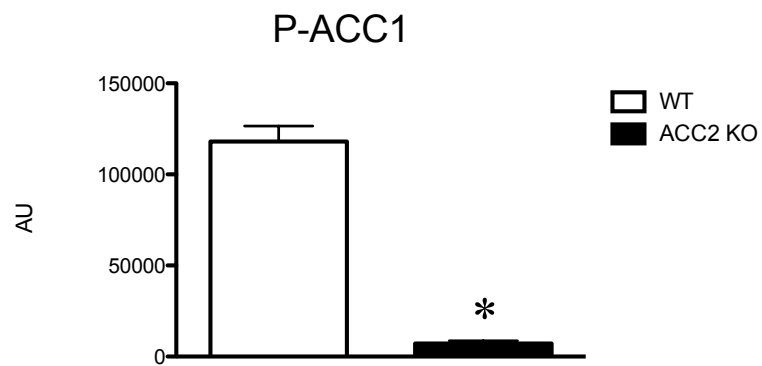
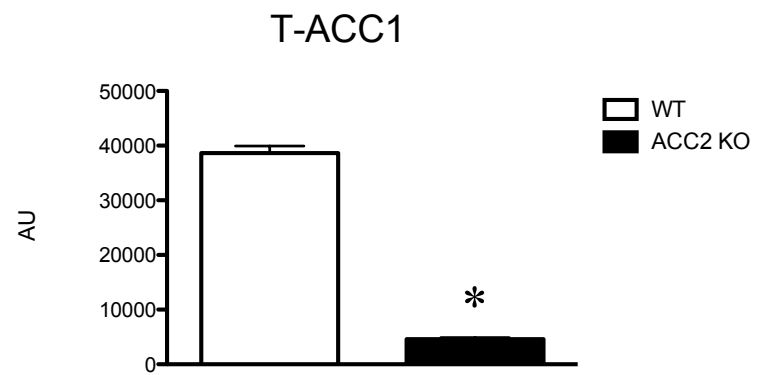
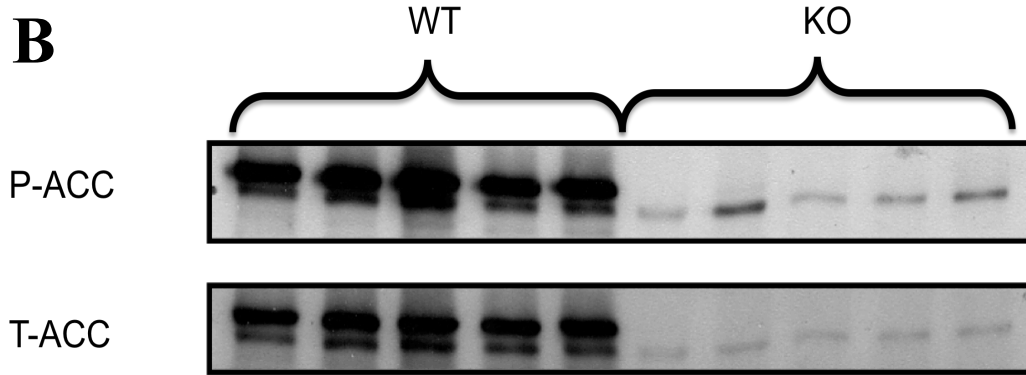


FIGURE 4-1

Figure 4-2: *Glucose and palmitate oxidation in isolated working ACC2 KO and WT hearts aerobically perfused with or without insulin.*

A: Palmitate oxidation markedly decreased in KO and WT hearts with insulin (*P<0.05 vs. WT baseline; **P<0.05 vs. KO baseline), but was still significantly higher in KO compared to WT (**P<0.05). **B:** In the absence of insulin, glucose oxidation rates were low in both KO and WT hearts. Following the addition of 100 μ U/mL of insulin, glucose oxidation spiked significantly in both groups (*P<0.05 vs. WT baseline; **P<0.05 vs. KO baseline). Values are mean \pm SE and statistical analysis was performed with 1-way ANOVA.

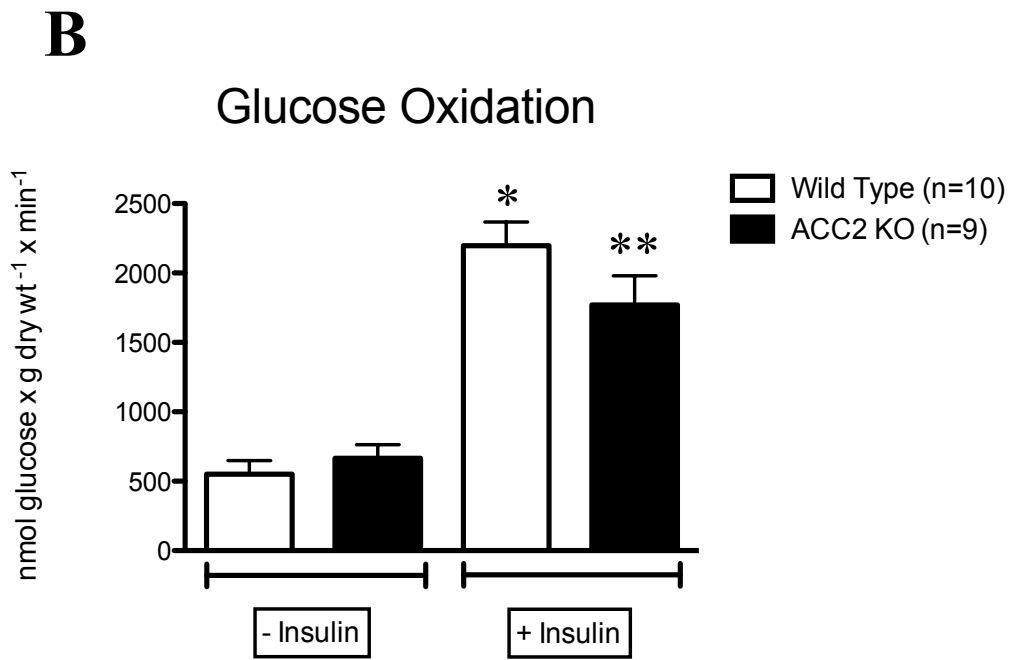
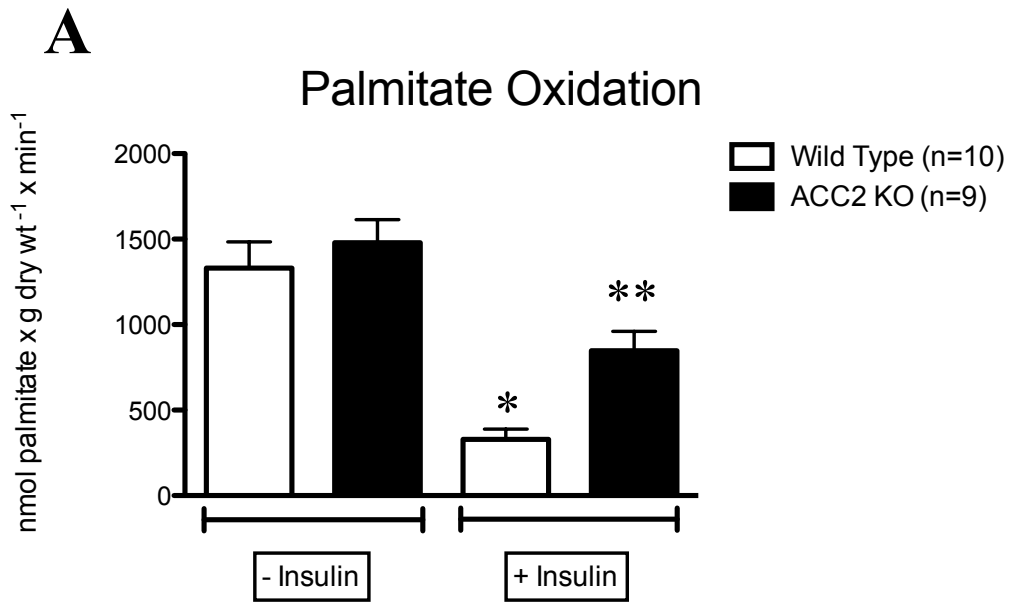


FIGURE 4-2

Figure 4-3: *Cardiac work and efficiency in ACC2 KO and WT hearts during aerobic perfusion with or without insulin.*

A: Cardiac work was unchanged during the course of the perfusions. **B:** TCA acetyl CoA production in WT hearts significantly decreased in the presence of insulin (* $P < 0.05$ vs. baseline; $n = 8-9$). **C:** Cardiac efficiency was calculated as cardiac work per TCA acetyl CoA. The WT hearts were significantly more efficient than their KO counterparts during perfusion with insulin (* $P < 0.05$; $n = 5-7$). Values are mean \pm SE and statistical analysis was performed with 1-way ANOVA.

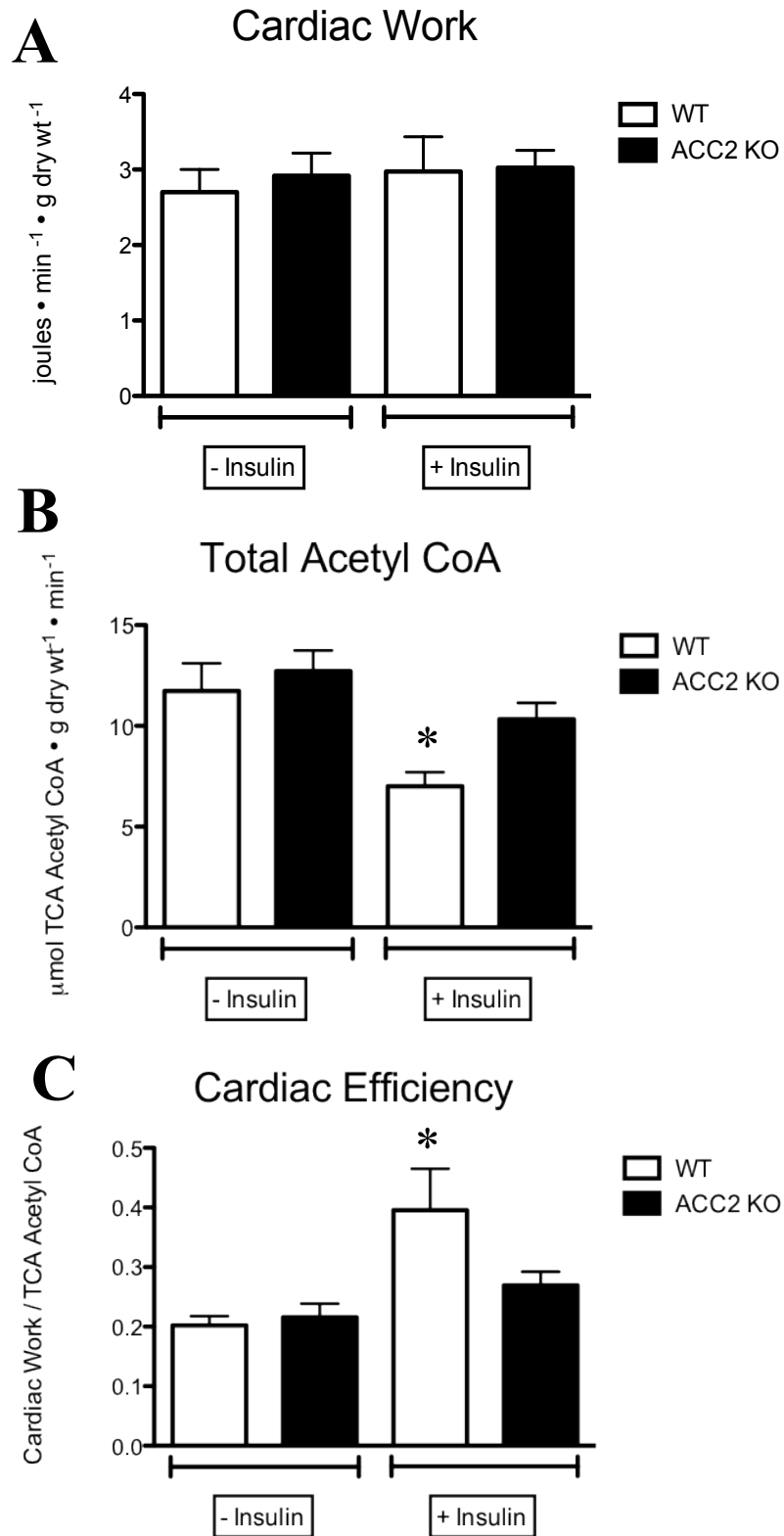


FIGURE 4-3

Figure 4-4: *Short chain CoA analysis of aerobically perfused ACC2 KO and WT heart tissue.*

A: Malonyl CoA levels are significantly lower in the KO hearts compared to WT (*P<0.05; n=6-8). **B:** Acetyl CoA:free CoA is significantly increased in KO hearts (*P<0.05; n=8). Values represent mean \pm SE and statistical analysis was performed with Student's two-tailed *t* test.

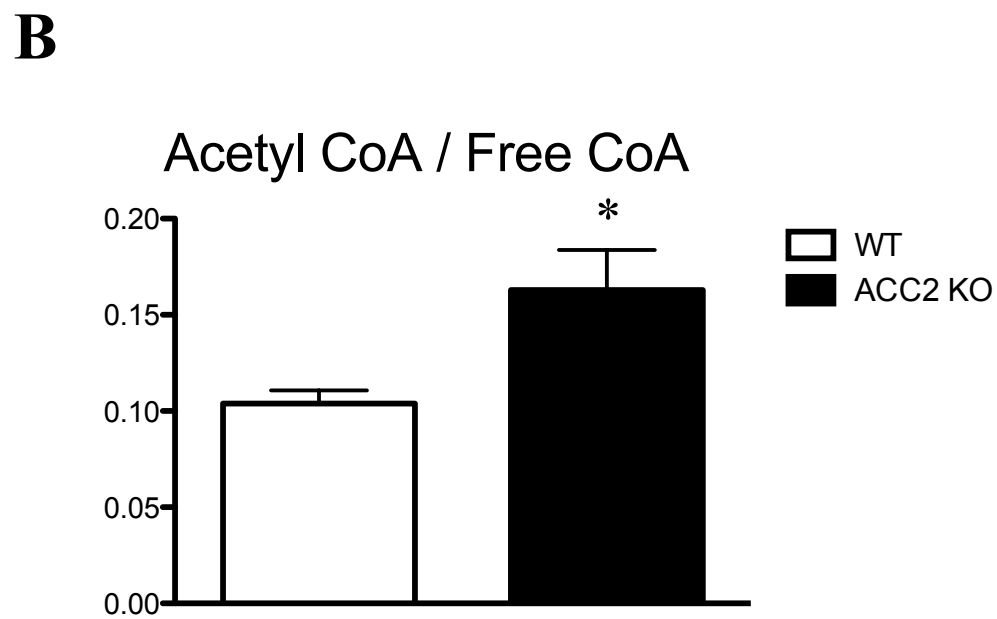
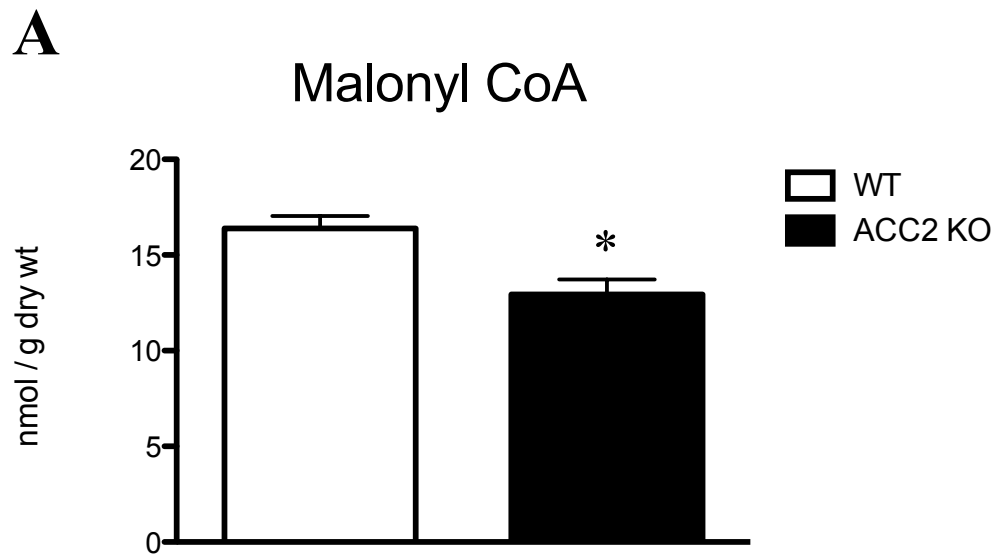
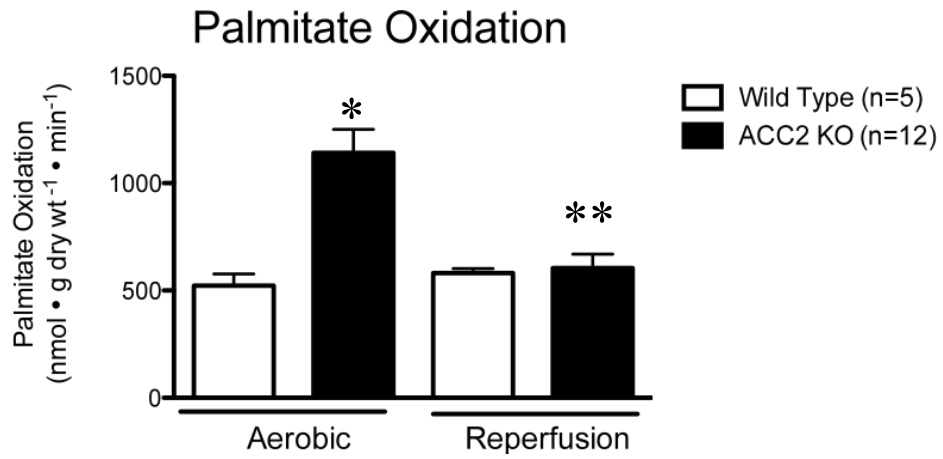
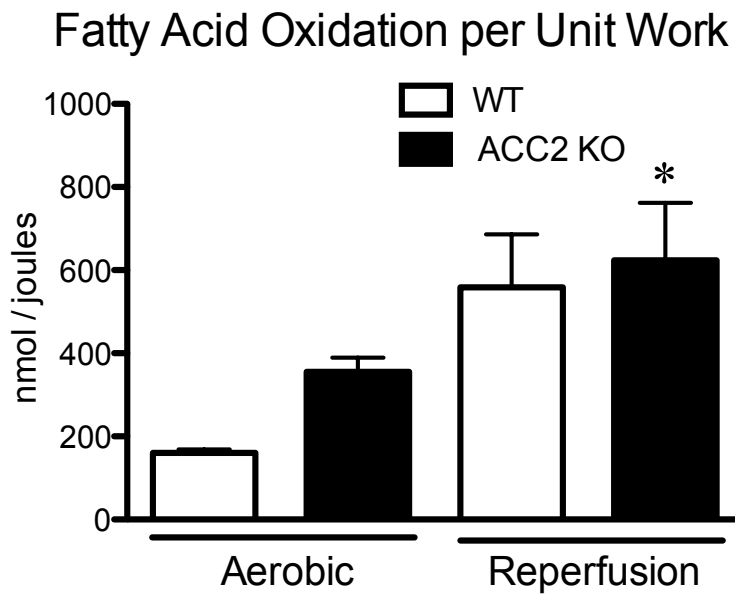


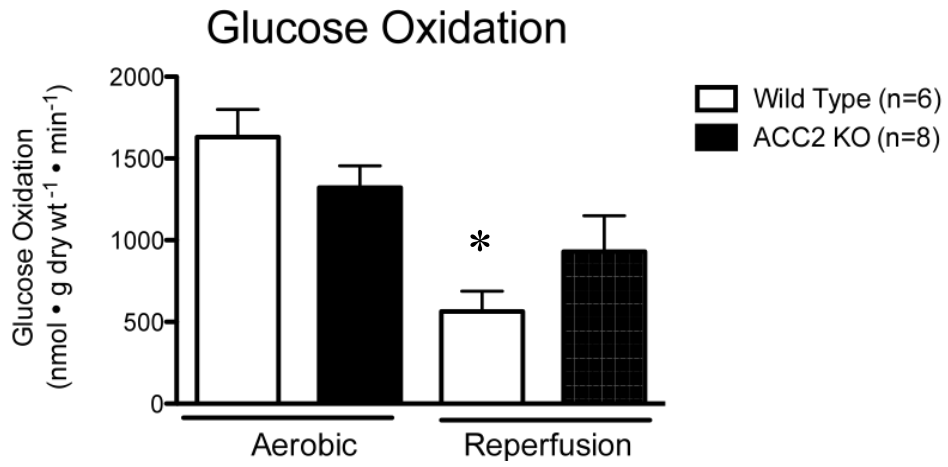
FIGURE 4-4

Figure 4-5: *Cardiac energy metabolism in ACC2 KO and WT isolated working hearts during aerobic and reperfusion periods.*

A: ACC2 KO mice exhibited an elevated rate of palmitate oxidation compared to WT during aerobic perfusions (* $P < 0.001$), which was significantly reduced following ischemia (** $P < 0.001$). Values are mean \pm SE and statistical analysis was performed with 2-way ANOVA. **B:** FAO normalized to cardiac work was significantly elevated during reperfusion in both KO and WT hearts to an equal extent compared to the aerobic values (* $P < 0.05$). **C:** There was a trend for decreased glucose oxidation in ACC2 KO compared to WT in the aerobic phase. Following ischemia glucose oxidation decreased in both KO and WT groups (* $P < 0.001$). Values are mean \pm SE and statistical analysis was performed with 2-way ANOVA. **D:** Glucose oxidation normalized to cardiac work was significantly higher in the WT hearts in reperfusion compared to the aerobic phase (* $P < 0.05$) and a similar trend was observed in the KO hearts. **E:** Lactate oxidation was markedly lower in ACC2 KO compared to WT (* $P < 0.05$) at baseline and was similar to WT in reperfusion. In the reperfusion phase lactate oxidation in WT was significantly reduced relative to the aerobic phase (** $P < 0.05$). Values are mean \pm SE and statistical analysis was performed with 2-way ANOVA. **F:** Rate of glycolysis was slightly higher in ACC2 KO during both aerobic and reperfusion periods compared to WT (not statistically significant). Values are mean \pm SE and statistical analysis was performed with 2-way ANOVA.

A**B****FIGURE 4-5**

C



D

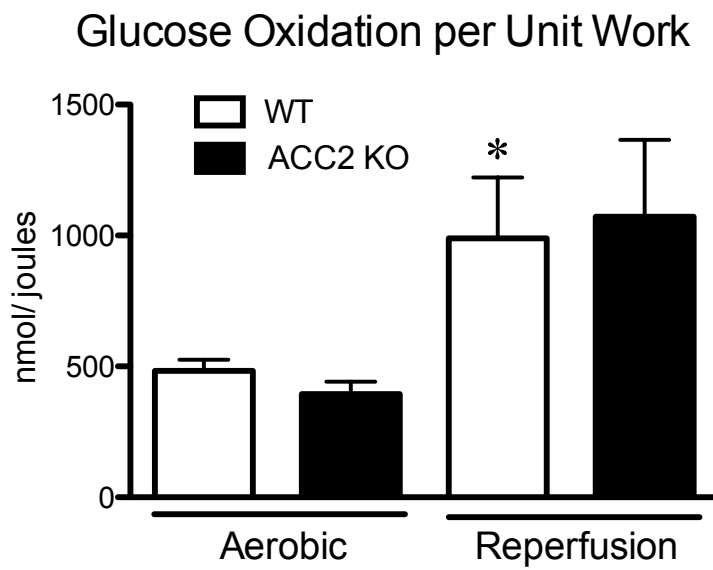


FIGURE 4-5

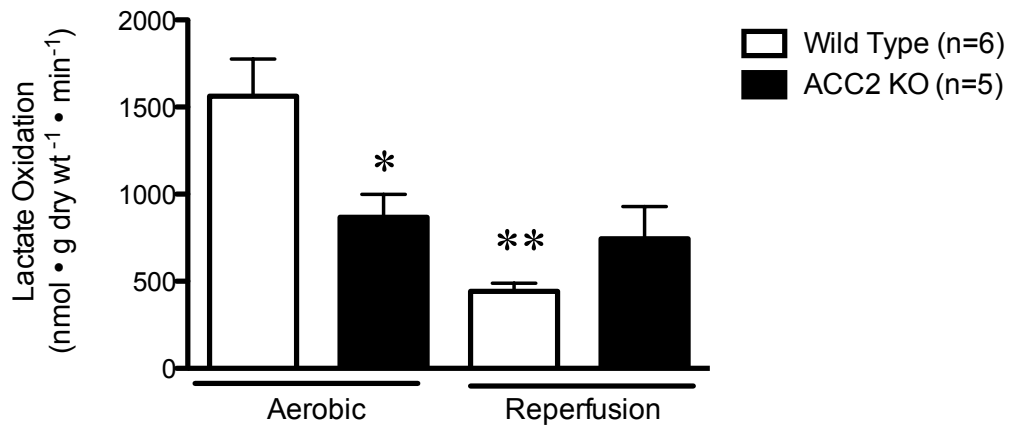
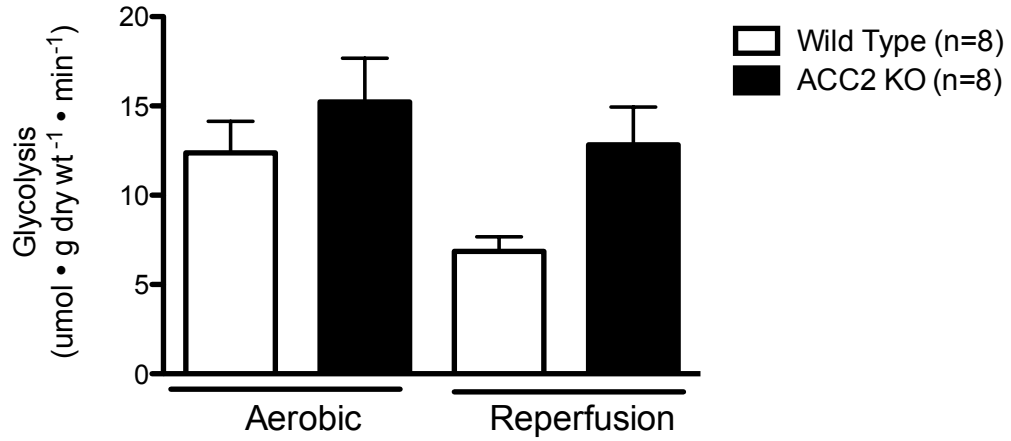
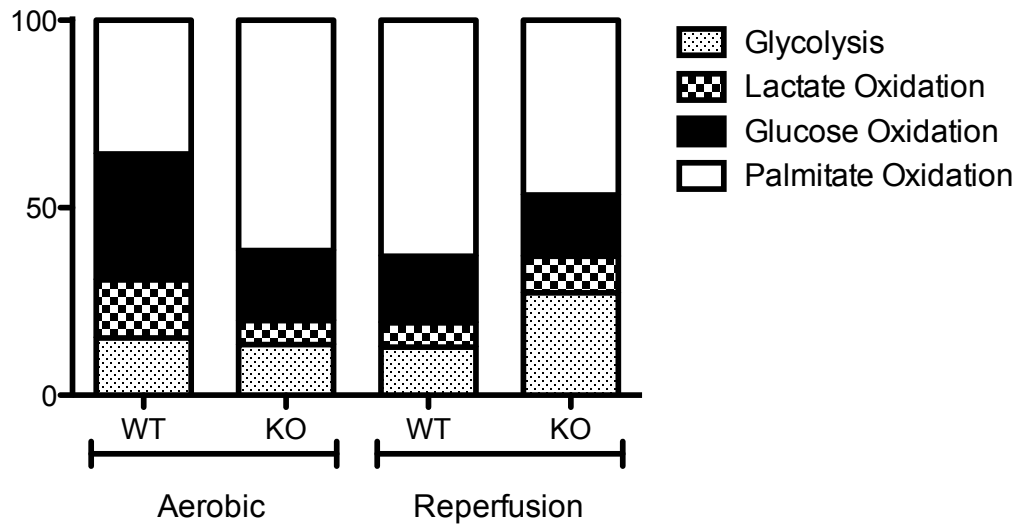
E**Lactate Oxidation****F****Glycolysis****FIGURE 4-5**

Figure 4-6: *ATP and TCA acetyl CoA production in isolated working ACC2 KO and WT hearts during aerobic and reperfusion periods.*

A: Overall contribution to ATP production from glycolysis, glucose, palmitate and lactate oxidation. **B:** Total ATP production significantly decreased during the reperfusion phase in both WT and KO groups compared to the aerobic phase (*P<0.05). **C:** Overall contribution of palmitate, glucose and lactate oxidation to TCA acetyl CoA production. **D:** Total TCA acetyl CoA is also reduced in the reperfusion phase in WT and KO hearts compared to the aerobic period (*P<0.05). Values are mean \pm SE and statistical analysis was performed with 1-way ANOVA (n=5).

A % Relative ATP Production



B

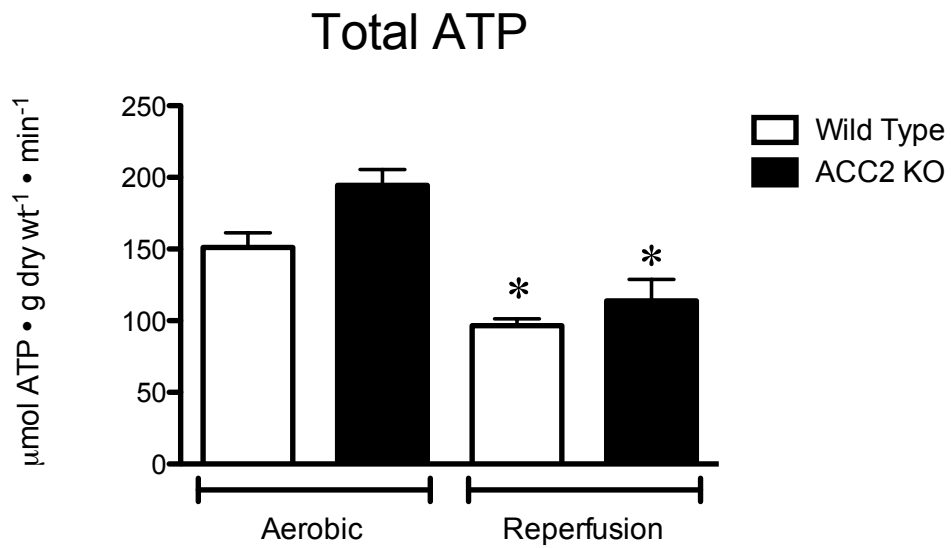


FIGURE 4-6

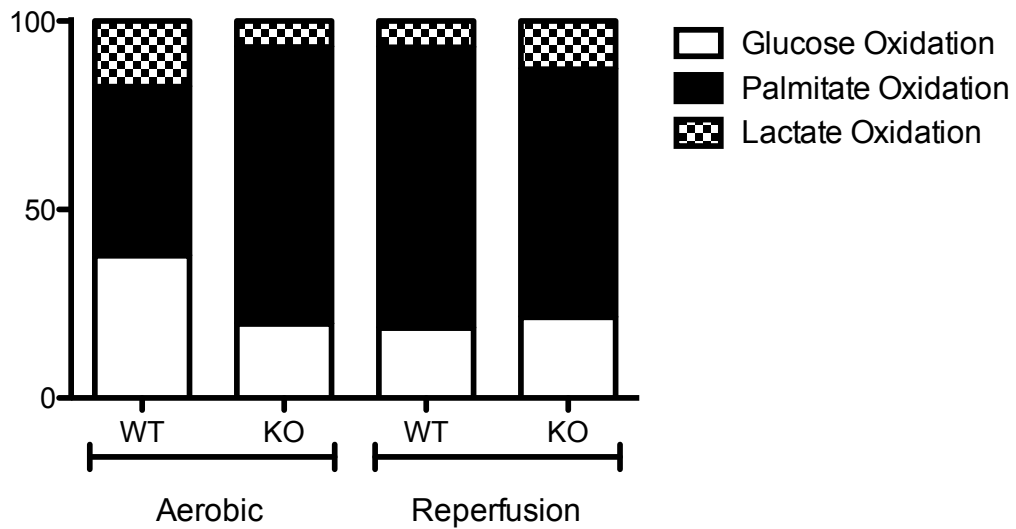
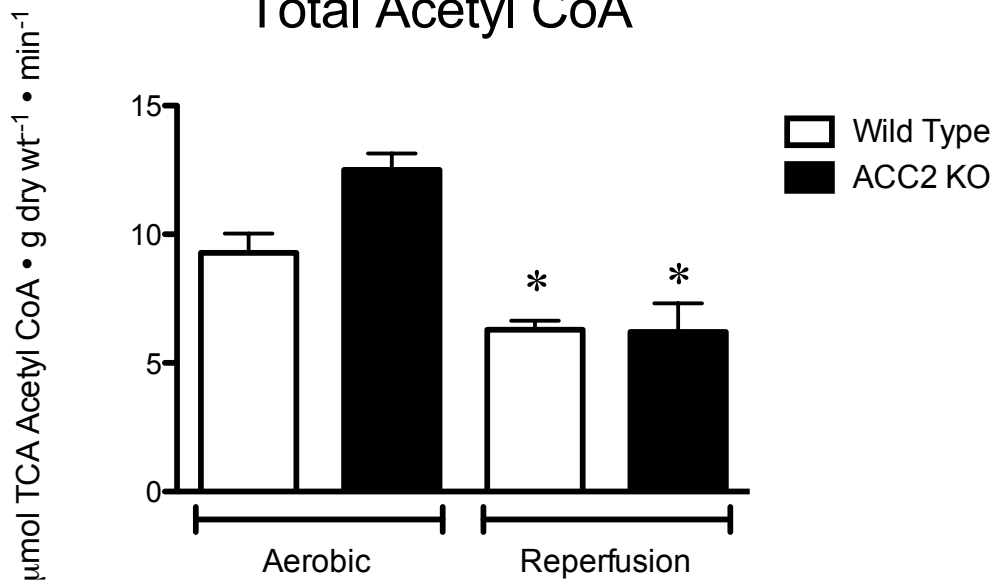
C**% Relative TCA Acetyl CoA****D****Total Acetyl CoA****FIGURE 4-6**

Figure 4-7: *Ex vivo* function in isolated working KO and WT hearts during aerobic perfusion and following ischemia-reperfusion.

A: ACC2 KO and WT mice had similar cardiac work in the aerobic period, but following ischemia cardiac work was slightly higher in KO group (not statistically significant). **B:** Oxygen consumption was consistently higher in the KO during the perfusion (* $P < 0.05$). **C:** Overall, cardiac efficiency in KO was comparable to WT during reperfusion. **D:** Cardiac output was similar across both groups during the perfusion period. Values are mean \pm SE and statistical analysis was performed with 2-way ANOVA (n=10-20).

Cardiac Work

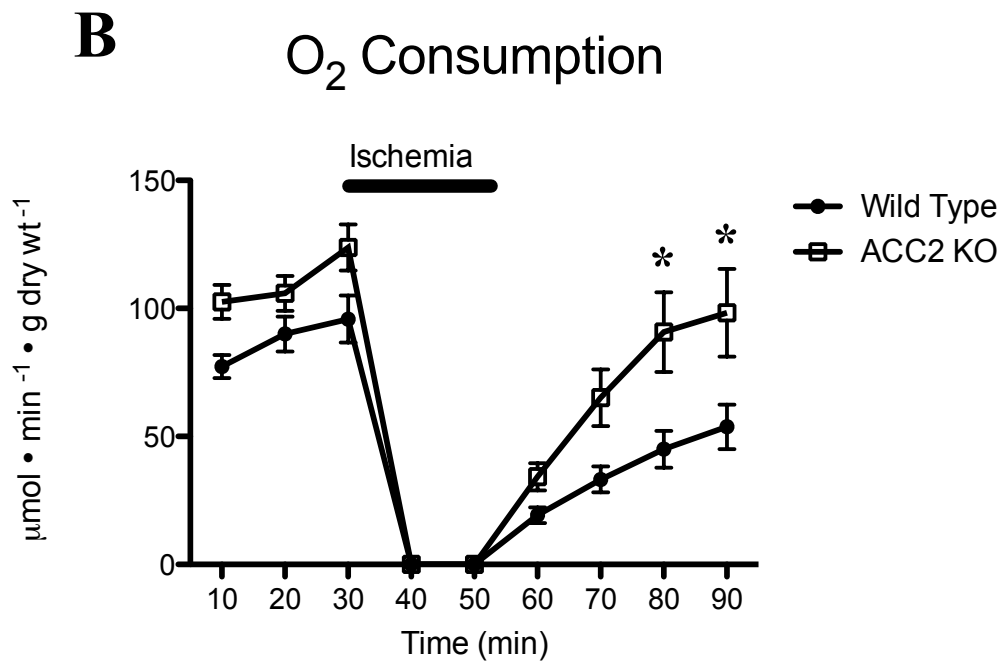
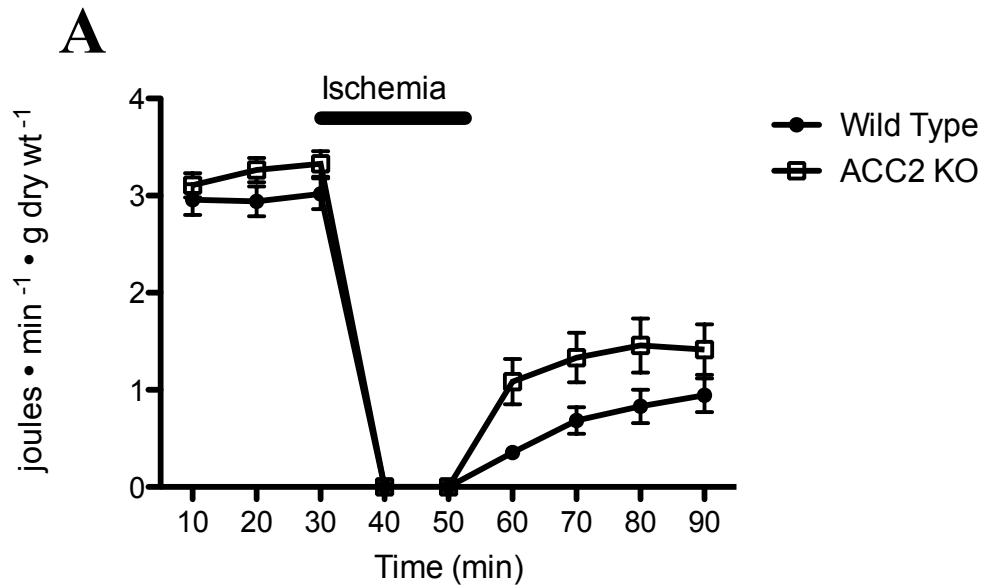


FIGURE 4-7

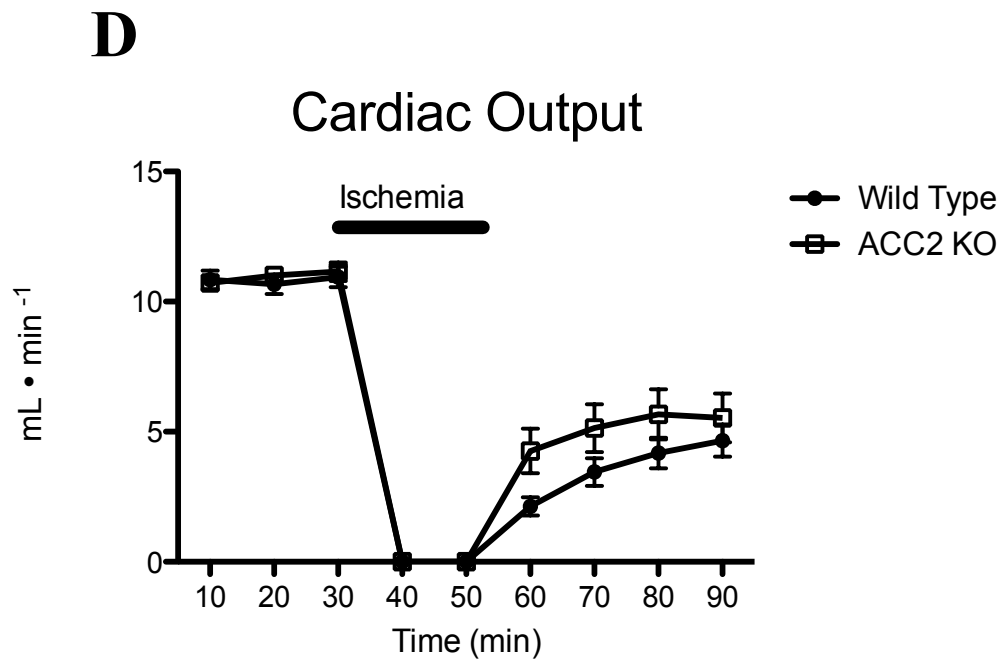
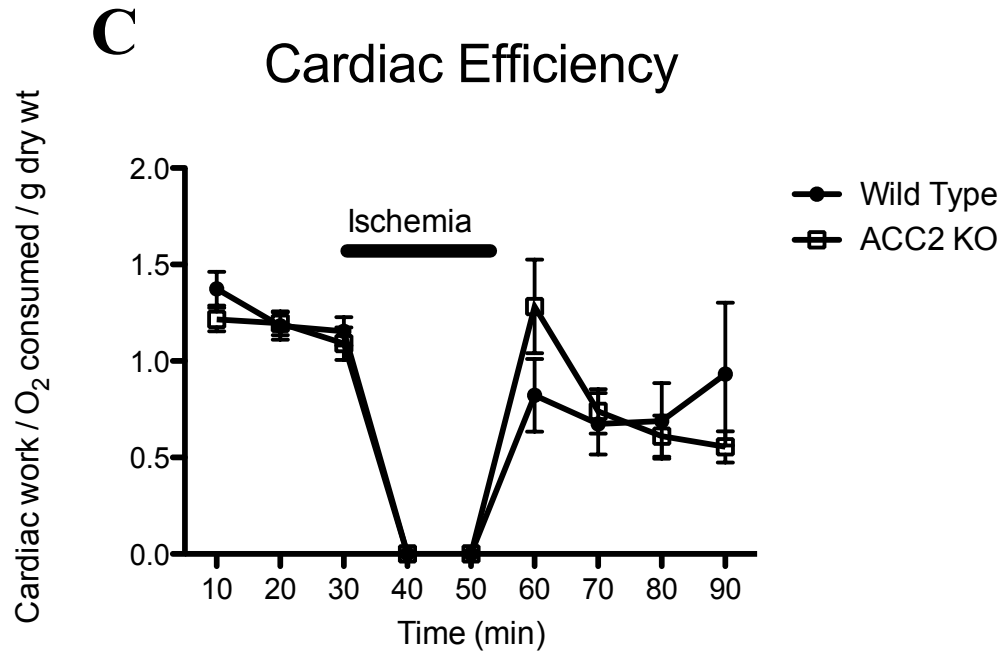


FIGURE 4-7

Table 4-1: *Ex vivo cardiac function in WT and KO hearts during aerobic and post-ischemic phases of isolated working heart perfusions.*

No difference in function was found between KO and WT groups in either aerobic or reperfusion phases. Values are mean \pm SE and statistical analysis was performed with Student's two-tailed *t* test.

	Aerobic	
	Wild Type (n=15)	ACC2 Knockout (n=20)
Heart Rate (bpm)	310±6	314±8
Rate Pressure Product (bpm x mmHg x 10⁻³)	22±0.4	22±0.5
Aortic Flow (mL/min)	7.9±0.3	7.8±0.2
Cardiac Output (mL/min)	10.8±0.4	11.0±0.3
Cardiac Power (mW)	1.4±0.05	1.4±0.04

	Post-Ischemic	
	Wild Type (n=10)	ACC2 Knockout (n=16)
Heart Rate (bpm)	204±25	237±22
Rate Pressure Product (bpm x mmHg x 10⁻³)	11±1.8	14±1.7
Aortic Flow (mL/min)	1.1±0.4	2.2±0.6
Cardiac Output (mL/min)	3.6±0.5	5.2±0.9
Cardiac Power (mW)	0.4±0.1	0.6±0.1

Table 4-1

Figure 4-8: *ACC activity, short chain CoA and triacylglycerol levels in cardiac tissue of ACC2 KO and WT mice following ischemia/reperfusion.*

A: Malonyl CoA levels in heart tissue were similar across both KO and WT mice following ischemia-reperfusion (n=8). **B:** The level of acetyl CoA was markedly elevated in the KO group (*P<0.05). Values are mean \pm SE and statistical analysis was performed with Student's two-tailed *t* test (n=8). **C:** Total ACC activity was measured in heart tissue subject to ischemia-reperfusion. No difference was found between KO and WT groups. Values are mean \pm SE and statistical analysis was performed with Student's two-tailed *t* test (n=10). **D:** Triacylglycerol levels in cardiac tissue were significantly lower in KO mice compared to WT (*P<0.05). Values are mean \pm SE and statistical analysis was performed with Student's two-tailed *t* test (n=5-8).

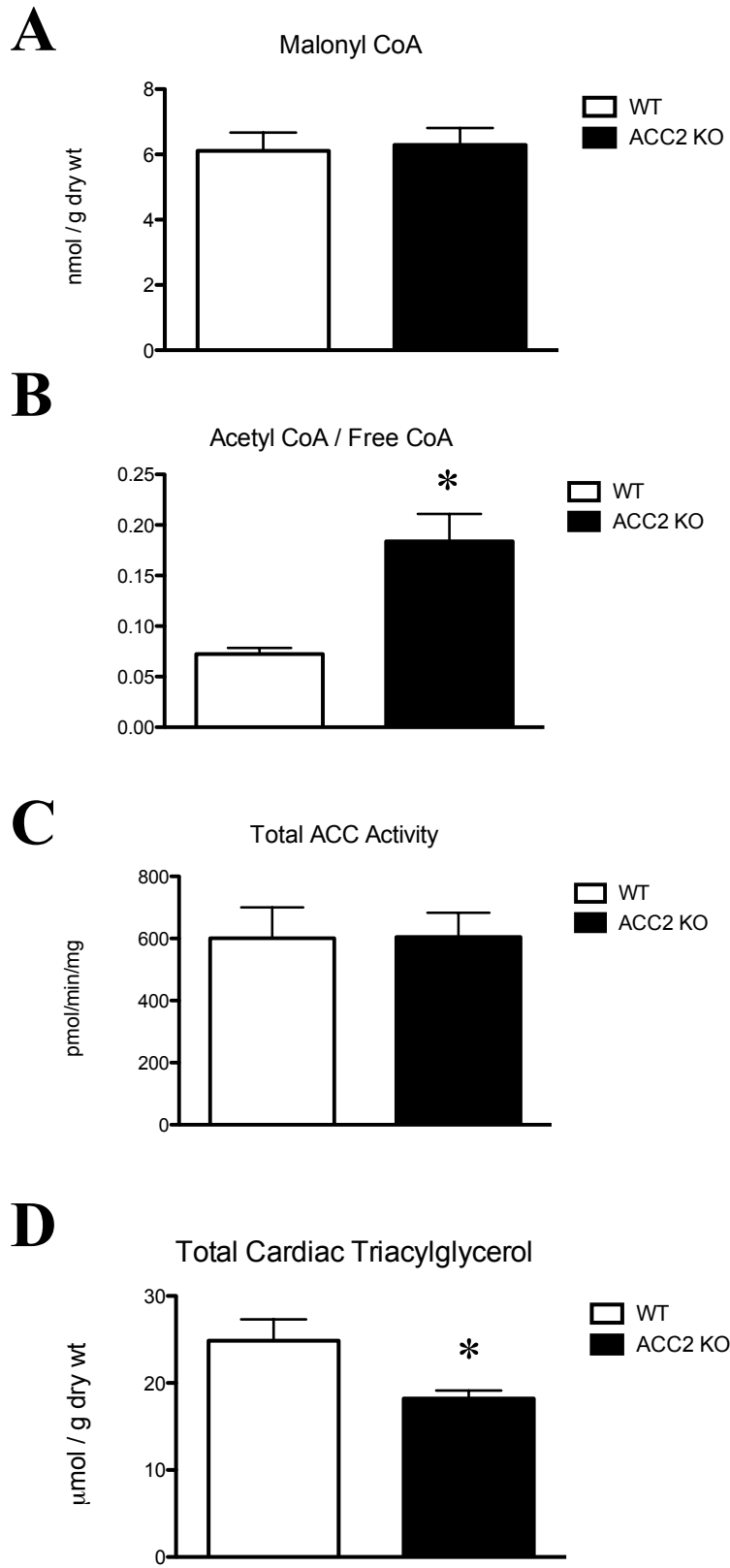


FIGURE 4-8

Figure 4-9: *P-AMPK protein expression in ACC2 KO and WT cardiac tissue.*

A, B: P-AMPK densitometry values are unchanged between ACC2 and WT hearts, while T-AMPK is increased in KO hearts (* $P < 0.05$; $n = 5$; Student's two-tailed t test). **C:** P-AMPK expression, when normalized to T-AMPK, is significantly downregulated in ACC2 KO hearts (* $P < 0.05$; $n = 5$; Student's two-tailed t test). Values represent mean \pm SE.

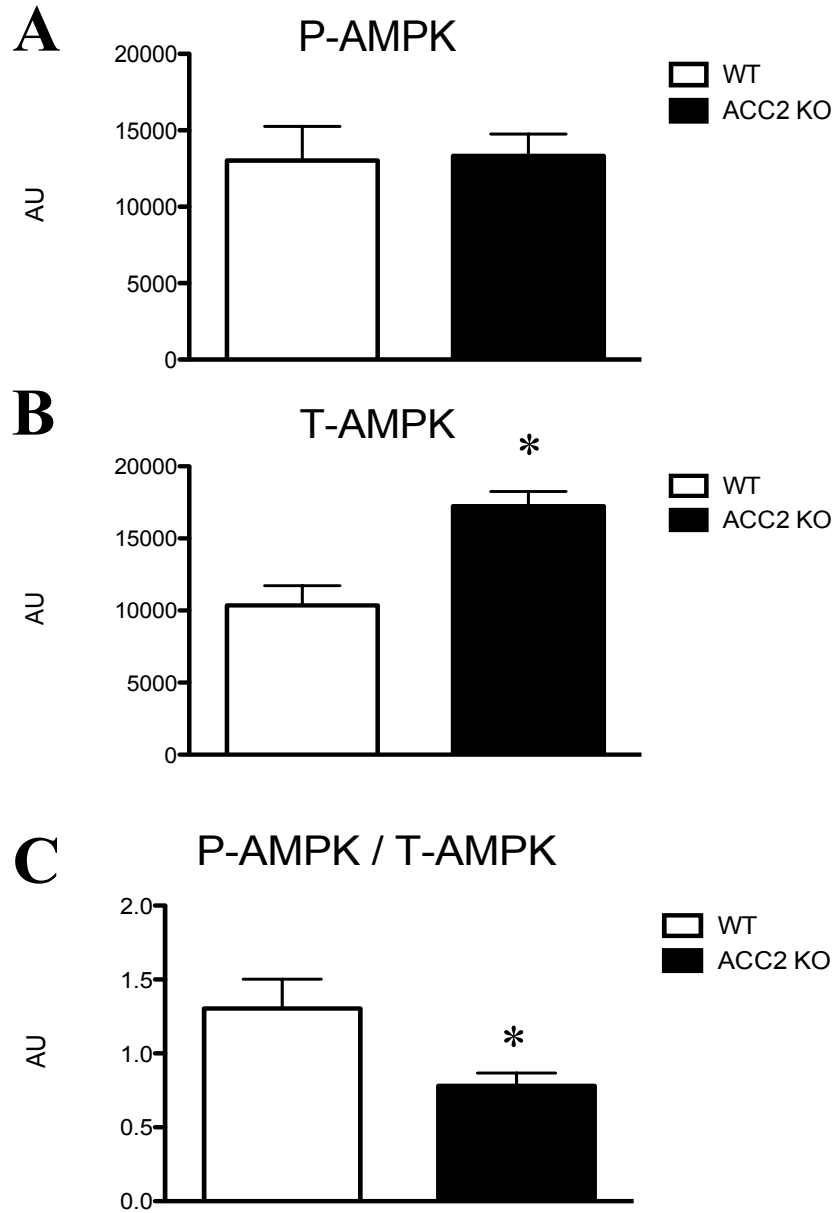
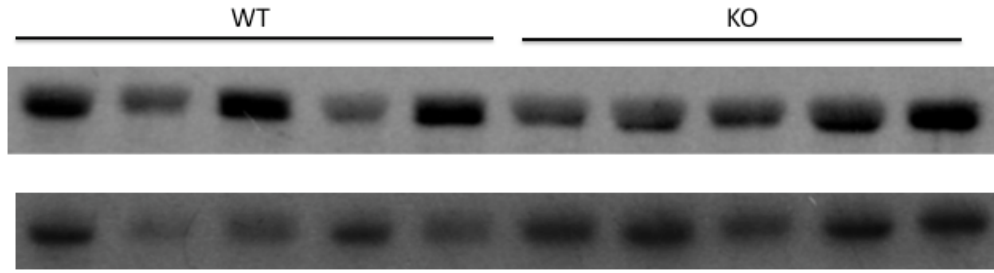


FIGURE 4-9

Figure 4-10: *P-PDH protein expression in ACC2 KO and WT cardiac tissue.*

Western blot analysis of KO and WT cardiac tissue revealed little change in the phosphorylation status of pyruvate dehydrogenase (PDH) following ischemia-reperfusion. Values are represented as mean \pm SE (n=5).

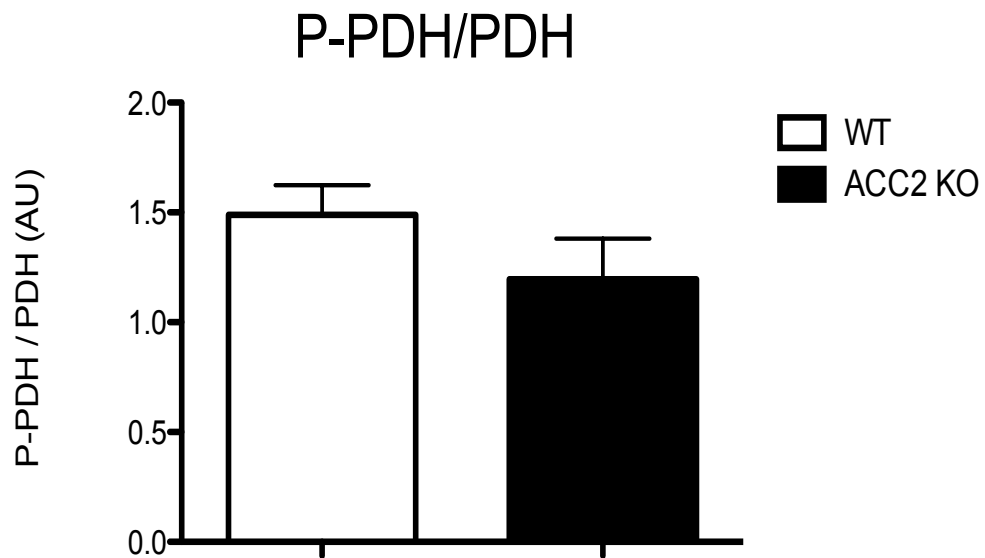
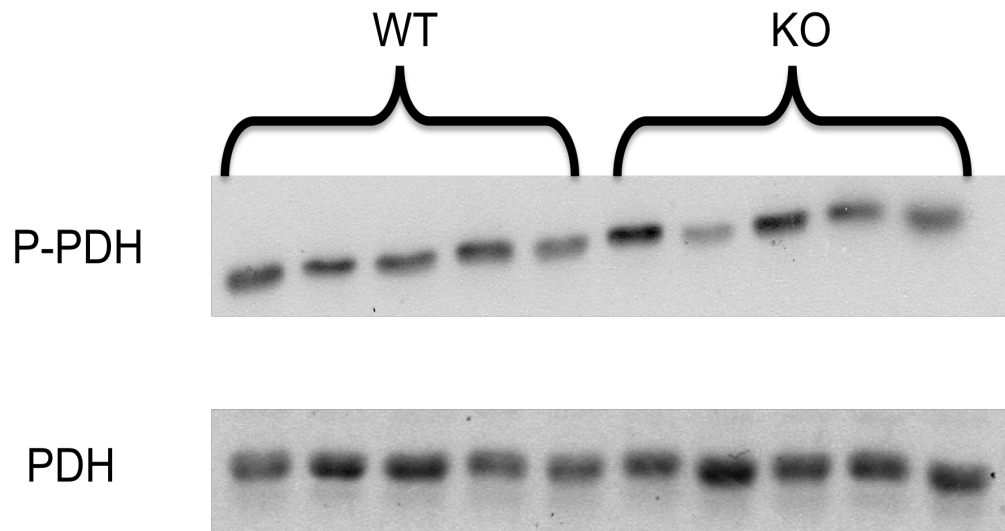


FIGURE 4-10

Figure 4-11: *MCD protein expression in ACC2 KO and WT cardiac tissue.*

Western blot analysis of MCD expression in cardiac tissue showed no difference between WT and KO mice. Values are represented as mean \pm SE (n=5).

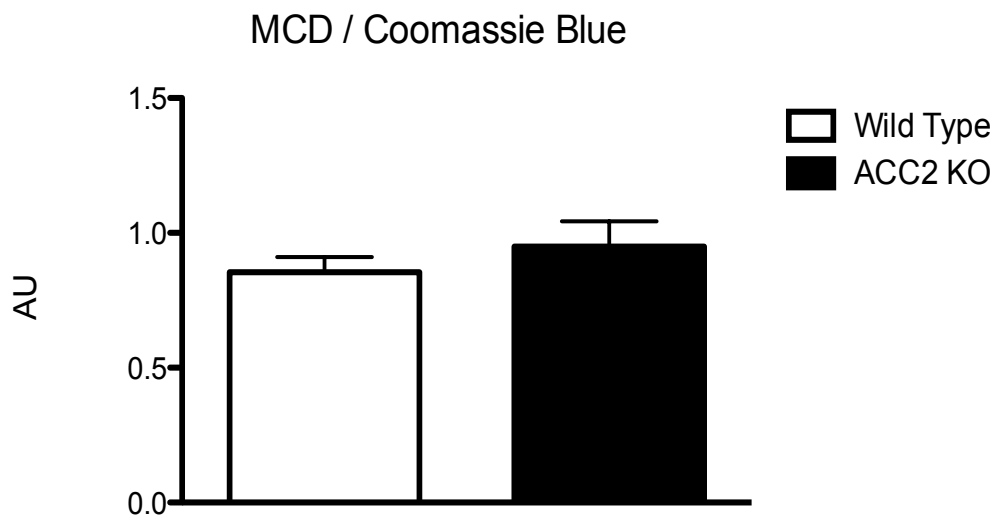
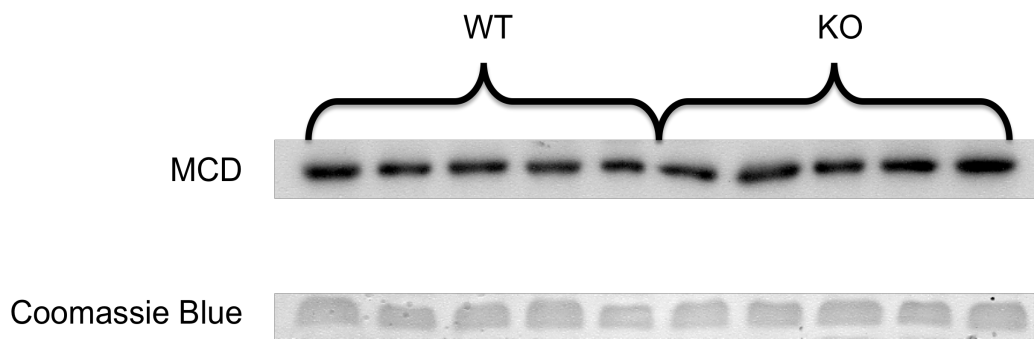


FIGURE 4-11

Discussion

It is well established that obesity is associated with numerous disorders such as type 2 diabetes, liver disease, and cancer, but by far the most prevalent are cardiovascular complications. The relative contributions of glucose and FAO to energy production dictate cardiac function as well as efficiency. In IHD as well as in acute myocardial infarction and early stage heart failure patients, this balance is disturbed and FAO predominates as a source of energy production (4). Therefore, accelerating FAO in these patients could exacerbate cardiac dysfunction. The study evaluated the viability of this therapeutic approach in hearts subject to an ischemic attack. Numerous studies have established that switching the energy source of the heart to fat serves a cardioprotective role and can therefore prevent ischemic injury. For example, in a study by Dyck *et al.*, MCD knockout mice demonstrated a lower rate of FAO, higher glucose oxidation and overall improved cardiac function during and following ischemia (50). This lead to our hypothesis that an ACC activator may be desirable, rather than ACC2 inhibitor, to treat ischemic heart disease because the switch in energy substrate from fatty acid to glucose oxidation would improve cardiac function and preserve cardiac efficiency. However, our data seem to suggest that ACC2 deletion has little detrimental effects on cardiac metabolism and function following an ischemic episode.

Research from our laboratory has previously shown that high rates FAO during reperfusion are, in part, due to low levels of malonyl CoA. The study by Kudo *et al.* reported a 39% drop in cardiac malonyl CoA following ischemia,

which further decreased after reperfusion. The investigators ruled out changes in sensitivity of CPT1 or CPT1 activity as possible contributors to the acceleration of FAO in reperfusion. However, these metabolic changes were associated with lower ACC activity and acetyl CoA (99). The authors explained that the upstream kinase, AMP-activated protein kinase (AMPK), is activated during ischemic stress and subsequently phosphorylates ACC, rendering it inactive. Thus, malonyl CoA levels decline allowing uninhibited uptake of fatty acids into the mitochondria for oxidation (99). In contrast to earlier studies, our study found lower rates of FAO into reperfusion, but after normalizing for cardiac work FAO tended to be higher in reperfusion while malonyl CoA and total ACC activity were maintained.

The preliminary data suggest that a compensatory mechanism may be responsible for the observed metabolic and functional profile. This compensation is likely at the level of ACC1. According to Saddik *et al.*, acetyl CoA supply is a key determinant of ACC activity and therefore malonyl CoA production. They demonstrated this concept by increasing cytosolic acetyl CoA with dichloroacetate, an indirect stimulator of glucose oxidation, which subsequently raised malonyl CoA production (91). The authors explained this observation as a result of the export of mitochondrial acetyl CoA into the cytosol by carnitine acetyltransferase (CAT) and carnitine acetyltranslocase. In this pathway carnitine acetyltransferase transfers acetyl moieties to acetylcarnitine in the mitochondrial matrix, and then carnitine acetyltranslocase shuttles the complex out into the cytosol in exchange for carnitine. Acetylcarnitine is then converted back into acetyl CoA to serve as a substrate for ACC. In terms of kinetics, ACC1 isolated

from adipose tissue had a K_m of 67 μM while ACC2 from cardiac tissue had a K_m of 117 μM (91). The higher affinity of ACC1 for acetyl CoA suggests that substrate availability is an important regulator of enzyme activity. In our study, increased acetyl CoA:CoA levels were measured in KO tissue and even though the assay is unable to distinguish between cytosolic and mitochondrial acetyl CoA, most of the acetyl CoA in the heart is intramitochondrial (91). The increase in acetyl CoA levels can be explained by the elevated rate of palmitate oxidation during the aerobic period. In terms of the malonyl CoA, the aerobic KO hearts had significantly reduced levels, but following aerobic reperfusion of the ischemic heart, we saw that the ischemic heart was able to compensate for low malonyl CoA. In order to elucidate this finding total ACC activity was measured in heart tissue and again we saw similar activity across both KO and WT. This activity assay measures total activity and is unable to decipher ACC1 activity from ACC2 (75), however it can still provide some insight into some of the molecular underpinnings of cardiac metabolism. Since total activity was the same between the groups, it can be inferred that ACC1 is responsible for the total ACC activity in KO mice. The majority of the ACC activity in the heart derives from the ACC2 isoform (100), therefore in the KO heart there may have been a compensatory increase in ACC1 activity, which would account for the increase in malonyl CoA. Elevated levels of malonyl CoA would theoretically inhibit CPT1 and thereby prevent fatty acid uptake into the mitochondrion and subsequent oxidation. Thus, this increase correlates with the reperfusion metabolic data where we see a marked decrease in FAO from aerobic values in KO to rates equivalent to that of

WT. According to the initial study, ACC2 deletion in skeletal muscle resulted in decreased total ACC activity, but FAO and malonyl CoA levels remained similar between KO and WT mice (75). The authors speculated a compensatory mechanism involving the downregulation of MCD might have been responsible for preventing excessive FAO. Our study focused on the heart, and although we did not look at MCD activity, MCD protein expression in the heart was unchanged between the groups (Figure 4-11).

The possible downregulation of P-AMPK in the KO hearts indicates reduced AMPK activation and therefore reduced AMPK-mediated inhibition of ACC. This finding may explain the decreased expression of P-ACC1 in the KO hearts since the activated form of AMPK, P-AMPK, is capable of phosphorylating and thereby inhibiting ACC. Since there is less of the inactivated form of ACC1, this may explain the observed increase in residual ACC activity.

Under aerobic conditions (without insulin), both KO and WT hearts displayed similar rates of glucose and fatty acid oxidation as well as similar cardiac efficiencies. Following the addition of insulin to the perfusate, the KO hearts were unable to efficiently switch to glucose oxidation as fatty acid oxidation remained significantly higher compared to WT. The lower levels of malonyl CoA in the KO hearts can explain this higher rate of palmitate oxidation. Unlike WT hearts, the KO hearts performed less cardiac work per unit TCA acetyl CoA production. As a result, the KO hearts were inefficient under aerobic perfusion with insulin. Even though cardiac efficiency was not compromised in the KO hearts following ischemia, the aerobic study with insulin shows that

knocking out ACC is associated with reduced cardiac efficiency. The difference in cardiac efficiencies between the two groups disappeared following I/R likely stemming from compensation by ACC1, as described above. Even though the KO hearts had increased cardiac work in reperfusion, these hearts were inefficient based on the increase in oxygen consumption.

Some of the limitations of this study include the lack of substantial metabolic and biochemical data immediately following the aerobic period, or at the end of ischemia. For example, ACC activity during the aerobic period is critical as is AMPK. This would provide a chronological picture of the molecular changes associated with the observed changes in cardiac metabolism. At this point, we are only able to compare the data from the nascent hearts in Olson's study to our ischemia-reperfused and aerobic hearts. It would be interesting to see the temporal relationship between FAO, AMPK, malonyl CoA and ACC. Future studies will try to address this and also examine activity of carnitine acetyltransferase in this strain.

Kolwicz *et al.* recently examined the effects of pressure-overload hypertrophy in a mouse model with cardiac-specific deletion of ACC2 (ACC2^{-/-}) (101). The authors concluded that maintaining the normal metabolic phenotype of the heart (by increasing FAO) is beneficial during the development of pathological cardiac hypertrophy. After 8 weeks of transverse aortic constriction (TAC), the ACC2^{-/-} mice had a metabolic profile similar to sham animals in terms of FAO and glucose oxidation, while the control TAC mice exhibited the fetal metabolic profile (reduced FAO and increased glycolysis) (101). The TAC

ACC2^{-/-} mice had lower glycolysis rates than TAC control mice, which might have been due to an increase in mitochondrial energy supply and therefore need for less glycolysis. Furthermore, the perceived benefit may have been due to better coupling of glucose oxidation and glycolysis, which was not as prominent in our study. The authors also reported that chronic elevation of FAO did not adversely affect the heart since lipid supply was maintained in the ACC2^{-/-} mouse hearts (101). This is in contrast to our studies where TAG levels were significantly lower in the KO hearts following I/R. Although these data suggest increasing FAO protects the heart from hypertrophy, it is still unknown whether chronic elevation of FAO is beneficial in other cardiac pathologies, especially in IHD.

Our study is the first to examine cardiac energy metabolism in the ACC2 KO mice in I/R. While it is well established that increased dependence on FAO is associated with poor cardiac function in ischemia, here we see that ACC2 KO hearts are able to maintain proper cardiac function and efficiency, despite increased FAO in the aerobic period. The underlying cause for this observation is the decrease in FAO following reperfusion, which is likely due to the fact that acetyl CoA, derived from fatty acid oxidation, is shuttled out from the mitochondria to the cytosol where it may be used by ACC1 to produce malonyl CoA.

Aerobically, the ACC2 KO hearts have higher rates of fatty acid oxidation and are thereby inefficient in the presence of insulin. Furthermore, these hearts may have decreased activation of AMPK, suggesting less inhibitory action on

ACC. Contrary to previous research on ischemia-reperfusion, which shows that AMPK is activated during ischemia leading to a decrease in malonyl CoA (99), our work suggests that the KO hearts may have an adaptation where basal AMPK expression/activity is suppressed which ultimately prevents the otherwise detrimental increase in fatty acid oxidation. It is this adaptation along with compensation by ACC1 that allows the hearts to evade post-ischemic injury. The compensation at the level of ACC1 may be acute, which warrants further study in a chronic model of ischemic heart disease before accelerating fatty acid oxidation is encouraged for cardiac patients.

CHAPTER 5.

Discussion and Conclusions

Final Conclusions

Considerable progress has been made over the last decade in the development of new therapies to combat cardiovascular disease. Optimizing energy metabolism has demonstrated therapeutic potential in the diseased heart and continues to be an evolving area of study. The metabolic approach to treating heart disease has evolved from a relatively broad concept of minimizing circulating fatty acid levels in the body to a more refined approach focusing on the enzymatic machinery in the metabolic pathway. Recent advances have led to the development of pharmacological agents targeting specific enzymes such as FAT/CD36, CPT1, MCD, 3-KAT, PDH and PDK. Currently, several metabolic therapies are used as adjunct treatments in heart disease and recent studies suggest that metabolic modulation could become a mainstay in the treatment of cardiovascular disease.

This thesis demonstrates the therapeutic potential of metabolic modulation in PAH, but also presents an aspect of metabolic modulation that may not be beneficial in IHD. Metabolic modulation in PAH holds promise as a treatment option for the associated cardiovascular morbidities. Our data show that DCA can restore oxidative metabolism in RVH and thereby improve the underlying cardiac dysfunction in PAH. On the other hand, modulation of ACC highlights the potential for myocardial injury in IHD. Our data show that knocking out ACC2 leads to inefficient hearts under normal aerobic perfusion, but an adaptation in the AMPK-ACC-malonyl CoA pathway protects these hearts from ischemic injury.

While metabolic modulation of PDK is promising, modulation of ACC requires more scrutiny before implementing this strategy.

Future Directions

As discussed in the preceding chapters, our findings have created some new avenues of research. For the PAH study, future experiments could include extending the acute DCA treatment time to 60 min in order to observe functional changes in the FH hearts. Novel PDK inhibitors with superior pharmacokinetics can also be studied. In addition, further examination of the molecular switch behind the glycolytic phenotype is crucial. Specifically, investigating FOXO-1 upregulation and how modifying this transcription factor can prevent the metabolic disturbance in PAH. As mentioned earlier, restoring glucose oxidation at the expense of fatty acid oxidation is garnering attention, thus it will be interesting to examine the utility of novel metabolic modulators in PAH.

For the ACC2 KO study, it is still premature to claim that inhibiting this enzyme is beneficial for the cardiac patient. It will be important to first track the metabolic changes in the KO strain in order to determine the origin of the compensation/adaptation. Additional isolated working heart perfusions as well as biochemical assays (i.e. Western blot, short chain CoA, ACC, AMPK activity assays) at different time points will be helpful in determining the temporal changes in oxidative metabolism. In addition, studying this phenotype in a different model of heart disease (i.e. myocardial infarction) will enhance our

understanding of how changes in ACC2 and fatty acid oxidation can impact the heart in different disease states. Aside from the heart, ACC2 is also highly expressed in skeletal muscle. Thus, future studies focusing on skeletal muscle fatty acid oxidation and insulin resistance could also be considered.

CHAPTER 6.

References

References

1. Klabunde, R.E. *Cardiovascular pharmacology concepts*. (2008). Retrieved November 20, 2008, from <http://cvpharmacology.com/index.html>.
2. World Health Organization. *Cardiovascular disease*. (2012). Retrieved August 7, 2012, from http://www.who.int/cardiovascular_diseases/en/.
3. Ussher JR, Lopaschuk GD. Targeting malonyl CoA inhibition of mitochondrial fatty acid uptake as an approach to treat cardiac ischemia/reperfusion. *Basic Res Cardiol* 2009;104:203-10.
4. Ussher JR, Lopaschuk GD. The malonyl CoA axis as a potential target for treating ischaemic heart disease. *Cardiovasc Res* 2008;79:259-68.
5. Di Lisa, F., Barbato, R., Menabo, R., & Siliprandi, N. (1995). Carnitine and carnitine esters in mitochondrial metabolism and function. In J.W. de Jong & R. Ferrari (Eds.), *The carnitine system: A new therapeutical approach to cardiovascular disease* (p. 21-38). Dordrecht: Kluwer Academic Publishers.
6. Lopaschuk GD, Stanley WC. Malonyl-CoA decarboxylase inhibition as a novel approach to treat ischemic heart disease. *Cardiovasc Drugs Ther* 2006;20:433-9.
7. Sung MM, Koonen DP, Soltys CL, Jacobs RL, Febbraio M, Dyck JR. Increased CD36 expression in middle-aged mice contributes to obesity-related cardiac hypertrophy in the absence of cardiac dysfunction. *J Mol Med (Berl)* 2011;89:459-69.
8. Lopaschuk GD, Ussher JR, Folmes CD, Jaswal JS, Stanley WC. Myocardial fatty acid metabolism in health and disease. *Physiol Rev* 2010;90:207-58.
9. Bremer, J. (1995). Carnitine-dependent pathways in heart muscle. In J.W. de Jong & R. Ferrari (Eds.), *The carnitine system: A new therapeutical approach to cardiovascular disease* (p. 7-20). Dordrecht: Kluwer Academic Publishers.
10. Kerner J, Hoppel C. Fatty acid import into mitochondria. *Biochim Biophys Acta* 2000;1486:1-17.
11. Jong, de J.W., & Ferrari, R. (1995). Introduction. In J.W. de Jong & R. Ferrari (Eds.), *The carnitine system: A new therapeutical approach to cardiovascular disease* (p. 1-3). Dordrecht: Kluwer Academic Publishers.
12. Hainline, B.E., & Wappner, R.S. (2006). Disorders of mitochondrial fatty acid oxidation: Carnitine palmitoyl transferase I and carnitine palmitoyl transferase II deficiencies. In J.A. McMillan, R.D. Feigin, C. DeAngelis, & M.D. Jones. (Eds.), *Oski's pediatrics*. Lippincott Williams & Wilkins. Retrieved from Books@Ovid.
13. Schulz H. Regulation of fatty acid oxidation in heart. *J Nutr* 1994;124:165-71.
14. Van Der Vusse, G.J. (1995). Accumulation of fatty acids and their carnitine derivatives during myocardial ischemia. In J.W. de Jong & R. Ferrari (Eds.), *The carnitine system: A new therapeutical approach to*

- cardiovascular disease* (p. 53-68). Dordrecht: Kluwer Academic Publishers.
15. Stanley WC, Recchia FA, Lopaschuk GD. Myocardial substrate metabolism in the normal and failing heart. *Physiol Rev* 2005;85:1093-129.
 16. Stanley WC, Lopaschuk GD, McCormack JG. Regulation of energy substrate metabolism in the diabetic heart. *Cardiovasc Res* 1997;34:25-33.
 17. McGarry JD, Brown NF. The mitochondrial carnitine palmitoyltransferase system. From concept to molecular analysis. *Eur J Biochem* 1997;244:1-14.
 18. Fraser F, Padovese R, Zammit VA. Distinct kinetics of carnitine palmitoyltransferase i in contact sites and outer membranes of rat liver mitochondria. *J Biol Chem* 2001;276:20182-5.
 19. Folmes CD, Lopaschuk GD. Role of malonyl-CoA in heart disease and the hypothalamic control of obesity. *Cardiovasc Res* 2007;73:278-87.
 20. Lopaschuk GD, Folmes CD, Stanley WC. Cardiac energy metabolism in obesity. *Circ Res* 2007;101:335-47.
 21. Saggerson D. Malonyl-CoA, a key signaling molecule in mammalian cells. *Annu Rev Nutr* 2008;28:253-72.
 22. Yue TL, Bao W, Jucker BM, et al. Activation of peroxisome proliferator-activated receptor-alpha protects the heart from ischemia/reperfusion injury. *Circulation* 2003;108:2393-9.
 23. Campbell FM, Kozak R, Wagner A, et al. A role for peroxisome proliferator-activated receptor alpha (PPARalpha) in the control of cardiac malonyl-CoA levels: reduced fatty acid oxidation rates and increased glucose oxidation rates in the hearts of mice lacking PPARalpha are associated with higher concentrations of malonyl-CoA and reduced expression of malonyl-CoA decarboxylase. *J Biol Chem* 2002;277:4098-103.
 24. Stanley WC, Lopaschuk GD, Hall JL, McCormack JG. Regulation of myocardial carbohydrate metabolism under normal and ischaemic conditions. Potential for pharmacological interventions. *Cardiovasc Res* 1997;33:243-57.
 25. Stanley WC, Hernandez LA, Spires D, Bringas J, Wallace S, McCormack JG. Pyruvate dehydrogenase activity and malonyl CoA levels in normal and ischemic swine myocardium: effects of dichloroacetate. *J Mol Cell Cardiol* 1996;28:905-14.
 26. Randle PJ, Garland PB, Hales CN, Newsholme EA. The glucose fatty-acid cycle. Its role in insulin sensitivity and the metabolic disturbances of diabetes mellitus. *Lancet* 1963;1:785-9.
 27. Opie LH. Myocardial ischemia, reperfusion and cytoprotection. *Rev Port Cardiol* 1996;15:703-8.
 28. Liu Q, Docherty JC, Rendell JC, Clanachan AS, Lopaschuk GD. High levels of fatty acids delay the recovery of intracellular pH and cardiac efficiency in post-ischemic hearts by inhibiting glucose oxidation. *J Am Coll Cardiol* 2002;39:718-25.

29. Avkiran M, Marber MS. Na(+)/H(+) exchange inhibitors for cardioprotective therapy: progress, problems and prospects. *J Am Coll Cardiol* 2002;39:747-53.
30. Lopaschuk GD. Targets for modulation of fatty acid oxidation in the heart. *Curr Opin Investig Drugs* 2004;5:290-4.
31. Piao L, Fang YH, Cadete VJ, et al. The inhibition of pyruvate dehydrogenase kinase improves impaired cardiac function and electrical remodeling in two models of right ventricular hypertrophy: resuscitating the hibernating right ventricle. *J Mol Med (Berl)* 2010;88:47-60.
32. Bonnet S, Michelakis ED, Porter CJ, et al. An abnormal mitochondrial-hypoxia inducible factor-1alpha-Kv channel pathway disrupts oxygen sensing and triggers pulmonary arterial hypertension in fawn hooded rats: similarities to human pulmonary arterial hypertension. *Circulation* 2006;113:2630-41.
33. Gomez A, Bialostozky D, Zajarias A, et al. Right ventricular ischemia in patients with primary pulmonary hypertension. *J Am Coll Cardiol* 2001;38:1137-42.
34. Piao L, Marsboom G, Archer SL. Mitochondrial metabolic adaptation in right ventricular hypertrophy and failure. *J Mol Med (Berl)* 2010;88:1011-20.
35. Fang YH, Piao L, Hong Z, et al. Therapeutic inhibition of fatty acid oxidation in right ventricular hypertrophy: exploiting Randle's cycle. *J Mol Med (Berl)* 2012;90:31-43.
36. Warburg O. On the origin of cancer cells. *Science* 1956;123:309-14.
37. Oikawa M, Kagaya Y, Otani H, et al. Increased [18F]fluorodeoxyglucose accumulation in right ventricular free wall in patients with pulmonary hypertension and the effect of epoprostenol. *J Am Coll Cardiol* 2005;45:1849-55.
38. Mattson DL, Kunert MP, Roman RJ, Jacob HJ, Cowley AW, Jr. Substitution of chromosome 1 ameliorates L-NAME hypertension and renal disease in the fawn-hooded hypertensive rat. *Am J Physiol Renal Physiol* 2005;288:F1015-22.
39. Morrell NW, Yang X, Upton PD, et al. Altered growth responses of pulmonary artery smooth muscle cells from patients with primary pulmonary hypertension to transforming growth factor-beta(1) and bone morphogenetic proteins. *Circulation* 2001;104:790-5.
40. Nagaoka T, Muramatsu M, Sato K, McMurtry I, Oka M, Fukuchi Y. Mild hypoxia causes severe pulmonary hypertension in fawn-hooded but not in Tester Moriyama rats. *Respir Physiol* 2001;127:53-60.
41. Sato K, Webb S, Tucker A, et al. Factors influencing the idiopathic development of pulmonary hypertension in the fawn hooded rat. *Am Rev Respir Dis* 1992;145:793-7.
42. Lam A, Lopaschuk GD. Anti-anginal effects of partial fatty acid oxidation inhibitors. *Curr Opin Pharmacol* 2007;7:179-85.
43. Lee L, Horowitz J, Frenneaux M. Metabolic manipulation in ischaemic heart disease, a novel approach to treatment. *Eur Heart J* 2004;25:634-41.

44. Lopaschuk GD, Wall SR, Olley PM, Davies NJ. Etomoxir, a carnitine palmitoyltransferase I inhibitor, protects hearts from fatty acid-induced ischemic injury independent of changes in long chain acylcarnitine. *Circ Res* 1988;63:1036-43.
45. Lopaschuk GD, McNeil GF, McVeigh JJ. Glucose oxidation is stimulated in reperfused ischemic hearts with the carnitine palmitoyltransferase I inhibitor, Etomoxir. *Mol Cell Biochem* 1989;88:175-9.
46. Schmidt-Schweda S, Holubarsch C. First clinical trial with etomoxir in patients with chronic congestive heart failure. *Clin Sci (Lond)* 2000;99:27-35.
47. Holubarsch CJ, Rohrbach M, Karrasch M, et al. A double-blind randomized multicentre clinical trial to evaluate the efficacy and safety of two doses of etomoxir in comparison with placebo in patients with moderate congestive heart failure: the ERGO (etomoxir for the recovery of glucose oxidation) study. *Clin Sci (Lond)* 2007;113:205-12.
48. Horowitz JD, Sia ST, Macdonald PS, Goble AJ, Louis WJ. Perhexiline maleate treatment for severe angina pectoris--correlations with pharmacokinetics. *Int J Cardiol* 1986;13:219-29.
49. Lee L, Campbell R, Scheuermann-Freestone M, et al. Metabolic modulation with perhexiline in chronic heart failure: a randomized, controlled trial of short-term use of a novel treatment. *Circulation* 2005;112:3280-8.
50. Dyck JR, Hopkins TA, Bonnet S, et al. Absence of malonyl coenzyme A decarboxylase in mice increases cardiac glucose oxidation and protects the heart from ischemic injury. *Circulation* 2006;114:1721-8.
51. Dyck JR, Cheng JF, Stanley WC, et al. Malonyl coenzyme a decarboxylase inhibition protects the ischemic heart by inhibiting fatty acid oxidation and stimulating glucose oxidation. *Circ Res* 2004;94:e78-84.
52. Stanley WC, Morgan EE, Huang H, et al. Malonyl-CoA decarboxylase inhibition suppresses fatty acid oxidation and reduces lactate production during demand-induced ischemia. *Am J Physiol Heart Circ Physiol* 2005;289:H2304-9.
53. Kantor PF, Lucien A, Kozak R, Lopaschuk GD. The antianginal drug trimetazidine shifts cardiac energy metabolism from fatty acid oxidation to glucose oxidation by inhibiting mitochondrial long-chain 3-ketoacyl coenzyme A thiolase. *Circ Res* 2000;86:580-8.
54. Chazov EI, Lepakchin VK, Zharova EA, et al. Trimetazidine in Angina Combination Therapy--the TACT study: trimetazidine versus conventional treatment in patients with stable angina pectoris in a randomized, placebo-controlled, multicenter study. *Am J Ther* 2005;12:35-42.
55. Ciapponi A, Pizarro R, Harrison J. Trimetazidine for stable angina. *Cochrane Database Syst Rev* 2005:CD003614.
56. Szwed H, Sadowski Z, Elikowski W, et al. Combination treatment in stable effort angina using trimetazidine and metoprolol: results of a

- randomized, double-blind, multicentre study (TRIMPOL II). TRIMetazidine in POLand. *Eur Heart J* 2001;22:2267-74.
57. Fragasso G, Salerno A, Spoladore R, Bassanelli G, Arioli F, Margonato A. Metabolic therapy of heart failure. *Curr Pharm Des* 2008;14:2582-91.
 58. Folmes CD, Clanachan AS, Lopaschuk GD. Fatty acid oxidation inhibitors in the management of chronic complications of atherosclerosis. *Curr Atheroscler Rep* 2005;7:63-70.
 59. McCormack JG, Barr RL, Wolff AA, Lopaschuk GD. Ranolazine stimulates glucose oxidation in normoxic, ischemic, and reperfused ischemic rat hearts. *Circulation* 1996;93:135-42.
 60. Belardinelli L, Shryock JC, Fraser H. Inhibition of the late sodium current as a potential cardioprotective principle: effects of the late sodium current inhibitor ranolazine. *Heart* 2006;92 Suppl 4:iv6-iv14.
 61. Morrow DA, Scirica BM, Chaitman BR, et al. Evaluation of the glycometabolic effects of ranolazine in patients with and without diabetes mellitus in the MERLIN-TIMI 36 randomized controlled trial. *Circulation* 2009;119:2032-9.
 62. Gralinski MR, Black SC, Kilgore KS, Chou AY, McCormack JG, Lucchesi BR. Cardioprotective effects of ranolazine (RS-43285) in the isolated perfused rabbit heart. *Cardiovasc Res* 1994;28:1231-7.
 63. Chandler MP, Stanley WC, Morita H, et al. Short-term treatment with ranolazine improves mechanical efficiency in dogs with chronic heart failure. *Circ Res* 2002;91:278-80.
 64. Zacharowski K, Blackburn B, Thiemermann C. Ranolazine, a partial fatty acid oxidation inhibitor, reduces myocardial infarct size and cardiac troponin T release in the rat. *Eur J Pharmacol* 2001;418:105-10.
 65. Chaitman BR, Skettino SL, Parker JO, et al. Anti-ischemic effects and long-term survival during ranolazine monotherapy in patients with chronic severe angina. *J Am Coll Cardiol* 2004;43:1375-82.
 66. Stone PH, Gratsiansky NA, Blokhin A, Huang IZ, Meng L. Antianginal efficacy of ranolazine when added to treatment with amlodipine: the ERICA (Efficacy of Ranolazine in Chronic Angina) trial. *J Am Coll Cardiol* 2006;48:566-75.
 67. Wilson SR, Scirica BM, Braunwald E, et al. Efficacy of ranolazine in patients with chronic angina observations from the randomized, double-blind, placebo-controlled MERLIN-TIMI (Metabolic Efficiency With Ranolazine for Less Ischemia in Non-ST-Segment Elevation Acute Coronary Syndromes) 36 Trial. *J Am Coll Cardiol* 2009;53:1510-6.
 68. Russell RR, 3rd, Li J, Coven DL, et al. AMP-activated protein kinase mediates ischemic glucose uptake and prevents postischemic cardiac dysfunction, apoptosis, and injury. *J Clin Invest* 2004;114:495-503.
 69. McVeigh JJ, Lopaschuk GD. Dichloroacetate stimulation of glucose oxidation improves recovery of ischemic rat hearts. *Am J Physiol* 1990;259:H1079-85.

70. Stacpoole PW, Henderson GN, Yan Z, Cornett R, James MO. Pharmacokinetics, metabolism and toxicology of dichloroacetate. *Drug metabolism reviews* 1998;30:499-539.
71. Lukas G, Vyas KH, Brindle SD, Le Sher AR, Wagner WE, Jr. Biological disposition of sodium dichloroacetate in animals and humans after intravenous administration. *Journal of pharmaceutical sciences* 1980;69:419-21.
72. Stacpoole PW, Nagaraja NV, Hutson AD. Efficacy of dichloroacetate as a lactate-lowering drug. *Journal of clinical pharmacology* 2003;43:683-91.
73. Harwood HJ, Jr. Treating the metabolic syndrome: acetyl-CoA carboxylase inhibition. *Expert opinion on therapeutic targets* 2005;9:267-81.
74. Seng TW, Skillman TR, Yang N, Hammond C. Cyclohexanedione herbicides are inhibitors of rat heart acetyl-CoA carboxylase. *Bioorganic & medicinal chemistry letters* 2003;13:3237-42.
75. Olson DP, Pulinilkunnil T, Cline GW, Shulman GI, Lowell BB. Gene knockout of *Acc2* has little effect on body weight, fat mass, or food intake. *Proc Natl Acad Sci U S A* 2010;107:7598-603.
76. McMurtry MS, Bonnet S, Wu X, et al. Dichloroacetate prevents and reverses pulmonary hypertension by inducing pulmonary artery smooth muscle cell apoptosis. *Circ Res* 2004;95:830-40.
77. Barr RL, Lopaschuk GD. Direct measurement of energy metabolism in the isolated working rat heart. *J Pharmacol Toxicol Methods* 1997;38:11-7.
78. Larsen TS, Belke DD, Sas R, et al. The isolated working mouse heart: methodological considerations. *Pflugers Arch* 1999;437:979-85.
79. Ussher JR, Wang W, Gandhi M, et al. Stimulation of glucose oxidation protects against acute myocardial infarction and reperfusion injury. *Cardiovasc Res* 2012;94:359-69.
80. Finegan BA, Lopaschuk GD, Gandhi M, Clanachan AS. Ischemic preconditioning inhibits glycolysis and proton production in isolated working rat hearts. *Am J Physiol* 1995;269:H1767-75.
81. Jaswal JS, Lund CR, Keung W, Beker DL, Rebeyka IM, Lopaschuk GD. Isoproterenol stimulates 5'-AMP-activated protein kinase and fatty acid oxidation in neonatal hearts. *Am J Physiol Heart Circ Physiol* 2010;299:H1135-45.
82. Belke DD, Larsen TS, Lopaschuk GD, Severson DL. Glucose and fatty acid metabolism in the isolated working mouse heart. *Am J Physiol* 1999;277:R1210-7.
83. King MT, Reiss PD, Cornell NW. Determination of short-chain coenzyme A compounds by reversed-phase high-performance liquid chromatography. *Methods Enzymol* 1988;166:70-9.
84. McHugh ML. Multiple comparison analysis testing in ANOVA. *Biochemia medica : casopis Hrvatskoga drustva medicinskih biokemicara / HDMB* 2011;21:203-9.
85. Piao L, Sidhu VK, Fang YH, et al. FOXO1-mediated upregulation of pyruvate dehydrogenase kinase-4 (PDK4) decreases glucose oxidation and

- impairs right ventricular function in pulmonary hypertension: therapeutic benefits of dichloroacetate. *Journal of molecular medicine* 2012.
86. Sutendra G, Bonnet S, Rochefort G, et al. Fatty acid oxidation and malonyl-CoA decarboxylase in the vascular remodeling of pulmonary hypertension. *Sci Transl Med* 2010;2:44ra58.
 87. Furuyama T, Kitayama K, Yamashita H, Mori N. Forkhead transcription factor FOXO1 (FKHR)-dependent induction of PDK4 gene expression in skeletal muscle during energy deprivation. *The Biochemical journal* 2003;375:365-71.
 88. Battiprolu PK, Hojaye B, Jiang N, et al. Metabolic stress-induced activation of FoxO1 triggers diabetic cardiomyopathy in mice. *The Journal of clinical investigation* 2012;122:1109-18.
 89. Whitmer JT, Idell-Wenger JA, Rovetto MJ, Neely JR. Control of fatty acid metabolism in ischemic and hypoxic hearts. *J Biol Chem* 1978;253:4305-9.
 90. Liu B, Clanachan AS, Schulz R, Lopaschuk GD. Cardiac efficiency is improved after ischemia by altering both the source and fate of protons. *Circ Res* 1996;79:940-8.
 91. Saddik M, Gamble J, Witters LA, Lopaschuk GD. Acetyl-CoA carboxylase regulation of fatty acid oxidation in the heart. *J Biol Chem* 1993;268:25836-45.
 92. Abu-Elheiga L, Matzuk MM, Abo-Hashema KA, Wakil SJ. Continuous fatty acid oxidation and reduced fat storage in mice lacking acetyl-CoA carboxylase 2. *Science* 2001;291:2613-6.
 93. Oh W, Abu-Elheiga L, Kordari P, et al. Glucose and fat metabolism in adipose tissue of acetyl-CoA carboxylase 2 knockout mice. *Proc Natl Acad Sci U S A* 2005;102:1384-9.
 94. Abu-Elheiga L, Oh W, Kordari P, Wakil SJ. Acetyl-CoA carboxylase 2 mutant mice are protected against obesity and diabetes induced by high-fat/high-carbohydrate diets. *Proc Natl Acad Sci U S A* 2003;100:10207-12.
 95. Choi CS, Savage DB, Abu-Elheiga L, et al. Continuous fat oxidation in acetyl-CoA carboxylase 2 knockout mice increases total energy expenditure, reduces fat mass, and improves insulin sensitivity. *Proc Natl Acad Sci U S A* 2007;104:16480-5.
 96. Essop MF, Camp HS, Choi CS, et al. Reduced heart size and increased myocardial fuel substrate oxidation in ACC2 mutant mice. *Am J Physiol Heart Circ Physiol* 2008;295:H256-65.
 97. Kuang M, Febbraio M, Wagg C, Lopaschuk GD, Dyck JR. Fatty acid translocase/CD36 deficiency does not energetically or functionally compromise hearts before or after ischemia. *Circulation* 2004;109:1550-7.
 98. Kovacic S, Soltys CL, Barr AJ, Shiojima I, Walsh K, Dyck JR. Akt activity negatively regulates phosphorylation of AMP-activated protein kinase in the heart. *J Biol Chem* 2003;278:39422-7.
 99. Kudo N, Barr AJ, Barr RL, Desai S, Lopaschuk GD. High rates of fatty acid oxidation during reperfusion of ischemic hearts are associated with a

decrease in malonyl-CoA levels due to an increase in 5'-AMP-activated protein kinase inhibition of acetyl-CoA carboxylase. *J Biol Chem* 1995;270:17513-20.

100. Lopaschuk GD, Gamble J. The 1993 Merck Frosst Award. Acetyl-CoA carboxylase: an important regulator of fatty acid oxidation in the heart. *Can J Physiol Pharmacol* 1994;72:1101-9.
101. Kolwicz SC, Jr., Olson DP, Marney LC, Garcia-Menendez L, Synovec RE, Tian R. Cardiac-specific deletion of acetyl CoA carboxylase 2 prevents metabolic remodeling during pressure-overload hypertrophy. *Circulation Research* 2012;111:728-38.